Financial Crises and Shadow Banks: A Quantitative Analysis

Matthias Rottner*
Deutsche Bundesbank

May 28, 2023

Abstract

Motivated by the build-up of shadow bank leverage prior to the financial crisis of 2007-2008, I develop a nonlinear macroeconomic model featuring excessive leverage accumulation and endogenous runs to capture the dynamics and quantify the build-up of instability. Incorporating monetary policy, I demonstrate that the zero lower bound increases the crises frequency and lowers welfare. The model is taken to U.S. data to estimate the run probability around the financial crisis of 2007-2008. The estimated run risk was already considerable in 2005 and kept increasing. Counterfactual simulations evaluate whether monetary interventions boost welfare and could have averted the financial crisis.

Keywords: Financial crises, leverage, nonlinear estimation, zero lower bound, monetary policy

JEL Codes: E32, E44, G23.

*Contact at matthias.rottner@bundesbank.de. I am indebted to Leonardo Melosi and Evi Pappa for their continued advice and guidance. I would like to thank Lawrence Christiano, Miguel Faria-e-Castro, Philipp Grübener, Brigitte Hochmuth, Tom Holden, Nikolay Hristov, Hanno Kase, Benedikt Kolb, Guido Lorenzoni, Francesca Loria, Galo Nuno, Johannes Poeschl, Andrea Prestipino, Giorgio Primiceri, Sebastian Rast, Michael Stiefel, Edgar Vogel and seminar participants at Northwestern University, the Federal Reserve Board, Deutsche Bundesbank, ECB WG on Econometric Modelling - Macro-at-Risk Group, Bank of Canada, Bank of England, Banque de France, Norges Bank, Danmarks Nationalbank, European University Institute, KU Leuven, the University of Konstanz, the University of Tuebingen, Bank of Estonia and the VfS Annual Conference 2020. I also thank Angélica Dominguez Cardoza and Jesús Laso Pazos for their excellent work as research assistants. The views presented in this paper are those of the author, and do not necessarily reflect those of the Deutsche Bundesbank or the Eurosystem.

1 Introduction

The financial crisis of 2007-2008 was, at the time, the most severe economic downturn in the US since the Great Depression. Although the origins of the financial crisis are complex and various, the financial distress in the shadow banking sector has been shown to be one of the key factors.[1] The shadow banking sector, which consists of financial intermediaries operating outside normal banking regulation, expanded considerably before the crisis. Crucially, there was an excessive build-up of leverage (asset to equity ratio) for these unregulated banks. The collapse of the highly leveraged major investment bank Lehman Brothers in September 2008 intensified then a run on the short-term funding of many financial intermediaries, with very severe repercussions for the real economy in the fourth quarter of 2008. Figure 1 documents these stylized facts about GDP growth and shadow bank leverage.

In this paper, I build a new nonlinear quantitative macroeconomic model with financial intermediaries and endogenous runs to capture the observed dynamics and to quantify the build-up of financial fragility. The model features endogenous boom-bust dynamics, which rely on the interaction among two features that correspond well to the shadow banking sector. First, the financial intermediaries face risk-shifting incentives and volatility shocks, which allow to account for extensive leverage accumulation similar to Adrian and Shin (2014) and Nuño and Thomas (2017). Second, the runs on the financial sector depend on economic and financial circumstances, as in Gertler et al. (2020b).

The boom-bust dynamics originate from a volatility paradox, in the spirit of Brunnermeier and Sannikov (2014). A period of low volatility reduces the risk-shifting incentives of financial intermediaries. This results in substantially elevated leverage, which implies low loss absorbing capacities, but also boosts credit and output. An increase in volatility can then trigger a self-fulfilling abrupt stop to the roll over of deposits, which triggers firesales and pushes the highly levered intermediaries into bankruptcy. This run on the financial sector causes a sharp contraction in output as observed in the great financial crisis in the fourth quarter of 2008. Importantly, the dynamics reconcile key empirical observations concerning financial crises since a run is preceded by a credit boom (Schularick and Taylor, 2012), low pre-crisis credit spreads (Krishnamurthy and Muir, 2017) and elevated shadow bank leverage as observed around 2008 (Adrian and Shin, 2010).

The model is embedded in a New Keynesian setup to study inflation dynamics and the zero lower bound (ZLB) in connection with financial crises. Financial fragility creates extensive downside risk for inflation. The ZLB increases the frequency and severity of financial crises substantially because it restricts the interventions of the monetary authority during a run. The ZLB also results in a considerable welfare loss of 0.3% in consumption equivalents.

The model is then taken to the data to obtain a structural estimate of the endogenous build-up of financial fragility in the U.S. around the great financial crisis. However, an estimation is very challenging because it requires to repeatedly solve the nonlinear model with global methods and then to filter it. To overcome this challenge, I apply a two-step procedure

[1] See e.g. Adrian and Shin (2010), Bernanke (2018), Brunnermeier (2009) and Gorton and Metrick (2012).

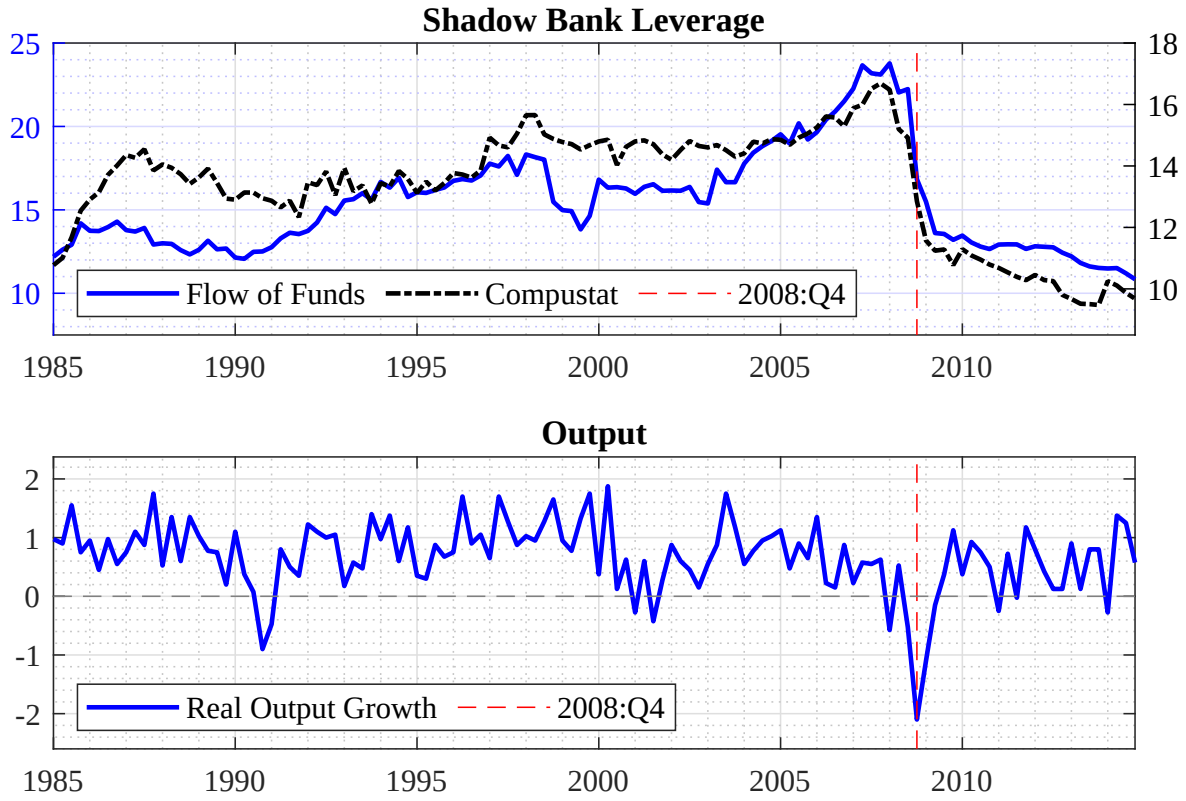

Figure 1: The upper graph shows two measures of U.S. shadow bank book leverage. The first measure is based on balance sheet data from the Flow of Funds (left axis). The alternative one uses Compustat data (right axis). The leverage series rely on the book value of equity. Appendix A shows the details. The lower graph shows the quarter-on-quarter real output growth rate in percent.

that reduces the computational burden, while still providing an estimate of financial fragility through the lens of a structural nonlinear model. In the first step, the nonlinear model is calibrated to key features of the U.S. and the shadow banking sector. The calibrated model is used as input for a nonlinear filter in the second step. The filter extracts the sequence of shocks and estimates the endogenous run probability over time conditional on the paths of selected data (shadow bank leverage and real output growth). In particular, I employ a particle filter to account for the nonlinear setup with endogenous financial crisis and the ZLB. This general approach provides a model-based growth-at-risk estimate.

According to the estimation, the run probability starts to increase significantly from 2005 onwards and peaks in 2008 due to rising shadow bank leverage. The estimation selects a run to explain the data in 2008:Q4. The run itself accounts for 70% of the severe output drop in this period. In addition to this, the results highlight the importance of low volatility because it causes the rise in leverage and makes the financial system prone to instability. As an external validation, the estimated path of volatility is also compared to a data proxy.

The model and estimation lend itself for a joint welfare analysis and counterfactual simulation of monetary and macroprudential strategies. Specifically, the focus is on a monetary policy rule that responds to the financial situation. The monetary policy response to financial conditions can be classified into interventions before (ex-ante) and after (ex-post) the crisis. Monetary policy can act in advance and lean against the wind through tightening measures,

such as raising interest rates. Conversely, the ex-post component captures the monetary authority committing to a loose policy after the crisis. The welfare-maximizing rule enhances welfare by 0.6% (expressed in consumption equivalents) and succeeds in avoiding almost all runs. Most of these gains stem from the credible ex-post commitment, while ex-ante leaning provides only small, albeit positive, effects. To evaluate the policy, I compare it with a comparable macroprudential policy. Even though macroprudential policy would be preferable from a welfare perspective, monetary policy can in some cases serve as a good substitute that is easier to implement in practice, especially with respect to shadow banks.

Using the results from the estimation, the counterfactual paths for economic activity and financial fragility under alternative policies can be constructed. I demonstrate that the described welfare-maximizing rule would have mitigated the estimated build-up of financial fragility and averted the run in 2008. This outcome, however, hinges on a credible commitment to a loose ex-post policy, as ex-ante leaning alone would have not been sufficient.

Related Literature Gertler et al. (2020b) and Gertler et al. (2020a) pioneer the incorporation of self-fulfilling runs into macroeconomic models to explain financial crises.[2] My paper contributes to this literature in three ways. First, I introduce volatility shocks as a new channel to quantify the financial crisis. This mechanism captures key macroeconomic and financial series, in particular the build-up of leverage prior to 2008 and endogenous boom-bust dynamics.[3] Second, I outline an approach to estimate the endogenous probability of a financial crisis through the lens of a microfounded nonlinear model. Taking the model to the data, I provide a novel nonlinear structural estimate of financial fragility around the financial crisis in 2008. Finally, I evaluate the economic and welfare implications of monetary policy with a special emphasis on the zero lower bound and responding to the financial situation. Combining the estimation with the policy analysis allows to show under what conditions a monetary interventions could have avoided the run on the financial sector in 2008. Other papers that incorporate runs into quantitative macro frameworks are Amador and Bianchi (2021), Faria-e-Castro (2019), Ferrante (2018), De Groot (2021), Ikeda and Matsumoto (2021), Hakamada (2021), Mikkelsen and Poeschl (2019), Paul (2020) and Poeschl (2020).[4]

I also contribute to the large large growing body of empirical work on growth-at-risk that was inspired by Adrian et al. (2019). Their work links macrofinancial conditions and the future distribution of output growth using quantile regressions. More recently, Adrian et al.

[2]Gertler and Kiyotaki (2015) and Gertler et al. (2016) are important preceding contributions that integrate bank runs in the spirit of Diamond and Dybvig (1983) into standard macro models. Cooper and Corbae (2002) is an early study with runs that can be interpreted as roll-over crises.

[3]The risk-shifting incentives have a very different impact on leverage compared to that of a run-away constraint, where an intermediary can divert a fraction of assets that cannot be reclaimed, as used in Gertler et al. (2020b). Risk-shifting incentives combined with the volatility shock generate procyclical leverage, while leverage is normally countercyclical with the run-away constraint. The run-away constraint can be reconciled with the evidence for credit booms that generate busts if intermediaries are overly optimistic about future news. An alternative approach to obtain procyclical leverage is to have sticky net worth accumulation of financial intermediaries (Ikeda and Matsumoto, 2021).

[4]Other approaches to capture boom-bust dynamics are asymmetric information, optimistic beliefs and learning (e.g. Boissay et al., 2016; Bordalo et al., 2018; Boz and Mendoza, 2014). Other studies (e.g. Justiniano et al., 2019; Guerrieri and Lorenzoni, 2017) emphasize the role of housing.

(2020) develop a semi-structural macroeconomic model with an ad-hoc specific vulnerability function to capture downside risk. My paper provides a novel structural empirical perspective on growth-at-risk through the combination of a fully microfounded nonlinear model and the particle filter. Based on the estimation, I also conduct (policy) counterfactuals on the estimated build-up of financial fragility and the occurrence of a financial crisis.

To obtain an estimate for the probability of a financial crisis through the lens of nonlinear model, I build on the literature that empirically assesses models with multiple equilibria. Following Aruoba et al. (2018), I use a particle filter (Fernández-Villaverde and Rubio-Ramírez, 2007) that is adapted to account for the multiplicity of equilibria.[5] A considerable difference to Aruoba et al. (2018) is the nature of the sunspot shock, which helps to select the equilibrium. While they use a Markov-switching sunspot shock to capture a switch in the inflation environment, I rely on an iid sunspot shock to capture the one-time event of a run. Furthermore, Bocola and Dovis (2019) use a particle filter to estimate the likelihood of a government default. Faria-e-Castro (2019) applies a particle filter to conduct a counterfactual with countercyclical capital requirements in a model with bank runs.

2 Model

The setup is a dynamic stochastic general equilibrium model with a financial sector that faces endogenous runs. It is embedded in a New Keynesian setup with a zero lower bound (ZLB). Financial intermediaries have risk-shifting incentives based on Adrian and Shin (2014) and Nuño and Thomas (2017), which microfounds their leverage constraint. The financial sector occasionally faces system-wide runs, which are state-dependent, or in other words endogenous, similar to Gertler et al. (2020b). The occurrence of a run depends jointly on fundamentals and a self-fulfilling element. The intermediaries can be best thought of as shadow banks, as they are unregulated and not protected by deposit insurance.[6] The model featuring runs and the ZLB is solved in its nonlinear specification with global methods.

2.1 Household

There is a continuum of identical households. The representative household consists of workers and financial intermediaries that have perfect insurance for their consumption C_t. Workers supply labor L_t and earn the wage W_t. Intermediaries die with a probability of $1-\theta$ and return their net worth to the household to avoid self-financing. Simultaneously, new intermediaries enter each period and receive a transfer from the household. The household owns the non-financial firms and receives the profits. The variable Ξ_t captures all transfers.

The household is a net saver and holds two different assets. The first asset are one-period deposits D_t for which the financial intermediaries promise to pay a predetermined gross interest rate $\bar{R}_t$. However, the occurrence of a run alters the intermediary's ability to

[5] I adjust the filter to handle equilibrium probabilities that are endogenously time-varying.

[6] While assuming the absence of deposit insurance is a characteristic in line with shadow banks, a run could also occur in the presence of a deposit insurance system provided that the insurance is imperfect.

honor its commitment. Households receive then only a fraction $x_t^\star$, which is the recovery ratio, of the promised return. The gross rate R_t is thus state-dependent:

$$R_t = \begin{cases} \bar{R}_{t-1} & \text{if no run takes place in period } t \\ x_t^\star \bar{R}_{t-1} & \text{if a run takes place in period } t \end{cases} \tag{1}$$

The other asset are securities. I distinguish between beginning-of-period securities K_t that are used to produce output and end-of-period securities S_t. The end of period securities S_t^H give them an ownership in the non-financial firms. The household earns the stochastic rental rate Z_t and can trade the securities with other households as well as intermediaries at the market price Q_t. The securities of households and intermediaries, where the latter are denoted as S_t^B, are perfect substitutes. Total end-of-period securities S_t are $S_t = S_t^H + S_t^B$.

The households are less efficient in managing capital holdings, as in the framework of Brunnermeier and Sannikov (2014). Following the shortcut of Gertler et al. (2020b), capital holdings are costly in terms of utility. The utility function is given as:

$$U_t = E_t\Big\{ \sum_{\tau=t}^{\infty} \beta^{\tau-t} \Big[\frac{(C_\tau)^{1-\sigma^h}}{1-\sigma^h} - \frac{\chi L_\tau^{1+\varphi}}{1+\varphi} - \frac{\Theta}{2}\Big(\frac{S_\tau^H}{S_\tau} - \gamma^F\Big)^2 S_\tau \Big] \Big\}, \tag{2}$$

where $\Theta > 0$ and $\gamma^F > 0$. Thus, holding a share of securities share above γ^F becomes increasingly costly. The households maximize their utility subject to the budget constraint:

$$C_t = W_t L_t + D_{t-1} R_t - D_t + \Xi_t - Q_t S_t^H + (Z_t + (1-\delta)Q_t) S_{t-1}^H. \tag{3}$$

2.2 Financial Intermediaries

The financial intermediaries' leverage decision depends on the risk-shifting incentives and the possibility of a run on the financial system. The intermediaries face a moral hazard problem due to risk-shifting incentives that limits their leverage. They can invest in two different securities with distinct risk profiles. Limited liability protects the intermediaries' losses in case of default and creates incentives to choose a strategy that is too risky from the depositors' point of view.[7] This results in an incentive and a participation constraint for the intermediaries' maximization problem, which also accounts for the threat of runs.

There is a continuum of financial intermediaries indexed by j, who intermediate funds between households and non-financial firms. The intermediaries hold net worth N_t^j and collect deposits D_t^j to buy securities S_t^B from the goods producers: $Q_t S_t^{Bj} = N_t^j + D_t^j$. Their leverage is defined as $\phi_t^j = Q_t S_t^{Bj} / N_t^j$. The intermediary chooses its security and deposit holdings to maximize the value of its franchise V_t. The maximization problem also depends on the run because the intermediary can only continue operating or return its net worth in the absence of a run. The probability that the intermediary defaults due to a run next period

[7] This formulation microfounds a value-at-risk constraint - a common risk management approach for shadow banks - and corresponds to a contracting problem from corporate finance theory. Adrian and Shin (2010) provide evidence on the value-at-risk constraint and the leverage decision of security broker-dealers.

is denoted as p_t, which is derived in the next subsection. The value V_t^j is:

$$V_t^j(N_t^j) = (1-p_t)E_t^N\left[\Lambda_{t,t+1}\left(\theta V_{t+1}^j(N_{t+1}^j) + (1-\theta)(R_{t+1}^K Q_t S_t^{Bj} - R_{t+1}D_t^j)\right)\right], \quad (4)$$

where net worth accumulates as the return on assets net the cost of deposits: $N_t^j = R_t^K Q_{t-1} S_{t-1}^{Bj} - R_t D_{t-1}^j$. $E_t^N[\cdot]$ is the expectation conditional on no run in $t+1$. A superscript denotes if the expectations are conditioned on the absence (N) or occurrence of a run (R). The intermediary maximizes V_t subject to an incentive and participation constraint due to risk-shifting incentives, as described now. Appendix B.3 contains the formal derivation.

Risk-Shifting Incentives and Volatility After purchasing the securities, the financial intermediary converts, at the end of the period, the securities into efficiency units ω_{t+1} that are subject to idiosyncratic volatility similar to Christiano et al. (2014). The arrival of the idiosyncratic shock is iid over time and intermediaries. The intermediary has to choose between two different conversions - a good security ω and a substandard security $\tilde{\omega}$ - that differ in their cross-sectional idiosyncratic volatility. They have the following distinct distributions:

$$\log \omega_t = 0, \qquad \text{and} \qquad \log \tilde{\omega}_t \overset{iid}{\sim} N\left(\frac{-\sigma_t^2 - \psi}{2}, \sigma_t\right), \quad (5)$$

where $\psi < 1$. σ_t affects the idiosyncratic volatility and is an exogenous driver specified below. I abstract from idiosyncratic volatility for the good security so that its distribution is a dirac delta function with $\Delta_t(\omega)$ denoting the cumulative distribution function. The substandard one follows a log normal distribution, where $F_t(\tilde{\omega}_t)$ is the cumulative distribution function.

The good security is superior as it has a higher mean and a lower variance due to $\psi < 1$:[8]

$$E(\omega) = \omega = 1 > e^{-\frac{\psi}{2}} = E(\tilde{\omega}), \quad \text{and} \quad Var(\omega) = 0 < [e^{\sigma^2} - 1]e^{-\psi} = Var(\tilde{\omega}). \quad (6)$$

However, the substandard security features a higher upside risk due to the possibility of a large idiosyncratic shock $\tilde{\omega}$.[9] Appendix B.2 contains a graphical characterization.

The variable σ_t is labeled as volatility since it affects the relative cross-sectional idiosyncratic volatility of the securities. In particular, it changes the upside risk, while preserving the mean spread $E(\omega) - E(\tilde{\omega})$. Volatility σ_t is exogenous and follows an AR(1) process:

$$\sigma_t = (1-\rho^\sigma)\sigma + \rho^\sigma \sigma_{t-1} + \sigma^\sigma \epsilon_t^\sigma, \qquad \text{where } \epsilon_t^\sigma \sim N(0,1). \quad (7)$$

The intermediary earns the return $R_t^{K,j}$ on its securities that depends on the stochastic aggregate return R_t^K and the realized idiosyncratic shock conditional on its conversion choice. While the return for the good type $R_t^{Kj} = \omega_t^j R_t^K = R_t^K$ is independent of the idiosyncratic shock, the shock affects the return for the substandard type $R_t^{Kj} = \tilde{\omega}_t^j R_t^K$.

[8] More formally, I assume that $\Delta_t(\omega)$ cuts $F_t(\tilde{\omega})$ once from below to ensure this property. This means that there is a single ω^*, such that $(\Delta_t(\omega) - \tilde{F}_t(\omega))(\omega - \omega^*) \geq 0 \ \ \forall \omega$.

[9] Ang et al. (2006) find empirically that stocks with high idiosyncratic variance have low average returns.

The aggregate return depends on price Q_t and the profits per unit of effective capital Z_t: $R_t^K = [(1-\delta)Q_t + Z_t]/Q_{t-1}$. Based on this, a threshold value $\overline{\omega}_t^j$ for the idiosyncratic shock defines when the intermediary can exactly cover the face value of the deposits:

$$\overline{\omega}_t^j = (\bar{R}_{t-1} D_{t-1}^j)/(R_t^K Q_{t-1} S_{t-1}^{Bj}). \tag{8}$$

As it stands so far, the financial entities would choose to invest in the good security as it has a higher mean and lower variance. However, limited liability protects the financial entities, which distorts the choice between the securities. If the realized idiosyncratic volatility is below $\overline{\omega}_t^j$, the financial intermediary declares bankruptcy. The households seize then all assets, but they do not receive the promised repayment. This limits the downside risk of the substandard security, while the upside risk is unaffected. The gain from limited liability is:

$$\tilde{\pi}_t^j = \int^{\overline{\omega}_{t+1}^j} (\overline{\omega}_{t+1}^j - \tilde{\omega}) dF_t(\tilde{\omega}) > 0. \tag{9}$$

In contrast to this, the gain from limited liability due to idiosyncratic risk is zero for the good technology. This creates a trade-off between the good securities' higher mean return versus the gains from limited liability for the substandard security.

To ensure an investment in the good security, the intermediary faces an incentive constraint that deals with the risk-shifting incentives resulting from limited liability. The incentive constraint ensures that the good security is the only equilibrium choice.[10] The constraint limits the leverage of the intermediaries to force them to have enough "skin in the game" because the gain from limited liability increases in leverage. The microfoundation behind the leverage constraint is very different to the incentive constraint in Gertler et al. (2020b) and the collateral constraint in Jermann and Quadrini (2012). One crucial strength is that this financial friction in combination with the volatility shock accounts for procyclical leverage dynamics and other key empirical observations concerning financial crises, as shown later.

The incentive constraints is as follows, as derived in Appendix B.3:

$$(1-p_t) E_t^N \Lambda_{t,t+1} R_{t+1}^K (\theta \lambda_{t+1}^j + (1-\theta))[1 - e^{\frac{-\psi}{2}} - \tilde{\pi}_{t+1}^j] \geq p_t E_t^R \Lambda_{t,t+1} R_{t+1}^K (e^{-\frac{\psi}{2}} - \overline{\omega}_{t+1}^j + \tilde{\pi}_{t+1}^j), \tag{10}$$

The LHS shows the trade-off between the higher mean return $(1 - e^{\frac{-\psi}{2}})$ and the upside risk $\tilde{\pi}_{t+1}^j$. This is the relevant consideration if there is no run next period. The RHS displays an additional gain of investing in the substandard security in case of a run. The substandard security offers the possibility to have positive net worth despite a run if the realized shock satisfies $\tilde{\omega}_t^i > \overline{\omega}_t$.[11] λ_t^j is the multiplier on the participation constraint, which is derived next.

[10] This also implies the absence of idiosyncratic default in equilibrium. However, the risk-shifting is not affected by the choice to not have idiosyncratic default in equilibrium. In that regard, idiosyncratic default in equilibrium, as e.g. in Ferrante (2019) or Nuño and Thomas (2017), can be seen as an additional element.

[11] Investing in substandard securities is an outside equilibrium strategy, which allows financial intermediaries to survive a run in the event of a very high realization of the idiosyncratic shock. It is assumed that the surviving intermediaries repay their depositors fully and return their remaining net worth to the households.

The return on deposits needs to be sufficient such that households provide deposits to the intermediaries. While the households earn the predetermined interest rate $\bar{R}_t$ in normal times, the households recovers the gross return of the securities if a run takes place. As the return in a run is lower, an increase in p_t augments the funding costs to compensate for the run risk. The participation constraint can be written as:

$$(1-p_t)E_t^N[\beta\Lambda_{t,t+1}\bar{R}_t^D D_t^j] + p_t E_t^R[\beta\Lambda_{t,t+1}R_{t+1}^K Q_t S_t^{Bj}] \geq D_t^j. \tag{11}$$

Both constraints are assumed to be binding in equilibrium. This implies for their respective multipliers $\kappa_t > 0$ and $\lambda_t > 1$ in all periods. I verify these assumptions numerically using a simulation and show that these conditions are satisfied in more than 99.5% periods.[12]

Aggregation The participation and incentive constraint do not depend on intermediary-specific characteristics so that the optimal choice of leverage is independent of net worth as shown in Appendix B.3. Therefore, I can sum up across individual intermediaries to obtain the aggregate values. Their asset demand depends on leverage and net worth: $Q_t S_t^B = \phi_t N_t$.

The net worth evolution is as follows. In the absence of a run, surviving intermediaries retain their earnings. A run eradicates the net worth of the surviving intermediaries ($N_{S,t} = 0$), so that they stop operating. New intermediaries, which receive their net worth $N_{N,t}$ as a transfer from households, enter each period (independent of a run taking place or not):

$$N_{S,t} = \max\{R_t^K Q_t S_{t-1}^B - R_t^D D_t, 0\}, \qquad \text{and} \qquad N_{N,t} = (1-\theta)\zeta S_{t-1}. \tag{12}$$

Aggregate net worth N_t is given as $N_t = \theta N_{S,t} + N_{N,t}$.

2.3 Endogenous Runs and Multiple Equilibria

There are occasional runs, in which depositors stop rolling over their deposits. Importantly, the possibility of such a run is endogenous because the existence of this equilibrium depends on economic circumstances, following Gertler et al. (2020b). In these states, the model features multiple equilibria in the spirit of Diamond and Dybvig (1983). The multiplicity of equilibria originates from heterogeneous asset demand of households and intermediaries.[13] During normal times households roll over their deposits. Financial intermediaries and households demand securities and the market clears at the fundamental price Q_t. The intermediary can cover the promised repayments for Q_t, that is $[(1-\delta)Q_t + Z_t]S_{t-1}^B > \bar{R}_{t-1}D_{t-1}$.

In contrast to this, a run wipes out the entire existing financial sector, so that $N_{S,t} = 0$. Households cease to roll over their deposits in a run, forcing intermediaries to liquidate their entire assets to repay the households. However, this eliminates their demand for securities. Households plus the newly entering financial intermediaries are the only remaining agents to

[12] The reason for these rare violations is that the intermediaries accumulate too much net worth. This could be addressed, for instance, by allowing for state-dependent dividend payments. The payments could be modeled as an occasionally binding constraint similar to the equity injections of Gertler et al. (2020a). Appendix B.3.3 contains more details and shows the dynamics of the multipliers in a boom-bust scenario.

[13] There is no explicit distinction between households and typical lenders on the wholesale market.

buy the securities. Subsequently, the asset price falls to clear the market at a firesale price. The drop is particularly severe because it is costly for households to hold large amounts of securities. This firesale price $Q_t^\star$ depresses the potential liquidation value of intermediaries' securities. The run can then occur in the first place if the intermediaries do not have sufficient means to cover the claims of the households under $Q_t^\star$. This is the case if the recovery ratio $x_t^\star$, that is the firesale liquidation value relative to the promised repayments, is below 1:

$$x_t^\star \equiv \frac{[(1-\delta)Q_t^\star + Z_t^\star]S_{t-1}^B}{\bar{R}_{t-1}D_{t-1}} < 1. \tag{13}$$

The recovery ratio $x_t^\star$ partitions the state space into a safe region without runs ($x_t^\star \geq 1$) and a fragile region with multiple equilibria ($x_t^\star < 1$). Appendix B.4 contains more details and a graphical characterization. There is also a third scenario, in which the intermediaries cannot repay the depositors even under the fundamental price, which is the case if $[(1-\delta)Q_t + Z_t]S_{t-1}^B < \bar{R}_{t-1}D_{t-1}$. While this third case is accounted and checked for, this scenario is neglected because its probability is infinitesimally small in the quantitative model.

If there exists multiple equilibria, a sunspot shock selects the equilibrium, following Cole and Kehoe (2000).[14] The sunspot ι_t takes the value 1 with probability Υ and 0 with probability $1-\Upsilon$. A run takes place if $\iota_t = 1$ and $x_t^\star < 1$ is jointly the case. If $x_t^\star > 1$, then the sunspot shock has no impact on the equilibrium choice. Taken together, the probability for a run in period $t+1$ is endogenous because it depends on the probability of being in the crisis region in $t+1$ and of drawing a sunspot shock:

$$p_t = \text{prob}(x_{t+1}^\star < 1)\Upsilon. \tag{14}$$

2.4 Production, Monetary Policy and Resource Constraint

The non-financial firms sector consists of intermediate goods producers, final goods producers and capital goods producers. The central bank follows a Taylor rule with a ZLB.

There is a continuum of competitive intermediate goods producers. The representative producer produces the output Y_t with labor L_t and working capital K_t as input: $Y_t^j = A_t(K_{t-1}^j)^\alpha(L_t^j)^{1-\alpha}$. A_t is total factor productivity (TFP), which follows an AR(1) process.

The firm pays the wage W_t to the households. The firm purchases in period $t-1$ capital S_{t-1} at the market price Q_{t-1}. The firm finances the capital with securities S_{t-1}^B from the financial sector and the households S_{t-1}^H, so that $K_{t-1} = S_{t-1}^H + S_{t-1}^B$. The intermediate firm pays the state-contingent return $R_{K,t}$. After using the capital in period t for production, the firm sells the undepreciated capital at the market. The intermediate output is sold at price M_t, which turns out to be equal to the marginal costs φ^{mc}. The firm problem is given as:

$$\max_{K_{t-1},L_t} \sum_{i=0}^{\infty} \beta^i \Lambda_{t,t+i} \left(M_{t+i}Y_{t+i} + Q_{t+i}(1-\delta)K_{t-1+i} - R_{k_{t+i}}Q_{t-1+i}K_{t-1+i} - W_{t+i}L_{t+i} \right).$$

The final goods retailers buy the intermediate goods and transform them into the final

[14] An alternative way could be global games, as used in Ikeda and Matsumoto (2021).

good using a CES production technology:

$$Y_t = \left[\int_0^1 (Y_t^j)^{\frac{\epsilon-1}{\epsilon}} df\right]^{\frac{\epsilon}{\epsilon-1}}. \tag{15}$$

The price index and intermediate goods demand are given by:

$$P_t = \left[\int_0^1 (P_t^j)^{1-\epsilon} df\right]^{\frac{1}{1-\epsilon}}, \quad \text{and} \quad Y_t^j = \left(P_t^j/P_t\right)^{-\epsilon} Y_t. \tag{16}$$

The final retailers are subject to Rotemberg price adjustment costs:

$$E_t\Big\{\sum_{i=0}^{T} \Lambda_{t,t+i}\Big[\Big(\frac{P_{t+i}^j}{P_{t+i}} - \varphi_{t+i}^{mc}\Big)Y_{t+i}^j - \frac{\rho^r}{2} Y_{t+i}\Big(\frac{P_{t+i}^j}{\Pi P_{t+i-1}^j} - 1\Big)^2\Big]\Big\}, \tag{17}$$

where Π is the inflation target of the monetary authority.

Competitive capital goods producers produce new end of period capital using final goods. They create $\Gamma(I_t/S_{t-1})S_{t-1}$ new capital out of an investment I_t, which they sell at price Q_t:

$$\max_{I_t} Q_t \Gamma\left(I_t/S_{t-1}\right) S_{t-1} - I_t, \tag{18}$$

where the functional form is $\Gamma(I_t/S_{t-1}) = a_1(I_t/S_{t-1})^{1-\eta} + a_2$. The FOC gives a relation for the price Q_t. The law of motion for capital is $S_t = (1-\delta)S_{t-1} + \Gamma\left(I_t/S_{t-1}\right) S_{t-1}$.

The monetary authority sets the interest rate R_t^I using a Taylor Rule subject to the ZLB:

$$R_t^I = \max\left\{R^I \left(\frac{\Pi_t}{\Pi}\right)^{\kappa_\Pi} \left(\frac{\varphi_t^{mc}}{\varphi^{mc}}\right)^{\kappa_y}, 1\right\}, \tag{19}$$

where deviations of marginal costs from its deterministic steady state φ^{mc} capture the output gap.[15] To connect this rate to the household, there exists one-period bond in zero net supply that pays the riskless nominal rate R_t^I. The associated Euler equation reads as follows: $\beta\Lambda_{t,t+1}R_t^I/\Pi_{t+1} = 1$. The resource constraint is $Y_t = C_t + I_t + G + \frac{\rho^r}{2}(\Pi_t/\Pi - 1)^2 Y_t$, where G is government spending. The equilibrium description can be found in Appendix B.1.

2.5 Multiple Equilibria, ZLB and Global Solution Method

The model features an occasionally binding constraint and multiplicity of equilibria. The main focus is on the role of multiplicity that is generated by runs. The occasionally binding constraint originates from the ZLB. On top of that, the ZLB introduces many equilibria such as the targeted-inflation equilibrium, deflation equilibria as well as sunspot equilibria (see Benhabib et al., 2001; Aruoba et al., 2018). This paper focuses on the targeted-inflation equilibrium, in which inflation fluctuates around the central bank's inflation target.

The model is solved with global methods, specifically policy function iteration, to account for all nonlinear features. Within the class of policy function iteration methods, I use time

[15] The model could be extended to assess negative interest rates, e.g. following Darracq Pariès et al. (2020).

iteration with linear interpolation, as Richter et al. (2014). Additionally, I use a piecewise representation of the policy functions to account for the multiplicity of equilibria generated by the runs on the financial sector in the spirit of Aruoba et al. (2018) and Aruoba et al. (2021). In particular, the numerical approximation of the policy functions has distinct functions for the run equilibrium and the no run equilibrium, which allows to locate the run equilibrium with a high precision. The details of the numerical solution are left to Appendix C.

3 Model Dynamics: Volatility, Endogenous Runs and the ZLB

This section explains how the model is mapped to the data and analyzes the dynamics.

3.1 Model Parameterization and Selected Key Moments

The emphasis of the calibration is on the recent financial crisis in the U.S. and the shadow banking sector. The financial sector variables and shock processes are set to match selected moments, while the conventional parameters are chosen based on the literature. The focus is mostly on quarterly data from 1985:Q1 to 2014:Q4 to accommodate the changing regulation of shadow banking activities. The starting point coincides with major changes in the contracting conventions of the repurchasement agreement (repo) market - an important source of funding for shadow banks - that took place after the failure of a number of dealers in the early 1980s (Garbade, 2006). It also captures the period after the Great Inflation. After the financial crisis, new regulatory reforms such as Basel III and the Dodd-Frank overhauled the financial system, suggesting to end the sample a few years after 2008. Table 1 summarizes the calibration and the match with targeted moments in the data.

The discount factor is set to 0.9975, which corresponds to a low rate environment with an annualized long-run real interest rate of 1%. The Frisch elasticity is set to match an elasticity of 0.75. Risk aversion is parameterized to 1. TFP A normalizes output to 1 in the deterministic steady state (DSS). Government spending G is 20% of total GDP in the DSS. The production parameter α matches a capital income share of 33%. The depreciation rate is 10% annually. The price elasticity of demand is set to 10. The Rotemberg adjustment costs correspond to a five-quarter average duration of resetting prices in the related Calvo framework. The elasticity of the asset price ρ^r is 0.25. The parameters of the investment function normalize the asset price to $Q = 1$ and the investment $\Gamma(I/K) = I$ in the DSS. Monetary policy responds to deviations of marginal costs ($\kappa_y = 0.125$) and inflation ($\kappa_\pi = 2.0$), where the target inflation rate is normalized to 2% per annum.

The parameters related to the financial sector and the shock processes are set to target selected moments of the shadow banking sector, the frequency of financial crises and the dynamics of output. The financial sector represents the shadow banking sector. Specifically, I define these as entities that rely on short-term deposits that are not protected by the Federal Deposit Insurance Corporations and do not have access to the FED's discount window.[16]

[16]This definition applies to the following entities: Money market mutual funds, government-sponsored

a) Conventional Parameters		Value	Target / Source
Discount factor	β	0.9975	Risk free rate = 1.0% p.a.
Frisch labor elasticity	$1/\varphi$	0.75	Chetty et al. (2011)
Risk aversion	σ^H	1	Log utility for consumption
TFP level	A	0.407	Output = 1
Government spending	G	0.2	Govt. spending to output = 0.2
Capital share	α	0.33	Capital income share = 33 %
Capital depreciation	δ	0.025	Depreciation rate = 10% p.a.
Price elasticity of demand	ϵ	10	Markup = 11%
Rotemberg adjustment costs	ρ^r	178	Calvo duration of 5 quarters
Elasticity of asset price	η_i	0.25	Bernanke et al. (1999)
Investment Parameter 1	a_1	0.530	Asset Price Q = 1
Investment Parameter 2	a_2	-.008	$\Gamma(I/K) = I$
Target inflation	Π	1.005	Inflation Target of 2%
MP response to inflation	κ_π	2.0	Standard
MP response to output	κ_y	0.125	Standard

(b) Financial Sector & Shocks		Value	Moment	Data	Model
Parameter asset share HH	γ^F	0.33	Share shadow banking sector	33%	35%
Mean Substandard Security	ψ	0.01	Mean shadow bank leverage	15.5	15.5
Intermediation cost HH	Θ	0.04	Financial crisis probability	2.0%	1.9%
Survival rate	ζ	0.88	Mean credit spread	2.3%	3.0%
Persistence volatility	ρ^σ	0.96	Persistence of leverage	0.96	0.95
Std. dev. volatility shock	σ^σ	0.0031	Std. dev. of leverage	3.0	2.9
Persistence TFP	ρ^A	0.95	Persistence TFP	0.95	0.95
Std. dev. TFP shock	σ^A	0.0026	Std. dev. of output growth	0.6	0.5
Sunspot Shock	Υ	0.50	Output drop during run	2.8%	2.8%

Table 1: Calibration and Targeted Moments

The share of total assets held directly by the shadow banking sector was 37.1% in 2006 and dropped to 28.3% in 2012, as shown by Gallin (2015). Thus, the parameter γ^F specifies that the shadow banking sector holds 33% of total assets on average. The leverage measure combines balance sheet data from security broker dealers and finance companies using the U.S. Flow of Funds data, as discussed in Appendix A. The leverage series relies on book equity, which is the difference between the market value of the portfolio and the liabilities.[17] The return of $\psi = 0.01$ for the substandard security is used to target a mean leverage ratio of 15.5. The intermediation costs Θ are set to match an annual run probability of 2.0% (every 50 years on average). This moment is based on the historical database of Jordà et al. (2017), in which the crisis probability is around 2.7% for the U.S. and 1.9% for a sample of advanced economies since World War II. The survival rate θ is set such that the finance

enterprises, agency- and GSE-backed mortgage pools, private-label issuers of asset-backed securities, finance companies, real estate investment trusts, security brokers and dealers, and funding corporations.

[17] An alternative measure is the intermediaries' market capitalization, as emphasized in He et al. (2010) and He et al. (2017). However, the appropriate concept here is book equity (net worth) since the run depends on it. Market capitalization would be relevant for the issuance of shares or acquisitions (Adrian et al., 2013).

premium targets an average spread of 2.3% as observed between the BAA bond yield and a 10 year Treasury bond. The start capital parameter ζ is implied from the other parameters.

The volatility shock's persistence ρ^{σ} and standard deviation σ^{σ} are set to match its counterpart for shadow bank leverage. The standard deviation of the TFP shock σ^{A} targets the standard deviation of real quarterly GDP growth. The persistence is aligned with the persistence of the TFP series of Fernald (2014). Finally, the sunspot shock materializes with a probability of 50% to help to match the demeaned GDP growth of -2.8% in 2008:Q4.

3.2 Financial Crises Dynamics: Endogenous Runs, Volatility and Leverage

The model enables to study the vulnerability to a financial crisis. In particular, I evaluate how the combination of the volatility shock and the risk-shifting incentives can account for the key empirical observations that a financial crisis is preceded by a credit boom (Schularick and Taylor, 2012), low pre-crisis credit spreads (Krishnamurthy and Muir, 2017) and elevated shadow bank leverage as observed around 2008 (Adrian and Shin, 2010).

Figure 2 shows the impulse response of the economy to a sequence of volatility shocks. Starting from the steady state, one-standard-deviation negative shocks hit the economy in period 1 until period 8. The reduction in volatility lowers the risk-shifting incentives so that intermediaries increase leverage and extend their security holdings. This results in a credit boom and boosts output. The finance premium also falls. To capture the increase in financial fragilities during a boom, the leverage dynamics are key. The run probability does initially not respond because leverage is still rather low and the economy is still in the safe zone. However, once leverage increases further, the run probability rises considerably. The intermediaries have too low equity buffers to cover potential large losses from a run.

During the ongoing boom, the economy is hit by a two-standard-deviation positive volatility shock in period 9. The realization of this shock pushes the highly levered economy into the fragile region, as shown by a recovery ratio below 1. It is important to note that a sufficient large contractionary shock is necessary to push the economy in the fragile zone. If then the sunspot shock materializes simultaneously, a run on the financial sector occurs. Depositors stop to roll over their deposits so that intermediaries, which are forced to sell the securities at a firesale price, do not have enough equity to cover their losses. While the solid line shows a scenario with a sunspot shock and thus a run in period 9, the dashed line shows a credit boom without a run. The run results in a severe drop in output, increase in the finance premium and also a substantial fall in inflation. The economy also faces the ZLB during the run. This feature will be explored in Section 3.3. Finally, leverage is quite high in the run period, which overshoots the prediction in the data. As the old intermediaries fail, the returns for new intermediaries is very large so that they lever up. While this is a common problem in the literature, the increase in leverage is already much more in line with the data. As seen later, the model can actually track the leverage data in the estimation.

The reason for the boom-bust dynamics is the leverage-constraint via risk-shifting incentives, which provides procyclical leverage dynamics. On the contrary, an incentive constraint,

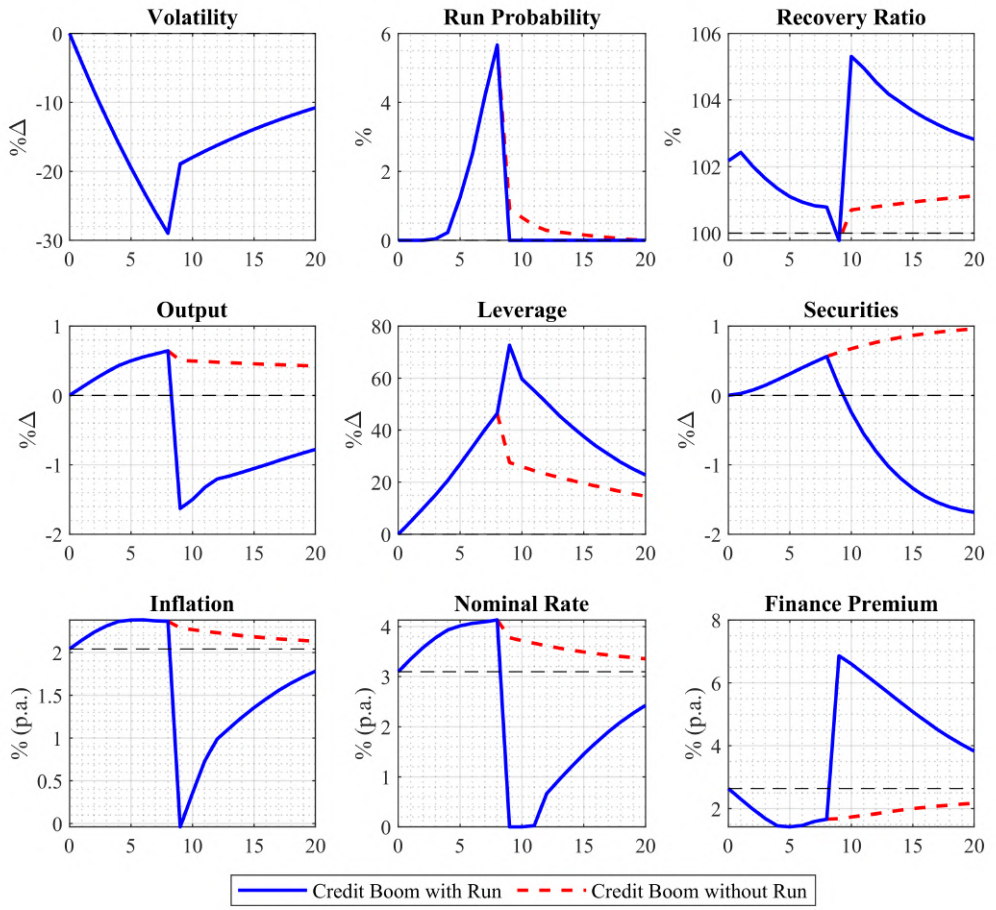

Figure 2: The role of volatility for a credit boom with a run. The simulation shows the impulse responses for a sequence of volatility shocks. The economy is initially at its stochastic steady state (SS). From period 1 until period 8, the economy is hit by a one-standard-deviation negative volatility shock in every period. In period 9, a two-standard-deviation positive volatility shock materializes. Afterwards, no more shocks occur. The scenario is shown for two cases: a) a boom with a run, which implies that the sunspot shock occurs in period 9 (blue solid line); b) a boom without a run, which implies that the sunspot shock does not materialize in period 9 (red dashed line). The scales are either percentage deviations from the stochastic SS (%Δ), annualized percent (% (p.a.)) or percent (%).

which generates countercyclical leverage, can not reconcile these boom-bust dynamics.

While extensive leverage raises the vulnerability to a run, the relationship is complex and highly nonlinear. If leverage is below some varying threshold value, which depends on the economic state, the run probability is zero. Once leverage increases above the threshold, then the run probability starts to respond nonlinearly. Additionally, the same level of leverage can result in different run probabilities depending on the economic circumstances. Thus, the relationship is not mechanic, and leverage alone is not a sufficient statistic to get the mapping to the probability of a run. Appendix D provides more details on this relationship.

The next step is to show that the discussed dynamics also represent a typical financial crisis in the model. For this reason, I conduct an event analysis around a financial crisis,

which is based on a simulation over 500,000 periods with $2,384$ runs. Figure 3 displays the run dynamics using an event window approach, where the window contains the path for ten quarters before and after a run. The dynamics are very similar as in the previous experiment and demonstrate that the typical run captures the key macroeconomic and financial features. The event window highlights that the underlying reason for the run is a period of low volatility, as even the 5% quantile of volatility is considerably below its long-run mean. Furthermore, a strong increase in volatility is then needed to trigger the run. While TFP is less important, a positive TFP level facilitates the boom.

The exercise also shows that there is a substantial increase in financial fragility prior to the run. The run probability peaks in the period before the run with a median value of 5%, corresponding to 20% as an annualized rate. At the same time, the upper bound of financial fragility is limited as it peaks around 10%. The reason is that agents are aware of the possibility of a run which endogenously limits the leverage of the financial sector. Thus, the model precludes a scenario in which the run probability becomes too large. Furthermore, the economy converges sometimes back to a safe zone without a crisis, which is in line with the empirical observation that not every boom ends in a bust (Gorton and Ordonez, 2020).

3.3 The Role of the Zero Lower Bound

The previous simulations have shown that the ZLB restricts the level of potential interest rate cuts during a financial collapse. Consequently, the ZLB can be an important amplification mechanism for financial fragility in a low rate environment.

To investigate this connection, I compare the run frequency and the run dynamics of the economy with and without the ZLB. First of all, the annual probability of a financial crisis drops significantly from 1.9% to 0.8% in the absence of the ZLB. This key moment emphasizes the relevance of the ZLB. The dynamics for the run itself are shown in Figure 3, which compares an economy with a ZLB (blue solid) and without a ZLB (red dashed). Due to the ZLB, the output fall is more severe, e.g around 0.6 percentage points in the initial run period. While the threat financial crisis is associated with a strong downside risk in inflation - as also empirically found in López-Salido and Loria (2020) - the ZLB exacerbates the downside risk of inflation even further. The fall in inflation is much more severe. Furthermore, the threat of encountering the ZLB creates deflationary pressure in periods of high financial fragility. This constitutes a further deflationary channel of the lower bound, in addition to the one which has already been studied in the literature, as e.g. in Bianchi et al. (2021). Finally, the relevance of TFP for financial fragility depends to some extent on the ZLB. A positive supply shock increases the probability of the ZLB. If this channel is absent, the level of TFP is much less important for the occurrence of a run.

A welfare comparison between the economy with and without the ZLB allows to capture the total costs of the interaction between the ZLB and endogenous runs. Welfare is measured as the utility of representative household, as in equation (2). The welfare gains of not having the ZLB correspond to 0.32% in consumption equivalents. In other words, agents would be

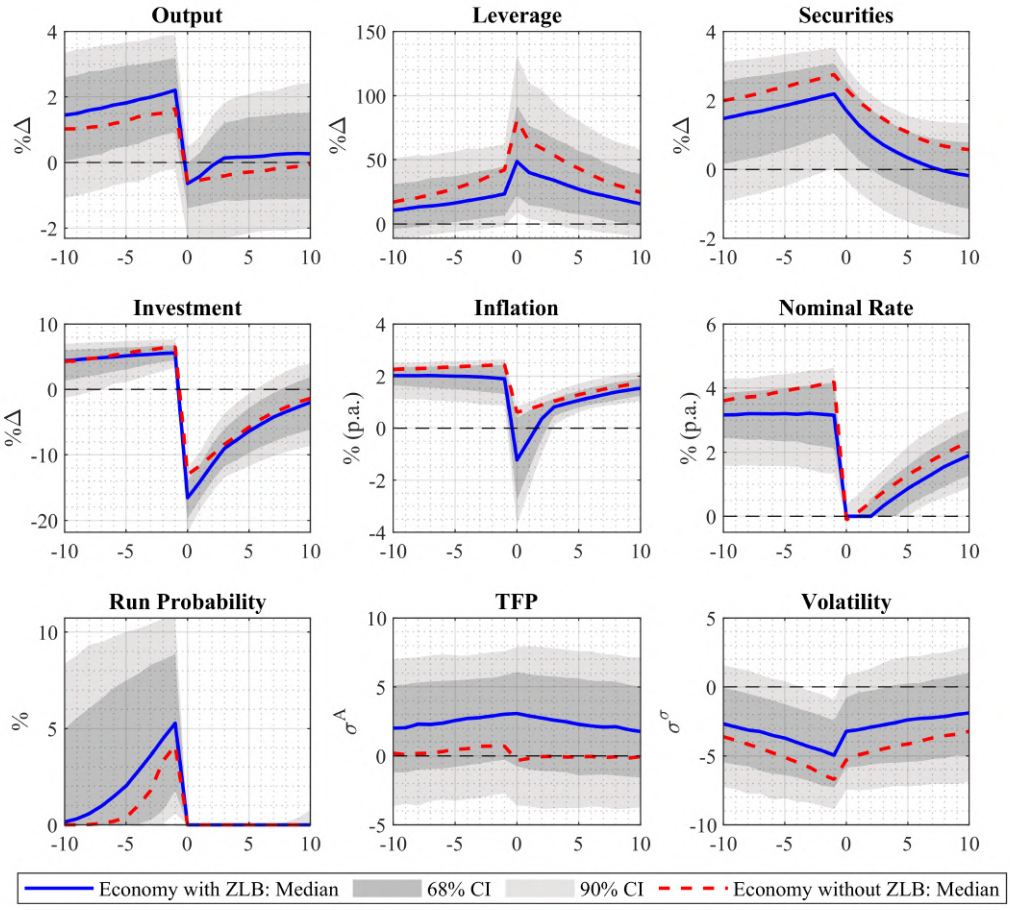

Figure 3: Event window around run episodes for an economy with and without a ZLB. Based on a simulation of 500,000 periods, the median path (blue solid) and the 68% as well as 90% confidence intervals of all runs are displayed ten quarters before and after a run in period 0 for the economy with the ZLB. For the economy without the ZLB, only the median is displayed. The scales are either percentage deviations from the simulated mean (%Δ), annualized percent, or percent.

willing to give up 0.32% of their consumption in each period to avoid facing the ZLB. These costs are substantial, especially considering that runs are rare events.

4 Estimation of Financial Fragility

I estimate the build-up of financial fragility around the financial crisis in 2008.

4.1 Estimation Approach, Particle Filter and Data

The model is taken to the data to obtain a structural estimate of the endogenous build-up of financial fragility and economic downside risk in the U.S. around the great financial crisis. However, an estimation is very challenging because it requires to repeatedly solve the nonlinear model with global methods and then to filter it. The time to solve and filter the model only once is around 2h55m using an Intel Xeon W-2295 processor with 18 cores.

To overcome this challenge, I apply a two-step procedure for the estimation. In the first step, the nonlinear model is calibrated to key moments, as already done in Section 3.1. Targeting key moments in the calibration results in a model that is well equipped to be taken to the data, while lowering the number of times that the model needs to be solved. The calibrated model is then used as input for the particle filter in the second step. The estimation strategy employs a particle filter to account for the nonlinear setup with endogenous runs and the ZLB. The filter retrieves the sequence of the shocks including the sunspot shock using the parameterized model. This sequence can, in turn, be used to obtain other objects of interest such as the estimated probability of a run. Importantly, this approach provides an estimate of financial fragility, while reducing the computational burden significantly.

I adapt the particle filter to specifically take into account the multiplicity of equilibria similar to Aruoba et al. (2018).[18] To account for endogenous runs, I extend their approach to handle not only multiplicity of equilibria, but also the state-dependence of the equilibria probabilities. The filter estimates the hidden states and shocks based on a set of observables. It is convenient to cast the model in a nonlinear state-space representation as a starting point:

$$\mathbb{X}_t = f(\mathbb{X}_{t-1}, v_t, \iota_t), \quad \text{and} \quad \mathbb{Y}_t = g(\mathbb{X}_t) + u_t. \tag{20}$$

The first set of equations contains the transition equations that depend on the state variables $\mathbb{X}_t$, the structural shocks v_t and the sunspot shock ι_t. In particular, the state variables and shocks determine endogenously the selected equilibrium of the model. The nonlinear functions f are obtained from the model that is solved with time iteration. The second set of equations contains the measurement equations, which connect the state variables with the observables $\mathbb{Y}_t$. It also includes an additive measurement error u_t.[19] The particle filter extracts a sequence of conditional distributions for the structural and sunspot shocks, which provides the empirical implications of the model. Thereby, the filter evaluates when a run occurs and provides the run probability. The algorithm is laid out in Appendix E.

The considered horizon stretches from 1985:Q1 to 2014:Q4. The observables are real GDP growth and shadow bank leverage, as used in the calibration. The observation equation is:

$$\begin{bmatrix} \text{Output Growth}_t \\ \text{Leverage}_t \end{bmatrix} = \begin{bmatrix} 100 \ln\left(\frac{Y_t}{Y_{t-1}}\right) \\ \phi_t \end{bmatrix} + u_t, \tag{21}$$

where GDP growth is quarterly and demeaned. The measurement error is $u_t \sim N(0, \Sigma_u)$. Its variance Σ_u is set to 25% of the sample variance, similar to Gust et al. (2017).

[18] The filter algorithm is also based on Atkinson et al. (2020) and Herbst and Schorfheide (2015).

[19] The particle filter requires a measurement error to avoid a degeneracy of the likelihood function. Another advantage is that it can take into account noisy data, which might be a concern for shadow bank leverage.

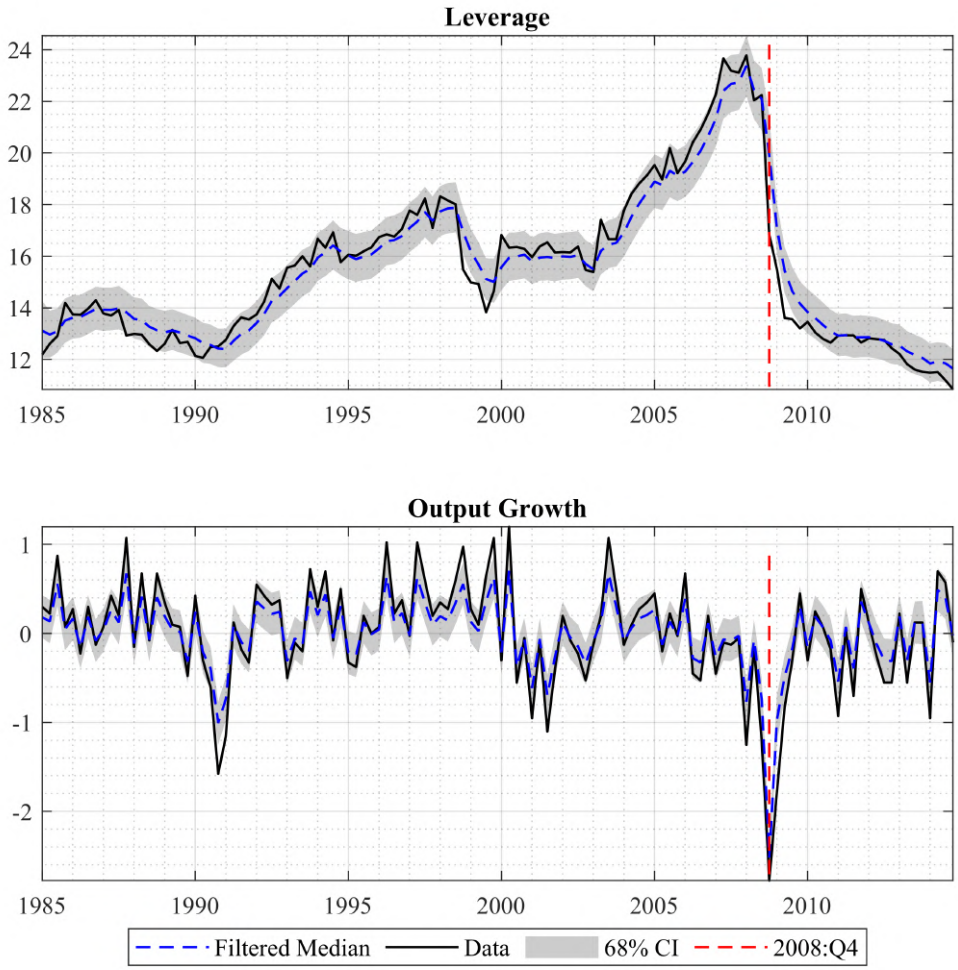

Figure 4: Filtered median of leverage and output growth is the blue line together with its 68% confidence interval. The observables are shadow bank leverage and (de-meaned) real quarter-on-quarter output growth. The red line corresponds to the fourth quarter of 2008:Q4.

4.2 Results

To establish that the filtered model captures the fluctuations in the observables, Figure 4 compares the estimated sequence for leverage and output against the data. In line with the data, leverage increases substantially prior to the financial crisis. The peak comes in 2008:Q1, with leverage close to 24. The filtered path also takes account of the strong decrease in output and leverage in the fourth quarter of 2008. Crucially, the model can account for this sharp drop in the fourth quarter of 2008 via two different channels: a run on the financial sector or large contractionary shocks. As the equilibria are not exogenously imposed, the particle filter selects the regime depending on the fit with the data. This gives an assessment if a run took place. The model clearly favors a run. The filter assigns a weight of 98% to a run in 2008:Q4, while the weight of the run regime is almost 0% in all other periods.

Bernanke (2018) and Gorton and Metrick (2012) argue that the run on the financial sector is behind the sharp and large economic contraction. To assess this through the lens of the

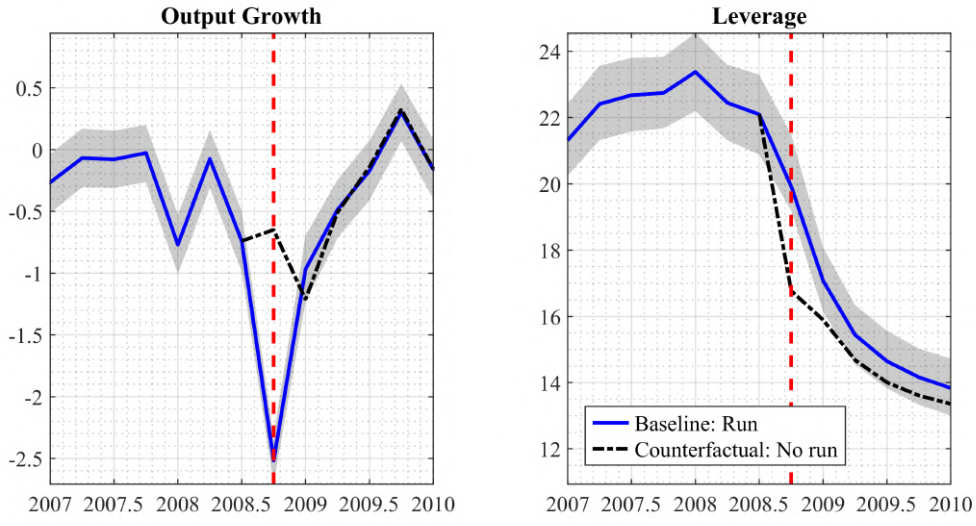

Figure 5: Comparison of baseline estimate to a counterfactual scenario without a run. The baseline median (blue line with its 68% confidence interval) is compared to the counterfactual median, where no sunspot shock materializes in 2008:Q4.

model, a counterfactual shown in Figure 5 compares the estimated path to a hypothetical scenario without a run (no sunspot shock in 2008:Q4). The main take-away is that the contraction would have been much smaller since the run alone accounts for 70% of the drop.

Figure 6 shows the filtered series for key variables. The estimation predicts a credit boom gone bust, a countercyclical finance premium and a period of low inflation after the run, which is line with the empirical evidence. The dynamics of volatility and TFP allow to inspect the economic drivers behind the run in 2008:Q4. A series of shocks reduces volatility σ_t prior to the financial crisis. In the spirit of the volatility paradox, this period sows the seed of a crisis as leverage and financial fragility increase. In 2008:Q4, contractionary volatility and TFP shocks in combination with a sunspot shock trigger the run.

The approach provides a novel model-implied estimate of financial fragility. The upper plot of Figure 7 shows the path of the estimated run probability p_t. While there is a slight increase around 1998, financial fragility starts to surge from 2005 onwards considerably. Thus, the model suggests that that there had already been a substantial build-up of fragilities a few years prior to the outbreak of the financial crisis. The median one-quarter-ahead forecast peaks in 2007:Q4 at around 8%, which is more than 25% in annualized terms. Note that the run probability is going down in shortly before the run as the level of leverage is slightly lower than at its peak.

A counterfactual analysis can disentangle the structural sources of financial fragility. The estimated series of TFP and volatility are evaluated in isolation by setting the other shock to zero for the entire horizon. While the volatility shock is the main driver, explaining most of the fragility in 2008, TFP causes no financial fragility. But, there are relevant nonlinear interaction between the shocks that can increase or decrease financial fragility. Importantly, financial fragility induces substantial macroeconomic downside risk. In fact, the multiplicity of equilibria due to the run characterizes macroeconomic risk as a multimodal distribution as in the empirical papers of Adrian et al. (2021), Caldara et al. (2021) and Mitchell et al.

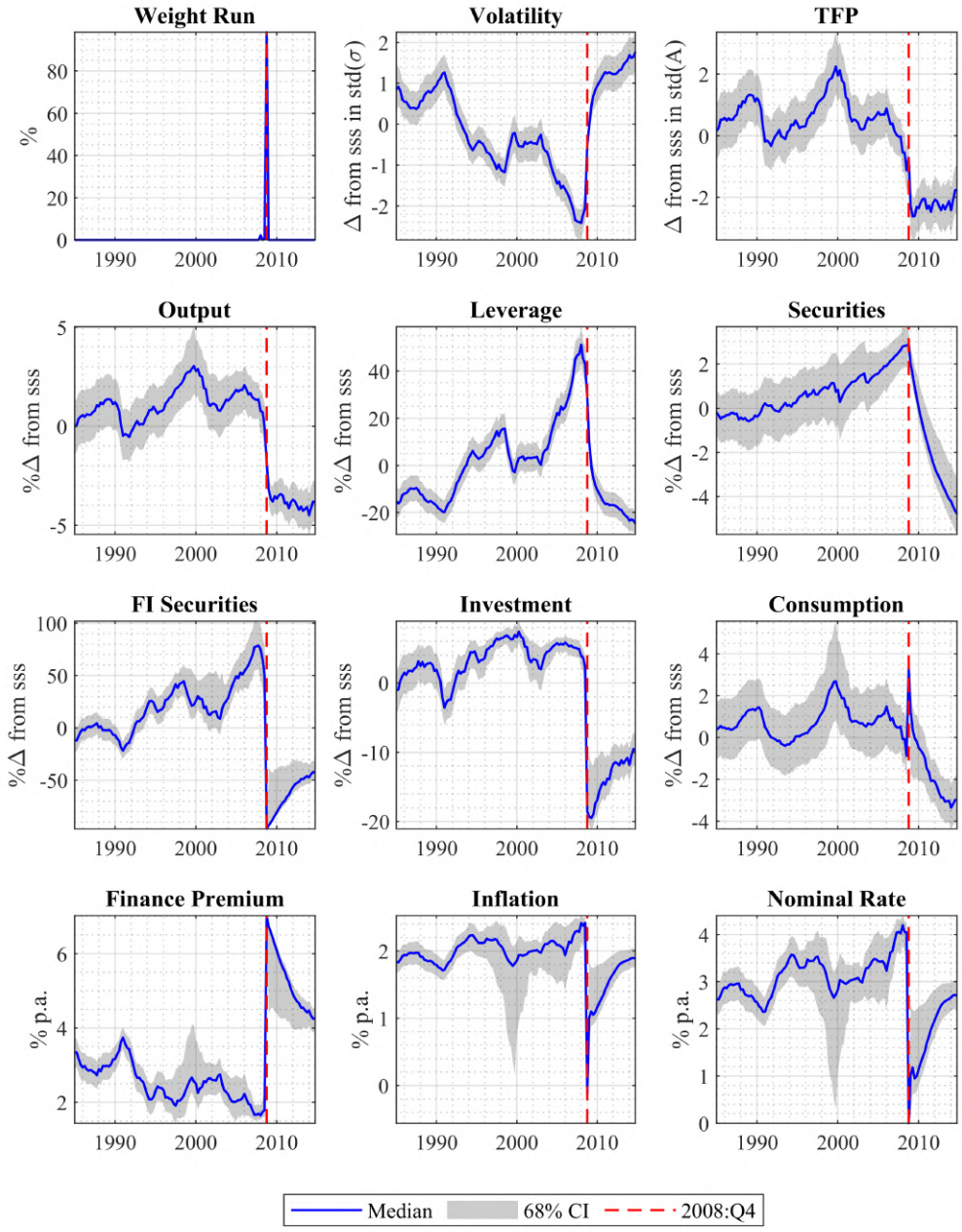

Figure 6: Filtered median with its 68% confidence interval for selected variables. The first plot shows the regime selection. The second and third plot show the exogenous drivers volatility and TFP. The remaining plots show other key variables. Note that for the third plot the weight of the run regime is shown. The red line indicates the fourth quarter of 2008. The scales are either percentage deviations from the stochastic SS, deviations from the stochastic SS measured in the unconditional variance of the variables for the two shocks, annualized percent, percent, or the level.

(2021). Appendix F.2 elaborates more on tail risk and multimodality.

I compare the model-implied filtered volatility series with a data proxy. Specifically, I use the volatility measure of Nuño and Thomas (2017), which is the cross-sectional variance of

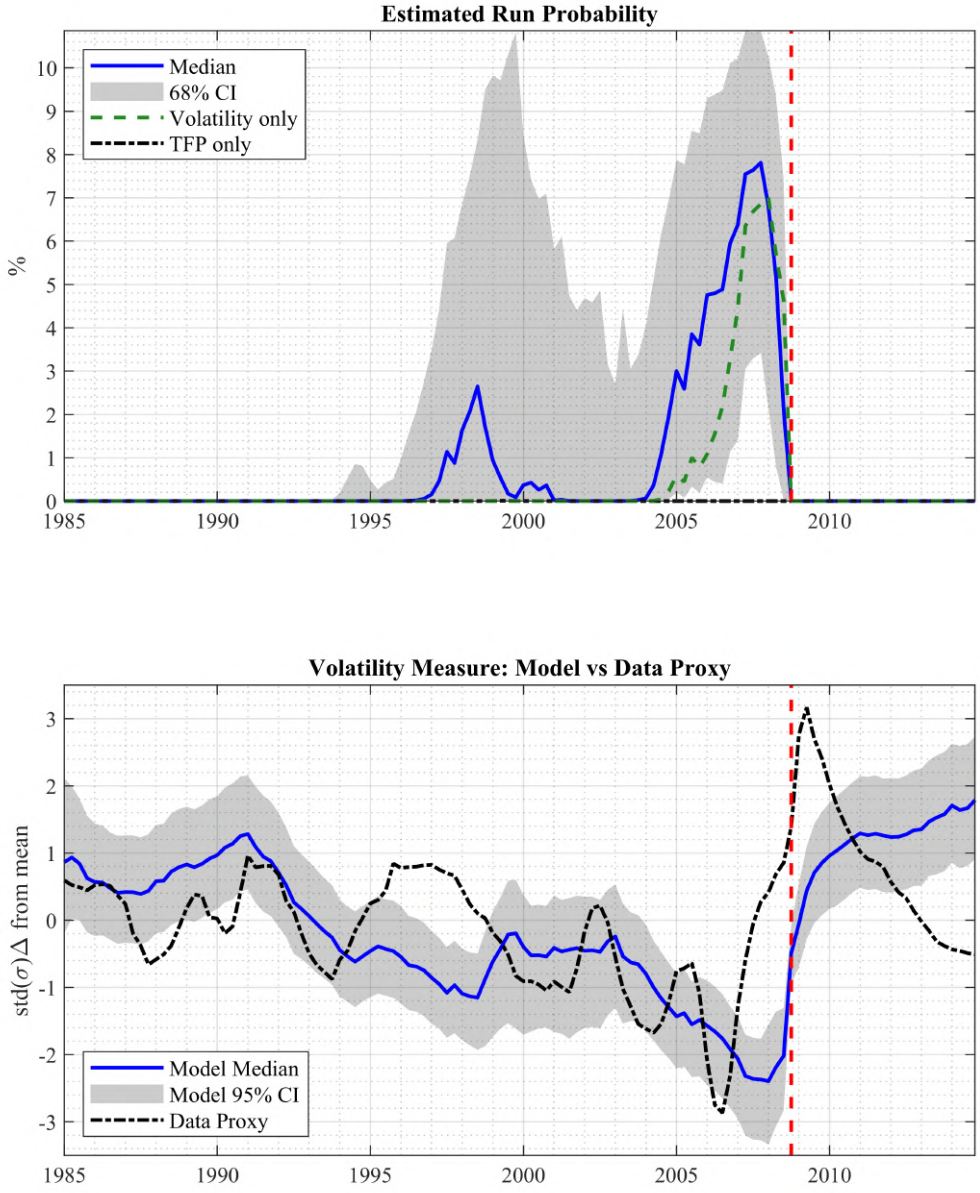

Figure 7: Run probability and external validation of the estimation. The upper plot shows the filtered median run probability p_t for t+1 with its 68% confidence interval measured in percent (%). To disentangle the impact of the structural shocks, the realizations of the volatility shock and TFP shock are set to 0 one at a time. The dashed green line and black dash-dotted line show the scenario using only the extracted volatility shocks and TFP shocks, respectively. The lower plot compares the filtered volatility series (blue solid line) with its 95% CI (grey shaded area) to a data proxy, which is a measure of cross-sectional variance of industry level TFP (black dashed line). The deviations from each volatility series mean are measured in their respective unconditional standard deviation. The red line indicates the fourth quarter of 2008.

industry level TFP based on data from the National Bureau of Economic Research and the US Census Bureau's Center for Economic Studies.[20] The filtered structural volatility series and the data proxy are shown in the lower plot of Figure 7. The key result is that both series comove most of the time, which provides an external validation to the dynamics of the volatility shock and the estimation in general. Both series suggest a drop in volatility during the early 2000s which then peaks before the financial crisis. During the financial crisis, there is a sharp increase in the volatility measure.

I also include three alternative specifications. First, I include the credit spread as additional observable in the observation equation. One advantage of the particle filter is that it can handle more observables than shocks. Second, I use a lower measurement error of 10% for the particle filter. The dynamics are quite similar for both checks. Even though there are some changes in the filtered series, the estimated probability of a run still predicts a strong build-up before 2008 and that the run itself occurred in 2008:Q4. The third check is a scenario, in which no shocks hit the economy after 2009. This points out that the model predicts a faster recovery than the data. The details are in Appendix F.1.

5 Monetary and Macroprudential Policies

There is an active debate about the costs and benefits of alternative monetary and macroprudential policies. I provide a novel perspective through the lens of the nonlinear model.

5.1 Monetary Policy and Financial Stability

Monetary policy can respond to financial conditions, which can be distinguished in interventions before (ex-ante) and after (ex-post) the crisis. Monetary policy can act in advance and lean-against-the-wind by raising rates during a boom. The second element is that monetary policy can commit to respond after the crisis by being more loose to "clean up". To begin with, the considered monetary policy rule features both elements. The central bank responds deviations of the level of security holdings relative to a target value. The monetary rule responding to financial conditions can be expressed as:

$$R_t^I = \max\left\{R^I\left(\frac{\Pi_t}{\Pi}\right)^{\kappa_\Pi}\left(\frac{\varphi_t^{mc}}{\varphi^{mc}}\right)^{\kappa_y}\left(\frac{S_t^B}{S^B}\right)^{\kappa_s}, 1\right\}, \tag{22}$$

where κ_s is the response to deviations from the target value S^B. The target value S^B is set to the median level of the intermediaries' security holdings in the baseline economy.

The financial stability and welfare impact is theoretically ambiguous. A rate hike during a boom can lead to a substitution towards more equity. The hike also reduces total securities and lowers the intermediaries' share of securities, resulting in enhanced financial resilience. At the same time, the increased funding cost due to higher rates can also result in less loss absorbing capacities, creating financial fragility. A rate cut during or after a run can stabilize

[20] The construction follows Nuno and Thomas (2017). I extend the series until 2014:Q4 to match the horizon of the quantitative exercise. The obtained series is then linearly detrended.

the economy. If the central bank can credibly commit to a loose policy stance ex-post, such a commitment can even alter the existence of the run equilibrium. However, this commitment can also incentivize risk-taking and the accumulation of assets in the first place.

The welfare impact of this rule is illustrated in the upper plot of Figure 8, where the response strength (κ_s) is varied. The welfare-maximizing rule, located at $\kappa_s^{opt} = 0.0102$, implies a substantial welfare gain of 0.57% in terms of consumption equivalents. The optimal rule is so effective that it reduces the run frequency to nearly zero.[21] Initially, a higher κ_s increases welfare because the monetary interventions reduce the financial risk. However, the gains start to reverse after reaching the peak at κ_s^{opt}. Raising κ_s further results in a too large accumulation of total securities, which makes the economy again more prone to runs and lowers welfare. This creates a hump-shaped welfare curve.

Does the success of the policy stem from the ex-ante leaning or the commitment for a loose ex-post policy stance? The two components can be analyzed separately. A policy with only the ex-ante leaning component has a positive, albeit small, impact on financial stability and welfare. The run probability is slightly reduced to 1.8% (from 1.9%), while welfare increases only by 0.05% in consumption equivalents. In contrast to this, a credible commitment to an ex-post loosening provides most of the welfare and stability gains. However, this requires a credible commitment from the central bank that is also understood by the economic actors. This finding also relates to Devereux et al. (2019), who evaluate the gains of a credible commitment in the context of sudden stops. More details can be found in Appendix G.1.

The impact of the ex-ante leaning policy is limited in the model, while the empirical study of Schularick et al. (2021) even suggests that rate hikes may actually increase crisis risk. To delve deeper, I examine how an unanticipated monetary policy shock affects financial stability during a boom. The following simulation assesses the transmission of an unanticipated rate hike during a boom. A sequence of one-standard-deviation negative volatility shocks hits the economy in period 1 until period 8. The monetary shock, which is normalized to an annualized 25 basis points, occurs in period 5. Figure 8 shows the percentage points difference in the run probability relative to a scenario without the monetary shock. Initially, the shock increases financial fragility. The true run probability, that is if the unanticipated shock would have been known, increases by an additional 0.4% percentage points in period 4. This effect then reverses and financial stability improves as a result of the monetary policy hike.[22] This trade-off between triggering a crisis in the short-term versus financial stability in the medium-term is also supported empirically by Ajello and Pike (2022). Appendix G.2 contains more details on the shock's transmission.

5.2 Macroprudential Policy and Financial Stability

To put the gains of monetary policy in context, I analyze the stability and welfare implications of a corresponding macroprudential policy. The focus is on a state-dependent leverage tax, which taxes or subsidizes the intermediaries' deposit holdings. Even though regulating the

[21] The model does not include some shocks (e.g. markup), which could reduce κ_s^{opt} and the rule's impact.
[22] This is a one-time shock. It takes longer until the run probability reverses for a more persistent shock.

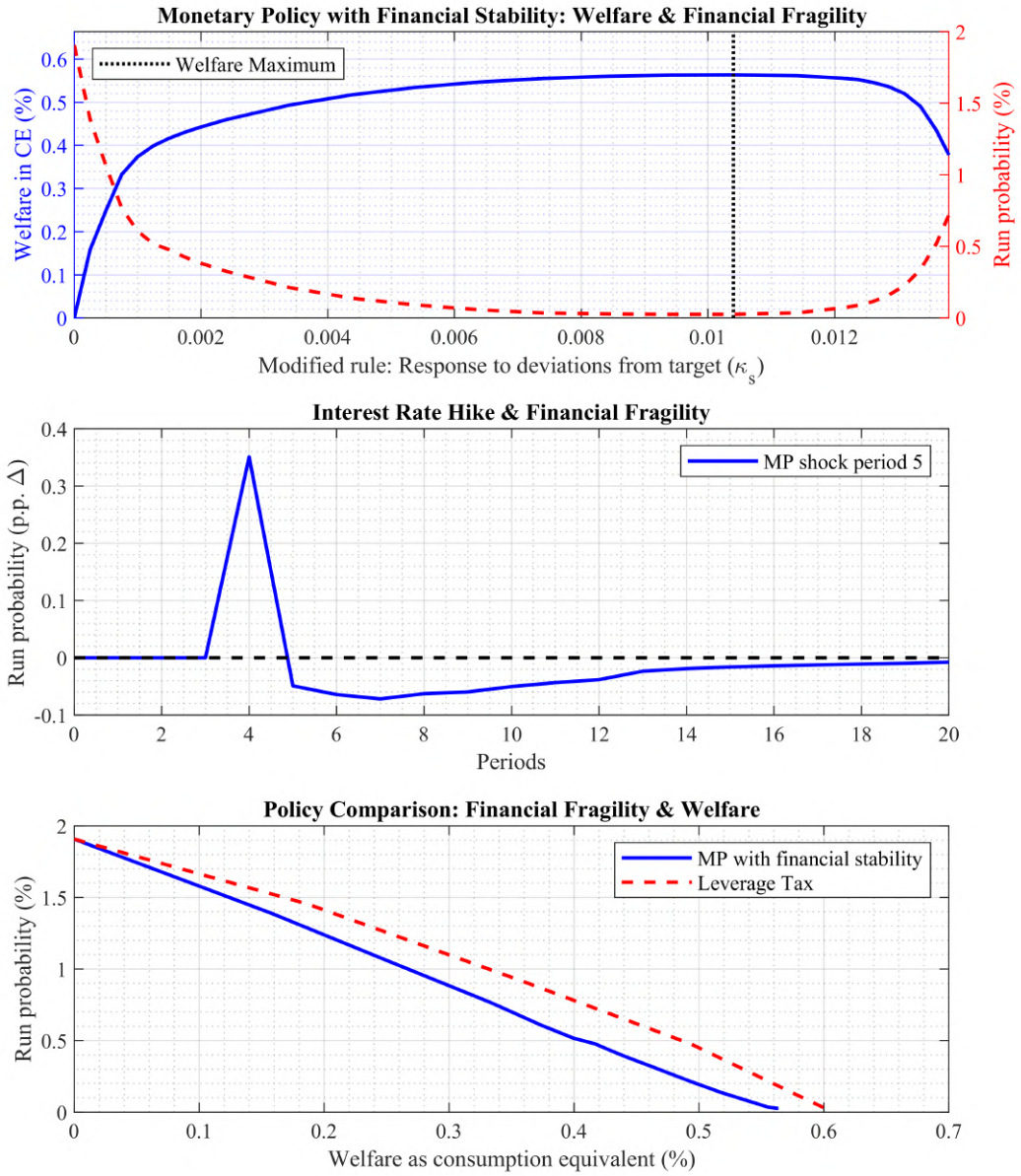

Figure 8: The upper plot shows the impact of varying the response of monetary policy with financial stability considerations (κ_s) on welfare (left axis) and the annual run probability (right axis). The dashed black line indicates the welfare-maximizing rule (κ_s^{opt}). The center plot shows the impact of an unanticipated monetary policy shock (25 bps) on the run probability during a boom scenario. The percentage points difference in the run probability relative to a scenario without a monetary policy shock is displayed. To generate the boom scenario, a sequence one-standard-deviation negative volatility shocks hits the economy in period 1 until period 8. Afterwards, no shock materializes. The lower plot shows the annual run probability-welfare-frontier for monetary policy with financial stability considerations for $\kappa_s \in [0, \kappa_s^{opt}]$. It is compared to the frontier of the leverage tax for $\tau_s \in [0, 0.012]$.

unregulated part of the financial sector is in practice potentially extremely difficult, the tax outlines the gains of macroprudential policy targeted at shadow banks. Furthermore, the gains of the macroprudential instrument provide a benchmark for monetary policy.

The leverage tax τ_t^{ϕ} requires the banker to pay a tax or receive a subsidy at the end of the period for its borrowings from households: $N_t = R_t^K Q_{t-1} S_{t-1}^B - R_{t-1}^D D_{t-1} - \tau_t^{\phi} D_{t-1} + \tau_t^L$. The intermediaries receive a lump sum transfer τ_t^L, which is chosen in a way that the leverage tax is budget neutral for each intermediary. Even though the tax is budget neutral in the end, the leverage tax still alters the intermediaries' problem and thus leverage decision.

The macroprudential authority responds to the security holdings of intermediaries similar to monetary rule. If the securities are above a target value, the central bank raises the tax. If the intermediaries hold only few securities, it increases the subsidy. The rule τ_t^{ϕ} is:

$$\tau_t^{\phi} = \left(\frac{S_t^B}{S^B}\right)^{\tau_s} - 1, \tag{23}$$

where τ_s is the response to deviations from the target value S^B set by the macroprudential authority. The target value S^B is calibrated to the same value as in the monetary rule.

To compare the policies, the lower plot of Figure 8 shows the combination of run probability and welfare for all $k_s \in [0, \kappa_s^{opt}]$ and $\tau_s \in [0, \tau_s^{up}]$, where τ_s^{up} is the lowest value that reduces the run frequency to zero. This shows that macroprudential policy has a superior stabilization-welfare combination, as the line is more outward. Furthermore, a forceful leverage tax can reduce the run probability to exactly zero. Nevertheless, monetary policy can be a good substitute. This is especially important because the advantage of monetary policy is that it gets in all of the cracks that macroprudential policy and supervision fail to reach.

However, there is an import caveat to this result. Ex-ante macroprudential policy in isolation can be quite effective in increasing financial stability. This is discussed in Appendix G.3 and aligns with Gertler et al. (2020a). This results contrasts with the findings for monetary policy, where the ex-ante effects were considerably smaller. Thus, monetary policy can be a good substitute for macroprudential policy only if the authorities can credibly commit to an ex-post looser policy stance.

5.3 Counterfactual Policy Analysis and the Financial Crisis in 2008

The policies can now be used to conduct a counterfactual scenario for the estimated financial fragility. Based on the sequence of distribution of shocks from the particle filter, an alternative scenario with adjusted policy functions can be studied. The filtered shocks are fed into the adapted model to calculate the counterfactual evolution of the economy.

Specifically, I evaluate if the welfare-maximizing monetary rule that responds to financial conditions (κ_s^{opt}) would have mitigated the estimated run probability and prevented the run in 2008. Figure 9 summarizes the counterfactual path. The build-up of financial fragility is now almost completely contained as it stays basically at zero. Furthermore, the run does not take place so that output decreases now only by 0.5% instead of 2.5% in 2008:Q4. Thus, the counterfactual scenario underlines the large financial stability gains and suggests that

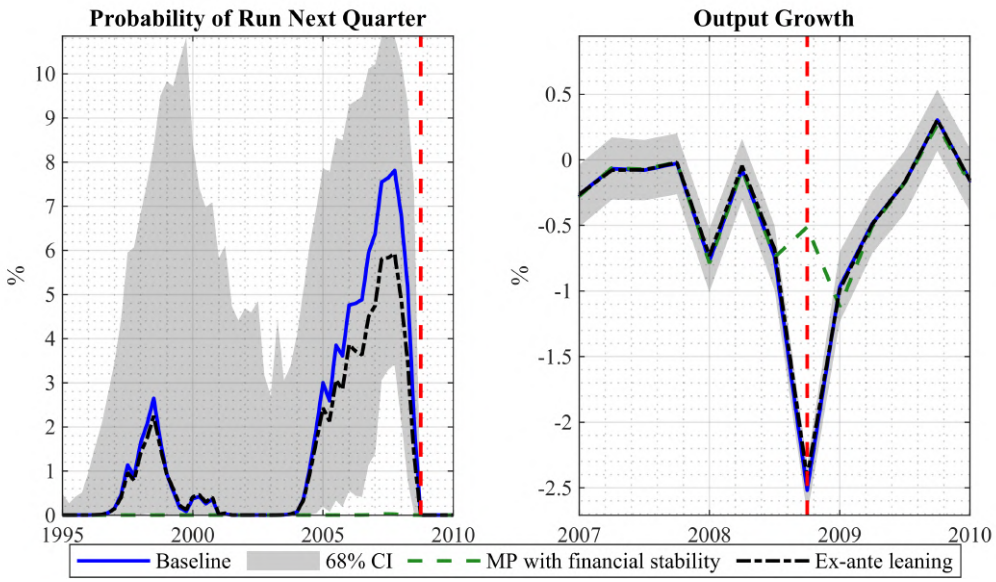

Figure 9: Counterfactual policy analysis of monetary policy with financial considerations. The filtered median probability of a run in the next quarter and output growth (solid blue) with its 68% confidence interval is shown for the baseline scenario. Using the estimated shocks, the median for the counterfactual scenario of the modified monetary policy with monetary policy with financial considerations (dashed green) and the scenario with only ex-ante leaning is shown (dash-dotted black). The red line indicates the fourth quarter of 2008.

monetary policy could have helped to avoid the run. However, this result depends again on the ex-post commitment. A scenario with only ex-ante leaning does not succeed in averting the financial crisis as the stabilization impact is insufficient. The run probability peaks at a slightly lower level, but output still declines by around 2.5% due to the occurrence of the run. Thus, an ex-ante leaning policy alone would have likely had only a limited impact. The outlined strategy is general and can be used for a range of alternatives policies.

6 Conclusion

I investigate the endogenous build-up of financial fragility with a new nonlinear macroeconomic model. The combination of volatility shocks and risk-shifting incentives accounts for key macroeconomic and financial features. I then take the model to data to obtain a novel structural estimate of financial fragility. The estimation suggests an considerable increase in financial fragility from 2005 onwards that ends up in a run in 2008. Finally, I show that the zero lower bound entails substantial welfare costs and use counterfactual simulations to assess whether monetary policy could have averted the run in 2008.

References

Adrian, T., Boyarchenko, N., Giannone, D., 2019. Vulnerable growth. American Economic Review 109, 1263–89.

Adrian, T., Boyarchenko, N., Giannone, D., 2021. Multimodality in macrofinancial dynamics. International Economic Review 62, 861–886.

Adrian, T., Colla, P., Shin, H., 2013. Which financial frictions? parsing the evidence from the financial crisis of 2007 to 2009. NBER Macroeconomics Annual 27, 159–214.

Adrian, T., Duarte, F., Liang, N., Zabczyk, P., 2020. Nkv: A new keynesian model with vulnerability. AEA Papers and Proceedings 110, 470–76.

Adrian, T., Shin, H.S., 2010. Liquidity and leverage. Journal of Financial Intermediation 19, 418–437.

Adrian, T., Shin, H.S., 2014. Procyclical leverage and value-at-risk. The Review of Financial Studies 27, 373–403.

Ajello, A., Pike, T., 2022. Getting in All the Cracks: Monetary Policy, Financial Vulnerabilities, and Macro Risk. Technical Report. mimeo.

Amador, M., Bianchi, J., 2021. Bank Runs, Fragility, and Credit Easing. Working Paper 29397. National Bureau of Economic Research.

Ang, A., Hodrick, R.J., Xing, Y., Zhang, X., 2006. The cross-section of volatility and expected returns. The Journal of Finance 61, 259–299.

Aruoba, B., Cuba-Borda, P., Schorfheide, F., 2018. Macroeconomic dynamics near the zlb: A tale of two countries. The Review of Economic Studies 85, 87–118.

Aruoba, S.B., Cuba-Borda, P., Higa-Flores, K., Schorfheide, F., Villalvazo, S., 2021. Piecewise-linear approximations and filtering for dsge models with occasionally-binding constraints. Review of Economic Dynamics 41, 96–120.

Atkinson, T., Richter, A.W., Throckmorton, N.A., 2020. The zero lower bound and estimation accuracy. Journal of Monetary Economics 115, 249–264.

Benhabib, J., Schmitt-Grohé, S., Uribe, M., 2001. Monetary policy and multiple equilibria. American Economic Review 91, 167–186.

Bernanke, B., 2018. The real effects of the financial crisis. Brookings Papers on Economic Activity 2018, 251–342.

Bernanke, B.S., Gertler, M., Gilchrist, S., 1999. The financial accelerator in a quantitative business cycle framework. Handbook of Macroeconomics 1, 1341–1393.

Bianchi, F., Melosi, L., Rottner, M., 2021. Hitting the elusive inflation target. Journal of Monetary Economics 124, 107–122.

Bocola, L., Dovis, A., 2019. Self-fulfilling debt crises: A quantitative analysis. American Economic Review 109, 4343–77.

Boissay, F., Collard, F., Smets, F., 2016. Booms and banking crises. Journal of Political Economy 124, 489–538.

Bordalo, P., Gennaioli, N., Shleifer, A., 2018. Diagnostic expectations and credit cycles. The Journal of Finance 73, 199–227.

Boz, E., Mendoza, E.G., 2014. Financial innovation, the discovery of risk, and the us credit crisis. Journal of Monetary Economics 62, 1–22.

Brunnermeier, M.K., 2009. Deciphering the liquidity and credit crunch 2007-2008. Journal of Economic Perspectives 23, 77–100.

Brunnermeier, M.K., Sannikov, Y., 2014. A macroeconomic model with a financial sector. American Economic Review 104, 379–421.

Caldara, D., Cascaldi-Garcia, D., Cuba-Borda, P., Loria, F., 2021. Understanding Growth-at-Risk: A Markov-Switching Approach. Technical Report. Mimeo.

Chetty, R., Guren, A., Manoli, D., Weber, A., 2011. Are micro and macro labor supply elasticities consistent? a review of evidence on the intensive and extensive margins. American Economic Review 101, 471–75.

Christiano, L.J., Motto, R., Rostagno, M., 2014. Risk shocks. The American Economic Review 104, 27–65.

Cole, H.L., Kehoe, T.J., 2000. Self-fulfilling debt crises. The Review of Economic Studies 67, 91–116.

Cooper, R., Corbae, D., 2002. Financial collapse: A lesson from the great depression. Journal of Economic Theory 107, 159–190.

Darracq Pariès, M., Kok, C., Rottner, M., 2020. Reversal interest rate and macroprudential policy. Working Paper Series 2487. European Central Bank.

De Groot, O., 2021. A financial accelerator through coordination failure. The Economic Journal 131, 1620–1642.

Devereux, M.B., Young, E.R., Yu, C., 2019. Capital controls and monetary policy in sudden-stop economies. Journal of Monetary Economics 103, 52–74.

Diamond, D.W., Dybvig, P.H., 1983. Bank runs, deposit insurance, and liquidity. Journal of Political Economy 91, 401–419.

Faria-e-Castro, M., 2019. A Quantitative Analysis of Countercyclical Capital Buffers. Working Paper 8D. FRB St. Louis.

Fernald, J., 2014. A quarterly, utilization-adjusted series on total factor productivity. Working Paper 2012-19. Federal Reserve Bank of San Francisco.

Fernández-Villaverde, J., Rubio-Ramírez, J.F., 2007. Estimating macroeconomic models: A likelihood approach. The Review of Economic Studies 74, 1059–1087.

Ferrante, F., 2018. A model of endogenous loan quality and the collapse of the shadow banking system. American Economic Journal: Macroeconomics 10, 152–201.

Ferrante, F., 2019. Risky lending, bank leverage and unconventional monetary policy. Journal of Monetary Economics 101, 100–127.

Gallin, J., 2015. Shadow Banking and the Funding of the Nonfinancial Sector, in: Measuring Wealth and Financial Intermediation and Their Links to the Real Economy. National Bureau of Economic Research, Inc. NBER Chapters, pp. 89–123.

Garbade, K., 2006. The evolution of repo contracting conventions in the 1980s. Economic Policy Review 12.

Gertler, M., Kiyotaki, N., 2015. Banking, liquidity, and bank runs in an infinite horizon economy. American Economic Review 105, 2011–43.

Gertler, M., Kiyotaki, N., Prestipino, A., 2016. Wholesale banking and bank runs in macroeconomic modeling of financial crises, in: Handbook of Macroeconomics. volume 2, pp. 1345–1425.

Gertler, M., Kiyotaki, N., Prestipino, A., 2020a. Credit booms, financial crises, and macroprudential policy. Review of Economic Dynamics 37, S8–S33.

Gertler, M., Kiyotaki, N., Prestipino, A., 2020b. A macroeconomic model with financial panics. The Review of Economic Studies 87, 240–288.

Gorton, G., Metrick, A., 2012. Securitized banking and the run on repo. Journal of Financial Economics 104, 425–451.

Gorton, G., Ordonez, G., 2020. Good booms, bad booms. Journal of the European Economic Association 18, 618–665.

Guerrieri, V., Lorenzoni, G., 2017. Credit crises, precautionary savings, and the liquidity trap. The Quarterly Journal of Economics 132, 1427–1467.

Gust, C., Herbst, E., López-Salido, D., Smith, M.E., 2017. The empirical implications of the interest-rate lower bound. American Economic Review 107, 1971–2006.

Hakamada, M., 2021. Risk Taking, Banking Crises, and Macroprudential Monetary Policy. Technical Report. Mimeo.

He, Z., Kelly, B., Manela, A., 2017. Intermediary asset pricing: New evidence from many asset classes. Journal of Financial Economics 126, 1–35.

He, Z., Khang, I.G., Krishnamurthy, A., 2010. Balance sheet adjustments during the 2008 crisis. IMF Economic Review 58, 118–156.

Herbst, E.P., Schorfheide, F., 2015. Bayesian estimation of DSGE models. Princeton University Press.

Ikeda, D., Matsumoto, H., 2021. Procyclical Leverage and Crisis Probability in a Macroeconomic Model of Bank Runs. Discussion Paper Series 21-E-01. Institute for Monetary and Economic Studies, Bank of Japan.

Jermann, U., Quadrini, V., 2012. Macroeconomic effects of financial shocks. American Economic Review 102, 238–71.

Jordà, Ò., Schularick, M., Taylor, A.M., 2017. Macrofinancial history and the new business cycle facts. NBER Macroeconomics Annual 31, 213–263.

Justiniano, A., Primiceri, G.E., Tambalotti, A., 2019. Credit supply and the housing boom. Journal of Political Economy 127, 1317–1350.

Kitagawa, G., 1996. Monte carlo filter and smoother for non-gaussian nonlinear state space models. Journal of computational and graphical statistics 5, 1–25.

Krishnamurthy, A., Muir, T., 2017. How credit cycles across a financial crisis. Technical Report. National Bureau of Economic Research.

López-Salido, J.D., Loria, F., 2020. Inflation at Risk. Finance and Economics Discussion Series 2020-013. Federal Reserve Board.

Mikkelsen, J., Poeschl, J., 2019. Banking Panic Risk and Macroeconomic Uncertainty. Working Paper No. 149. Danmarks Nationalbank.

Mitchell, J., Poon, A., Zhu, D., 2021. Constructing density forecasts from quantile regressions: Multimodality in macroeconomic dynamics .

Nuño, G., Thomas, C., 2017. Bank leverage cycles. American Economic Journal: Macroeconomics 9, 32–72.

Paul, P., 2020. A macroeconomic model with occasional financial crises. Journal of Economic Dynamics and Control 112, 103830.

Poeschl, J., 2020. The Macroeconomic Effects of Shadow Banking Panics. Working Paper No. 158. Danmarks Nationalbank.

Richter, A.W., Throckmorton, N.A., Walker, T.B., 2014. Accuracy, speed and robustness of policy function iteration. Computational Economics 44, 445–476.

Schularick, M., Steege, L.t., Ward, F., 2021. Leaning against the wind and crisis risk. American Economic Review: Insights 3, 199–214.

Schularick, M., Taylor, A.M., 2012. Credit booms gone bust: Monetary policy, leverage cycles, and financial crises, 1870-2008. American Economic Review 102, 1029–61.

A Data: Shadow Bank Leverage

The leverage series in this paper uses book equity, which is the difference between the value of the portfolio and liabilities of financial intermediaries. An alternative measure is the financial intermediaries' market capitalization (e.g. market valuation of financial intermediaries). Book equity is the appropriate concept in this context because the interest lies with credit supply and financial intermediaries' lending decisions, as stressed for instance in Adrian and Shin (2014).[23] In contrast to this, market capitalization is the appropriate measure when considering the issuance of new shares or acquisition decisions (Adrian et al., 2013). In the context of the model, the occurrence of a run also depends on book equity, which rationalizes this choice. With that in mind, book leverage based on book equity is the appropriate concept for my purposes.

A related issue is that marked-to-market value of book equity, which is the difference between the market value of portfolio claims and liabilities of financial intermediaries, is conceptually very different from market capitalization. As argued in Adrian and Shin (2014), the book value of equity should be measured as marked-to-market. In such a case, the valuation of the assets is based on market values. Importantly, the valuation of assets is marked-to-market in the balance sheet of financial intermediaries that hold primarily securities (Adrian and Shin, 2014). Crucially, the concept of marked-to-market value of book equity corresponds to the approach to leverage adopted in the model as the value of the securities depends on their market price. Therefore, I am interested in marked-to-market book leverage.

U.S. Flow of Funds The leverage measure for shadow banks uses U.S. Flow of Funds balance sheet data for security brokers and dealers and finance companies similar to Nuño and Thomas (2017).[24]

Equity is computed as the difference between book assets and book liabilities for both types of financial intermediaries:

$$\textit{Equity Brokers \& Dealers}_t = \textit{Assets Brokers \& Dealers}_t - \textit{Liabilities Brokers \& Dealers}_t \tag{24}$$

$$\textit{Equity Finance Companies}_t = \textit{Assets Finance Companies}_t - \textit{Liabilities Finance Companies}_t \tag{25}$$

The aggregate leverage measure is then defined as:

$$\textit{Leverage}_t = \frac{\textit{Assets Finance Companies}_t + \textit{Assets Brokers \& Dealers}_t}{\textit{Equity Finance Companies}_t + \textit{Equity Security Brokers \& Dealers}_t}. \tag{26}$$

Compustat An alternative measure of book leverage of the shadow banking sector can be constructed with individual balance sheet data from Compustat. I include financial firms that are classified with SIC codes between 6141 - 6172 and 6199 - 6221. This set contains credit institutions, business credit institutions, finance lessors, finance services, mortgage bankers

[23] He et al. (2010) and He et al. (2017) provide an opposing view with an emphasis on market leverage.
[24] The time series are adjusted for discontinuities and breaks in the data.

and brokers, security brokers, dealers and flotation companies, and commodity contracts brokers and dealers.[25]

Equity is computed as the difference between book assets and book liabilities for each firm:

$$Equity_{i,t} = Book\ Assets_{i,t} - Book\ Liabilities_{i,t}. \tag{27}$$

The leverage of the shadow banking sector is then defined as

$$Leverage_t = \frac{\sum_i Book\ Assets_{i,t}}{\sum_i Book\ Equity_{i,t}}, \tag{28}$$

where I sum up equity and assets over the different entities.

[25]Finance lessors and finance services with the SIC codes 6172 and 6199 are not official SIC codes, but are used by the U.S. Securities and Exchange Commission.

B Model: Equations, Derivations and Equilibrium

This section contains a description of all equilibrium equations and the equilibrium definition, a graphical characterization of the risk-shifting incentives, the formal derivation of the financial intermediary's problem including some simulations and a graphical characterization of the endogenous run problem.

B.1 Equations and Equilibrium

The system of equations that characterizes the economy is described below.

Households

$$C_t = W_t L_t + D_{t-1} R_t - D_t + \Xi_t + Q_t S_t^H + (Z_t + (1-\delta) Q_t) S_{t-1}^H, \tag{29}$$

$$\varrho_t = (C_t)^{-\sigma}, \tag{30}$$

$$\varrho_t W_t = \chi L_t^{\varphi}, \tag{31}$$

$$1 = \beta E_t \Lambda_{t,t+1} R_{t+1}, \tag{32}$$

$$1 = \beta E_t \Lambda_{t,t+1} \tfrac{Z_{t+1} + (1-\delta) Q_{t+1}}{Q_t + \Theta (S_t^H / S_t - \gamma^F)/\varrho_t}, \tag{33}$$

$$\beta E_t \Lambda_{t,t+1} = \beta E_t \varrho_{t+1} / \varrho_t. \tag{34}$$

Financial Intermediaries

$$Q_t S_t^B = \phi_t N_t, \tag{35}$$

$$\overline{\omega}_t = \tfrac{\phi_{t-1} - 1}{R_t^K \phi_{t-1}}, \tag{36}$$

$$(1-p_t) E_t^N [\beta \Lambda_{t,t+1} \bar{R}_t D_t] + p_t E_t^R [\beta \Lambda_{t,t+1} R_{t+1}^K Q_t S_t^B] = D_t, \tag{37}$$

$$(1-p_t) E_t^N [\Lambda_{t,t+1} R_{t+1}^K (\theta \lambda_{t+1} + (1-\theta))[1 - e^{\frac{-\psi}{2}} - \tilde{\pi}_{t+1}]] = p_t E_t^R [\Lambda_{t,t+1} R_{t+1}^K (e^{-\frac{\psi}{2}} - \overline{\omega}_{t+1} + \tilde{\pi}_{t+1})], \tag{38}$$

$$\lambda_t = \tfrac{(1-p_t) E_t^N \Lambda_{t,t+1} R_{t+1}^K [\theta \lambda_{t+1} + (1-\theta)](1 - \overline{\omega}_{t+1})}{1 - (1-p_t) E_t^N [\Lambda_{t,t+1} R_{t+1}^K \overline{\omega}_{t+1}] - p_t E_t^R [\Lambda_{t,t+1} R_{t+1}^K]}, \tag{39}$$

$$\kappa_t = \tfrac{\beta (1-p_t) E_t^N \Lambda_{t,t+1} [\lambda_t - (\theta \lambda_{t+1} + 1 - \theta)]}{(1-p_t) E_t^N \Lambda_{t,t+1} \left[(\theta \lambda_{t+1} + 1 - \theta) \tilde{F}_{t+1}(\overline{\omega}_{t+1}) \right] + p_t E_t^R \Lambda_{t,t+1} \left[(\theta \lambda_{t+1} + 1 - \theta) \left(1 - \tilde{F}_{t+1}(\overline{\omega}_{t+1}) \right) \right]}, \tag{40}$$

$$E_t[\tilde{\pi}_{t+1}] = E_t \left[\overline{\omega}_{t+1} \Phi \left(\tfrac{\log(\overline{\omega}_{t+1}) + \frac{1}{2}(\psi + \sigma_{t+1}^2)}{\sigma_{t+1}} \right) - e^{-\psi/2} \Phi \left(\tfrac{\log(\overline{\omega}_{t+1}) + \frac{1}{2}(\psi - \sigma_{t+1}^2)}{\sigma_{t+1}} \right) \right], \tag{41}$$

$$N_t = \theta N_{S,t} + N_{N,t}, \tag{42}$$

$$N_{N,t} = (1-\theta) \zeta S_{t-1}, \tag{43}$$

$$N_{S,t} = \begin{cases} R_t^K Q_{t-1} S_{t-1}^B - \overline{R}_{t-1} D_{t-1} & \text{if } x_t^\star \geq = 1 \vee \iota_t = 0 \text{ (no run)} \\ 0 & \text{if } x_t^\star < 1 \wedge \iota_t = 1 \text{ (run occurs)} \end{cases}, \tag{44}$$

$$R_t = \begin{cases} \bar{R}_{t-1} & \text{if } x_t^\star \geq = 1 \vee \iota_t = 0 \text{ (no run)} \\ x_t^\star \bar{R}_{t-1} & \text{if } x_t^\star < 1 \wedge \iota_t = 1 \text{ (run occurs)} \end{cases}. \tag{45}$$

Non-Financial Firms

$$Y_t = A_t(K_{t-1})^{\alpha}(L_t)^{1-\alpha}, \tag{46}$$

$$K_t = S_t, \tag{47}$$

$$\varphi_t^{mc}(1-\alpha)\tfrac{Y_t}{L_t} = W_t, \tag{48}$$

$$R_t^K = \tfrac{Z_t + Q_t(1-\delta)}{Q_{t-1}}, \tag{49}$$

$$Z_t = \varphi_t^{mc}\alpha\tfrac{Y_t}{K_{t-1}}, \tag{50}$$

$$\left(\tfrac{\Pi_t}{\Pi} - 1\right)\tfrac{\Pi_t}{\Pi} = \tfrac{\epsilon}{\rho^r}\left(\varphi_t^{mc} - \tfrac{\epsilon-1}{\epsilon}\right) + \Lambda_{t,t+1}\left(\tfrac{\Pi_{t+1}}{\Pi} - 1\right)\tfrac{\Pi_{t+1}}{\Pi}\tfrac{Y_{t+1}}{Y_t}, \tag{51}$$

$$\Gamma\left(\tfrac{I_t}{K_t}\right) = a_1\left(\tfrac{I_t}{K_t}\right)^{(1-\eta)} + a_2, \tag{52}$$

$$Q_t = \left[\Gamma'\left(\tfrac{I_t}{S_{t-1}}\right)\right]^{-1}, \tag{53}$$

$$S_t = (1-\delta)S_{t-1} + \Gamma\left(\tfrac{I_t}{S_{t-1}}\right)S_{t-1}. \tag{54}$$

Monetary Policy and Market Clearing

$$R_t^I = \max\left[1, R^I\left(\tfrac{\Pi_t}{\Pi}\right)^{\kappa_\Pi}\left(\tfrac{\varphi_t^{mc}}{\varphi^{mc}}\right)^{\kappa_y}\right], \tag{55}$$

$$\beta E_t \Lambda_{t,t+1}\tfrac{R_t^I}{\Pi_{t+1}} = 1, \tag{56}$$

$$Y_t = C_t + I_t + G + \tfrac{\rho^r}{2}\left(\tfrac{\Pi_t}{\Pi} - 1\right)^2 Y_t, \tag{57}$$

$$S_t = S_t^H + S_t^B. \tag{58}$$

Shocks

$$\sigma_t = (1-\rho^\sigma)\sigma + \rho^\sigma\sigma_{t-1} + \sigma^\sigma\epsilon_t^\sigma, \tag{59}$$

$$A_t = (1-\rho^A)A + \rho^A A_{t-1} + \sigma^A\epsilon_t^A, \tag{60}$$

$$\iota_t = \begin{cases} 1 & \text{with probability } \Upsilon \\ 0 & \text{with probability } 1-\Upsilon \end{cases}. \tag{61}$$

Definition

The recursive competitive equilibrium is a price system, policy functions for the households, the financial intermediaries, the final goods producers, intermediate goods producers and capital goods producers, law of motion of the aggregate state and perceived law of motion of the aggregate state, such that the policy functions solve the agents' respective maximization problem, the price system clears the markets and the perceived law of motion coincides with the law of motion. The aggregate state of the economy is described by the vector of state variables $\mathcal{S}_t = (N_t, S_{t-1}^B, A_t, \sigma_t, \iota_t)$, where ι_t is a sunspot shock.

B.2 Graphical Characterization of the Risk-Shifting Incentives

Figure 10 shows an example for the distributions of the good and substandard security. The figure highlights the difference in mean, variance and upside risk.

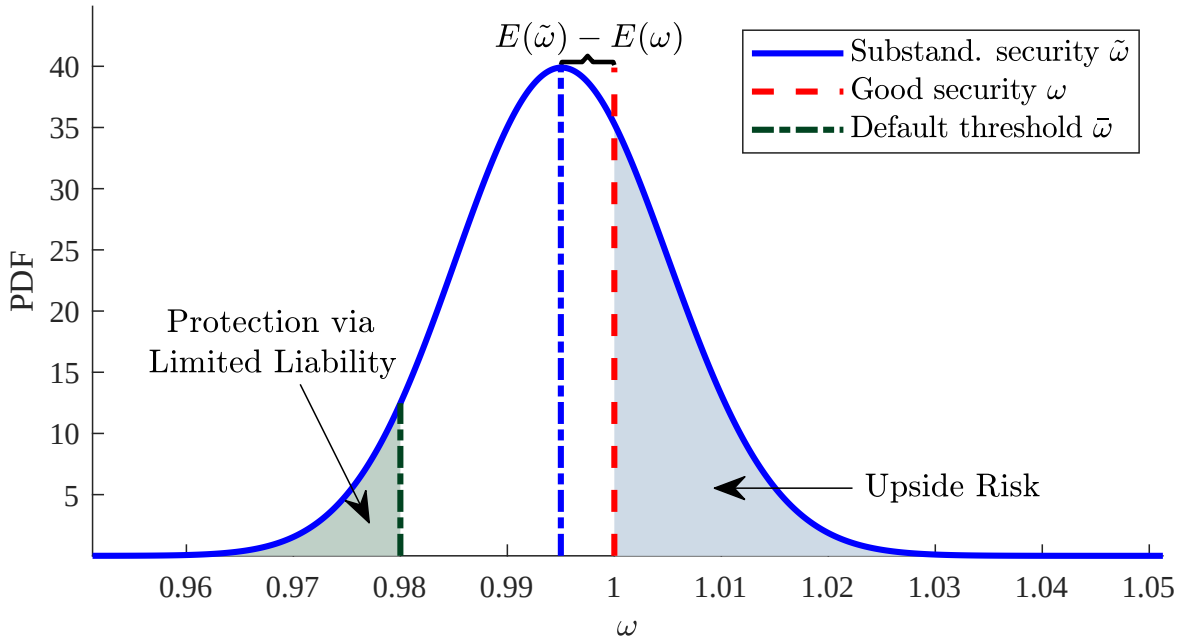

Figure 10: Trade-off between mean return, upside risk and limited liability. The blue line depicts the PDF of the substandard security (log normal distribution) and its mean (blue dashed dotted). The red dashed line is the (mean) return of the good security (dirac delta distribution). The green dash-dotted line is the default threshold value $\bar{\omega}$. The blue and green shaded areas indicate the area associated with the upside risk and protection from downside risk via limited liability, respectively.

B.3 Derivation of Financial Intermediary's Problem

In the following, I derive the financial intermediary's problem. For simplicity, I first derive the solution in the absence of runs. I then extend then the problem to account for runs. Finally, I show some numerical results regarding the incentive and participation constraint.

B.3.1 Absence of runs

The financial intermediary maximizes the value of its franchise V_t subject to a participation and incentive constraint, which reads as follows:[26]

$$V_t^j(N_t^j) = \max_{S_t^{Bj},\bar{D}_t} \beta E_t \Lambda_{t,t+1}\Big[\theta V_{t+1}^j(N_{t+1}^j) + (1-\theta)(R_{t+1}^K Q_t S_t^{Bj} - \bar{D}_t^j)\Big], \tag{62}$$

$$\text{subject to} \quad \beta E_t[\Lambda_{t,t+1}\bar{R}_t^D D_t^j] \geq D_t^j, \tag{63}$$

$$\beta E_t \Lambda_{t,t+1}\Big\{\theta V_{t+1}^j(S_t^{Bj},\overline{D}_t^j) + (1-\theta)[R_{t+1}^K Q_t S_t^{Bj} - \overline{D}_t^j]\Big\} \geq \tag{64}$$

$$\beta E_t \Lambda_{t,t+1} \int_{\overline{\omega}_{t+1}^j}^{\infty} \Big\{\theta V_{t+1}(\omega, S_t^{Bj},\overline{D}_t^j) + (1-\theta)[R_{t+1}^K Q_t S_t^{Bj}\omega_{t+1}^j - \overline{D}_t^j]\Big\} d\tilde{F}_{t+1}(\omega),$$

where $\bar{D}_t^j = \bar{R}_t D_t^j$.

The financial intermediary's problem can be written as the following Bellman equation:

$$\begin{aligned} V_t(N_t^j) = \max_{\{S_t^{Bj},\bar{b}_t^j\}} & \beta E_t \Lambda_{t,t+1}\Bigg[\theta V_{t+1}\Bigg(\Big(1-\tfrac{\bar{b}_t^j}{R_{t+1}^K}\Big)R_{t+1}^K Q_t S_t^{Bj}\Bigg) + (1-\theta)\big(1-\tfrac{\bar{b}_t^j}{R_{t+1}^K}\big)R_{t+1}^K Q_t S_t^{Bj}\Bigg] \\ & + \lambda_t^j\Big[\beta E_t \Lambda_{t,t+1} Q_t S_t^{Bj}\bar{b}_t^j - (Q_t S_t^{Bj} - N_t^j)\Big] \\ & + \kappa_t^j \beta E_t \Lambda_{t,t+1}\Bigg\{\Bigg[\theta V_{t+1}\Bigg(\Big(1-\tfrac{\bar{b}_t^j}{R_{t+1}^K}\Big)R_{t+1}^K Q_t S_t^{Bj}\Bigg) + (1-\theta)\Big(1-\tfrac{\bar{b}_t^j}{R_{t+1}^K}\Big)R_{t+1}^K Q_t S_t^{Bj}\Bigg] \\ & - \int_{\frac{\bar{b}_t^j}{R_{t+1}^K}}^{\infty}\Bigg[\theta V_{t+1}\Bigg(\Big(\omega-\tfrac{\bar{b}_t^j}{R_{t+1}^K}\Big)R_{t+1}^K Q_t S_t^{Bj}\Bigg) + (1-\theta)\Big(\omega-\tfrac{\bar{b}_t^j}{R_{t+1}^K}\Big)R_{t+1}^K Q_t S_t^{Bj}\Bigg] d\tilde{F}_{t+1}(\omega)\Bigg\} \end{aligned}$$

where I defined $\bar{b}_t^j = \left(\overline{R}_t D_t^j\right) / \left(Q_t S_t^B\right)$ and used that

$$N_t^j = \begin{cases} \Big(1-\frac{\bar{b}_{t-1}^j}{R_t^K}\Big)R_t^K Q_{t-1} S_{t-1}^{Bj} & \text{if standard security} \\ \Big(\omega-\frac{\bar{b}_{t-1}^j}{R_t^K}\Big)R_t^K Q_{t-1} S_{t-1}^{Bj} & \text{if substandard security} \end{cases} \tag{65}$$

λ_t^j and κ_t^j are the Lagrange multipliers of the participation and incentive constraint. The first order conditions are

$$\begin{aligned} 0 = & \beta E_t \Lambda_{t,t+1} R_{t+1}^K[\theta V_{t+1}'^{,j} + (1-\theta)](1-\overline{\omega}_{t+1}^j) + \lambda_t^j E_t[\beta \Lambda_{t,t+1} R_{t+1}^K \overline{\omega}_{t+1}^j - 1] \\ & + \kappa_t^j \beta E_t \Lambda_{t,t+1} R_{t+1}^K\Bigg\{[\theta V_{t+1}'^{,j} + (1-\theta)](1-\overline{\omega}_{t+1}^j) - \int_{\overline{\omega}_{t+1}^j}^{\infty}\Big[[\theta V_{t+1}'^{,j} + (1-\theta)](\omega - \overline{\omega}_{t+1}^j)\Big] d\tilde{F}_{t+1}(\omega)\Bigg\} \end{aligned}$$

[26] The derivation is based on Nuño and Thomas (2017).

and

$$\begin{aligned}0 = & -\beta E_t\Lambda_{t,t+1}[\theta V'^j_{t+1} + (1-\theta)] + \lambda^j_t \beta E_t \Lambda_{t,t+1} \\ & -\kappa^j_t \beta E_t \Lambda_{t,t+1}\Big\{[\theta V'^j_{t+1} + (1-\theta)] - \int_{\overline{\omega}^j_{t+1}}^{\infty}\Big[\theta V'^j_{t+1} + (1-\theta)\Big]d\tilde{F}_{t+1}(\omega) - \theta \tfrac{V_{t+1}(0)}{R^K_{t+1}Q_tS^{Bj}_t}\tilde{f}_t(\overline{\omega}^j_{t+1})\Big\}\end{aligned}$$

where I used $\overline{\omega}^j_{t+1} = \overline{b}^j_t / R^K_{t+1}$. The envelope condition is given as:

$$V'^j_t = \lambda^j_t \tag{66}$$

The first order conditions can be written as:

$$\begin{aligned}0 = & \beta E_t \Lambda_{t,t+1} R^K_{t+1}[\theta\lambda^j_{t+1} + (1-\theta)](1-\overline{\omega}^j_{t+1}) + \lambda^j_t E_t[\Lambda_{t,t+1}R^K_{t+1}\overline{\omega}^j_{t+1} - 1] \\ & +\kappa^j_t E_t R^K_{t+1}[\theta\lambda^j_{t+1} + (1-\theta)]\Big\{(1-\overline{\omega}^j_{t+1}) - \int_{\overline{\omega}^j_{t+1}}^{\infty}\Big[(\omega - \overline{\omega}^j_{t+1})\Big]d\tilde{F}_{t+1}(\omega)\Big\} \\ 0 = & -\beta E_t\Lambda_{t,t+1}[\theta\lambda^j_{t+1} + (1-\theta)] + \lambda^j_t \beta E_t \Lambda_{t,t+1} \\ & -\kappa^j_t \beta E_t \Lambda_{t,t+1}\Big\{[\theta\lambda^j_{t+1} + (1-\theta)] - \int_{\overline{\omega}^j_{t+1}}^{\infty}\Big[\theta\lambda^j_{t+1} + (1-\theta)\Big]d\tilde{F}_{t+1}(\omega) - \theta \tfrac{V_{t+1}(0)}{R_{t+1}{}^K Q_t S^{Bj}_t}\tilde{f}_t(\overline{\omega}^j_{t+1})\Big\}\end{aligned}$$

To continue solving the problem, I use a guess and verify approach. I guess that the value function is linear in net worth, so that the value function reads as follows:

$$V_t = \lambda^j_t N^j_t \tag{67}$$

Furthermore, I guess the multipliers are equal across intermediaries, that is $\lambda^j_t = \lambda_t$ and $\kappa^j_t = \kappa_t \ \forall j$. Using the guess, the incentive constraint can be written as:

$$\beta E_t\Lambda_{t,t+1}\left\{\begin{array}{l}\Big[\theta\lambda_{t+1}(1-\overline{\omega}^j_{t+1})R^K_{t+1}Q_tS^B_t + (1-\theta)(1-\overline{\omega}^j_{t+1})R^K_{t+1}Q_tS^B_t\Big] - \\ \int_{\overline{\omega}^j_{t+1}}^{\infty}\Big[\theta\lambda_{t+1}(\omega_t - \overline{\omega}^j_{t+1})R^K_{t+1}Q_tS^B_t + (1-\theta)(\omega_t - \overline{\omega}^j_{t+1})R^K_{t+1}Q_tS^B_t\Big]d\tilde{F}_{t+1}(\omega)\end{array}\right\} \geq 0$$

and reformulated to:

$$\beta E_t\Lambda_{t,t+1}(\theta\lambda_{t+1} + (1-\theta))\Big\{(1-\overline{\omega}^j_{t+1}) - \int_{\overline{\omega}^j_{t+1}}^{\infty}(\omega_t - \overline{\omega}^j_{t+1})d\tilde{F}_{t+1}(\omega)\Big\} \geq 0 \tag{68}$$

The next step is to simplify the first order conditions. I use that if either the incentive constraint binds or if not then $\lambda_t = 0$ (Kuhn Tucker conditions) to simplify the participation constraint and use that the guess for the value function evaluated at 0 so that the first order conditions are given as:

$$0 = E_t\Lambda_{t,t+1}R^K_{t+1}[\theta\lambda_{t+1} + (1-\theta)](1-\overline{\omega}_{t+1}) + \lambda_t E_t[\Lambda_{t,t+1}R^K_{t+1}\overline{\omega}^j_{t+1} - 1] \tag{69}$$

$$0 = -\beta E_t\Lambda_{t,t+1}[\theta\lambda_{t+1} + (1-\theta)] + \lambda_t\beta E_t\Lambda_{t,t+1} - \kappa_t\beta E_t\Lambda_{t,t+1}(\theta\lambda_{t+1} + (1-\theta))\tilde{F}_{t+1}(\overline{\omega}^j_{t+1}) \tag{70}$$

I can now get the following expression for the multipliers:

$$\lambda_t = \tfrac{\beta E_t\Lambda_{t,t+1}R^K_{t+1}[\theta\lambda_{t+1}+(1-\theta)](1-\overline{\omega}^j_{t+1})}{1-\beta E_t\Lambda_{t,t+1}R^K_{t+1}\overline{\omega}^j_{t+1}} \tag{71}$$

$$\kappa_t = \frac{\beta E_t \Lambda_{t,t+1}(\lambda_t - [\theta\lambda_{t+1} + (1-\theta)])}{\beta E_t \Lambda_{t,t+1}(\theta\lambda_{t+1} + (1-\theta))\tilde{F}_{t+1}(\overline{\omega}^j_{t+1})} \tag{72}$$

I now want to show that the multipliers are symmetric across intermediaries. Assuming that equation (68), which is the incentive constraint, is binding, I can get $\omega^j_t = \omega_t$. Due to $b^j_t = \overline{\omega}^j_{t+1} R^K_t$, $b^j_t = b_t$ can be obtained. At the same time, I have $\overline{\omega}^j_{t+1} = \overline{\omega}_{t+1}$ and $\overline{b}^j_t = \overline{b}_t$. Then, equation (71) implies that $\lambda^j_t = \lambda_t$ and equation (72) shows $\kappa^j_t = \kappa_t$. This verifies my guess that the multipliers are equalized. Note that $\lambda_t > 1$ implies that the financial intermediaries do not want to return their net worth as then $V_t > 1$. I then check numerically that the participation and incentive constraint are binding. Taken together, this implies $\lambda_t > 1$ and $\kappa_t > 0$ as conditions.

To show that the leverage ratio is symmetric, I use the participation constraint and assume that it is binding:

$$E_t \Lambda_{t,t+1} Q_t S^{Bj}_t \overline{b}^j_t - (Q_t S^{Bj}_t - N^j_t) = 0. \tag{73}$$

The leverage ratio is then given as:

$$\phi^j_t = \frac{1}{1 - E_t \Lambda_{t,t+1} R^K_{t+1} \overline{\omega}_{t+1}}. \tag{74}$$

As the leverage ratio does not depend on j, this implies that $\phi_t = \phi^j_t$.

The final step is to show that my guess $V_t = \lambda_t N^j_t$ is correct. The starting point is again the value function:

$$V_t(N^j_t) = \beta E_t\big[(\theta\lambda_{t+1} N_{t+1} + (1-\theta)\big(1 - \overline{\omega}_{t+1}\big) R^K_{t+1} Q_t S^{Bj}_t)\big],$$

where I used $N^j_{t+1} = (1 - \overline{\omega}_{t+1}) R^K_{t+1} Q_t S^{Bj}_t$. I insert the guess to obtain:

$$\lambda_t N^j_t = \phi_t N^j_t \beta E_t \Lambda_{t,t+1}\big[\theta\lambda_{t+1} + (1-\theta)\big]\big(1 - \overline{\omega}_{t+1}\big) R^K_{t+1}. \tag{75}$$

and reformulate it to

$$\lambda_t = \phi_t E_t \Lambda_{t,t+1}\big[\theta\lambda_{t+1} + (1-\theta)\big]\big(1 - \overline{\omega}_{t+1}\big) R^K_{t+1} \tag{76}$$

This gives us again a condition for λ_t:

$$\begin{aligned} \lambda_t &= E_t\big[(\theta\lambda_{t+1} N_{t+1} + (1-\theta)\big(1 - \overline{\omega}_{t+1}\big) R^K_{t+1} Q_t S^{Bj}_t)\big] && (77)\\ &= \phi_t \beta E_t \Lambda_{t,t+1}\big[\theta\lambda_{t+1} + (1-\theta)\big]\big(1 - \overline{\omega}_{t+1}\big) R^K_{t+1}. && (78) \end{aligned}$$

Inserting (74), the condition for λ_t becomes:

$$\lambda_t = \frac{\beta E_t \Lambda_{t,t+1}\big[\theta\lambda_{t+1} + (1-\theta)\big]\big(1 - \overline{\omega}_{t+1}\big) R^K_{t+1}}{1 - \beta E_t \Lambda_{t,t+1} R^K_{t+1} \overline{\omega}_{t+1}}. \tag{79}$$

This coincides with the equation (71). This verifies the guess.

B.3.2 With Runs on the Financial Sector

In this section, the possibility of runs is included. The financial intermediary maximizes V_t subject to a participation and incentive constraint, which reads as follows:

$$V_t^j(N_t^j) = \max_{S_t^{Bj},\bar{D}_t}(1-p_t^j)\beta E_t^N\Lambda_{t,t+1}\left[\theta V_{t+1}^j\left(N_{t+1}^j\right)+(1-\theta)(R_{t+1}^K Q_t S_t^{Bj}-\bar{D}_t^j)\right] \quad (80)$$

$$\text{s.t.} \quad (1-p_t^j)\beta E_t^N[\Lambda_{t,t+1}Q_t S_t^{Bj}\bar{b}_t^j]+p_t^j\beta E_t^R[R_{t+1}^K Q_t S_t^{Bj}] \geq (Q_t S_t^{Bj}-N_t^j) \quad (81)$$

$$(1-p_t^j)E_t^N\left[\Lambda_{t,t+1}\theta V_{t+1}\left(N_{t+1}^j\right)+(1-\theta)\Big(1-\frac{\bar{b}_t^j}{R_{t+1}^K}\Big)R_{t+1}^K Q_t S_t^{Bj}\right]\geq \quad (82)$$

$$\beta\Lambda_{t,t+1}E_t\left[\Lambda_{t,t+1}\int_{\frac{\bar{b}_t^j}{R_{t+1}^K}}^{\infty}\theta V_{t+1}\left(N_{t+1}^j\right)+(1-\theta)\Big(\omega-\frac{\bar{b}_t^j}{R_{t+1}^K}\Big)R_{t+1}^K Q_t S_t^{Bj}d\tilde{F}_{t+1}(\omega)\right]$$

The financial intermediary's specific can be written as Bellman equation:

$$\begin{aligned}V_t(N_t^j) = \max_{\{\phi_t^j,\bar{b}_t^j\}}&(1-p_t^j)\beta E_t^N\Lambda_{t,t+1}\left[\theta V_{t+1}\left(\Big(1-\frac{\bar{b}_t^j}{R_{t+1}^K}\Big)R_{t+1}^K\phi_t^j N_t^j\right)+(1-\theta)\big(1-\frac{\bar{b}_t^j}{R_{t+1}^K}\big)R_{t+1}^K\phi_t^j N_t^j\right]\\
&+\lambda_t^j\left[(1-p_t^j)\beta E_t^N[\Lambda_{t,t+1}\phi_t^j N_t^j\bar{b}_t^j]+p_t^j\beta E_t^R[R_{t+1}^K\phi_t^j N_t^j]-(\phi_t^j N_t^j-N_t^j)\right]\\
+\kappa_t^j\beta\Bigg\{&\left[(1-p_t^j)E_t^N\Lambda_{t,t+1}\left[\Lambda_{t,t+1}\theta V_{t+1}\left(\Big(1-\frac{\bar{b}_t^j}{R_{t+1}^K}\Big)R_{t+1}^K\phi_t^j N_t^j\right)+(1-\theta)\Big(1-\frac{\bar{b}_t^j}{R_{t+1}^K}\Big)R_{t+1}^K\phi_t^j N_t^j\right]\right]\\
&-\beta E_t\left[\Lambda_{t,t+1}\int_{\frac{\bar{b}_t^j}{R_{t+1}^K}}^{\infty}\theta V_{t+1}\left(\Big(1-\frac{\bar{b}_t^j}{R_{t+1}^K}\Big)R_{t+1}^K\phi_t^j N_t^j\right)+(1-\theta)\Big(\omega-\frac{\bar{b}_t^j}{R_{t+1}^K}\Big)R_{t+1}^K\phi_t^j N_t^j d\tilde{F}_{t+1}(\omega)\right]\Bigg\}\end{aligned}$$

The first order conditions with respect to ϕ_t^j can be written as

$$\begin{aligned}0 = \quad &(1-p_t^j)E_t^N\Lambda_{t,t+1}R_{t+1}^K[\theta V_{t+1}'^j+(1-\theta)](1-\overline{\omega}_{t+1}^j)\\
&+\lambda_t^j((1-p_t^j)E_t^N[\Lambda_{t,t+1}R_{t+1}^K\overline{\omega}_{t+1}^j]+p_t E_t^R[\Lambda_{t,t+1}R_{t+1}^K]-1)\\
&+\kappa_t^j((1-p_t^j)\beta E_t^N\Lambda_{t,t+1}R_{t+1}^K[\theta V_{t+1}'^j+(1-\theta)](1-\overline{\omega}_{t+1}^j)\\
&-\kappa_t^j\beta E_t\Lambda_{t,t+1}\int_{\overline{\omega}_{t+1}^j}^{\infty}\left[R_{t+1}^K[\theta V_{t+1}'^j+(1-\theta)](\omega-\overline{\omega}_{t+1}^j)\right]d\tilde{F}_{t+1}(\omega)\\
&-\frac{\partial p_t^j}{\phi_t^j}E_t^N\Lambda_{t,t+1}R_{t+1}^K[\theta V_{t+1}'^j+(1-\theta)](1-\overline{\omega}_{t+1}^j)\left(1+\kappa_t^j\right) \quad (83)\\
&-\frac{\partial p_t^j}{\phi_t^j}E_t^N\left(R_{t+1}^K\overline{\omega}_{t+1}^j-R_{t+1}^K\right) \quad (84)\end{aligned}$$

where I applied $\overline{\omega}_{t+1}^j = \overline{b}_t^j/R_{t+1}^K$. Gertler et al. (2020b) show that the even though the optimization of leverage ϕ^j affect the default probability p_t, this indirect effect on on the firm value V_t and the promised return R_t^D is zero. The reason is that at the cutoff value of default, net worth is zero, which implies $V_{t+1}=0$. Similarly, the promised return is unchanged. The cutoff values of default is defined as:

$$\xi_{t+1}^D(\phi_t^j) = \left\{(\sigma_{t+1},A_{t+1},\iota_{t+1}) : R_{t+1}^K\frac{\phi_t^j-1}{\phi_t^j}\overline{R}_t^D\right\}. \quad (85)$$

At the cutoff points, the intermediary can exactly cover the face value of the deposits, which implies

$$\overline{\omega}_t^j = 1. \tag{86}$$

Based on the derivation in Gertler et al. (2020b), the property $\overline{\omega}_t^j = 1$ implies that

$$-\frac{\partial p_t}{S_t^{Bj}} E_t^N \Lambda_{t,t+1} R_{t+1}^K [\theta V_{t+1}'^j + (1-\theta)](1-\overline{\omega}_{t+1}^j)\left(1+\kappa_t^j\right) = 0, \tag{87}$$

$$-\frac{\partial p_t}{S_t^{Bj}} E_t^N \left(R_{t+1}^K \overline{\omega}_{t+1}^j - R_{t+1}^K\right) = 0, \tag{88}$$

The first order condition with respect to ϕ_t^B becomes then

$$\begin{aligned} 0 = \quad & (1-p_t^j) E_t^N \Lambda_{t,t+1} R_{t+1}^K [\theta V_{t+1}'^j + (1-\theta)](1-\overline{\omega}_{t+1}^j) \\ & + \lambda_t^j ((1-p_t^j) E_t^N [\Lambda_{t,t+1} R_{t+1}^K \overline{\omega}_{t+1}^j] + p_t E_t^R [\Lambda_{t,t+1} R_{t+1}^K] - 1) \\ & + \kappa_t^j ((1-p_t^j) \beta E_t^N \Lambda_{t,t+1} R_{t+1}^K [\theta V_{t+1}'^j + (1-\theta)](1-\overline{\omega}_{t+1}^j) \\ & - \kappa_t^j \beta E_t \Lambda_{t,t+1} \int_{\overline{\omega}_{t+1}^j}^{\infty} \left[R_{t+1}^K [\theta V_{t+1}'^j + (1-\theta)](\omega - \overline{\omega}_{t+1}^j)\right] d\tilde{F}_{t+1}(\omega) \end{aligned}$$

The first order condition with respect to $\overline{b}_t^j$ is given as

$$\begin{aligned} 0 = \quad & -\beta(1-p_t^j) E_t^N \Lambda_{t,t+1} [\theta V_{t+1}'^j + (1-\theta)] \\ & + \lambda_t^j \beta (1-p_t^j) E_t^N \Lambda_{t,t+1} \\ & - \kappa_t^j \beta (1-p_t^j) E_t^N \Lambda_{t,t+1} \left\{ [\theta V_{t+1}'^j + (1-\theta)] \right\} \\ & + \kappa_t^j \beta (1-p_t^j) E_t \Lambda_{t,t+1} \int_{\overline{\omega}_{t+1}^j}^{\infty} \left[\theta V_{t+1}'^j + (1-\theta)\right] d\tilde{F}_{t+1}(\omega) - \theta \frac{V_{t+1}(0)}{R_{t+1}^K Q_t S_t^{Bj}} \tilde{f}_t(\overline{\omega}_{t+1}^j) \end{aligned} \tag{89}$$

where I applied $\overline{\omega}_{t+1}^j = \overline{b}_t^j / R_{t+1}^K$

Similar to before, I use the following guess for the value function

$$V_t = \lambda_t^j N_t^j \tag{90}$$

and also the fact that the multipliers are equal across intermediaries, that is $\lambda_t^j = \lambda_t$ and $\kappa_t^j = \kappa_t \forall j$. In addition, I also guess now that the probability of a run does not depend on individual characteristics, that is $p_t^j = p_t$.

The incentive constraint can then then be written as

$$\begin{aligned} & \beta(1-p_t^j) E_t^N \left[\Lambda_{t,t+1} (\theta \lambda_{t+1} + (1-\theta))(1-\overline{\omega}_{t+1}^j) R_{t+1}^K\right] \geq \\ & \beta E_t \left[\Lambda_{t,t+1} \int_{\frac{\overline{b}_t^j}{R_{t+1}^K}}^{\infty} (\theta \lambda_{t+1} + (1-\theta))\left(\omega - \overline{\omega}_{t+1}^j\right) R_{t+1}^K d\tilde{F}_{t+1}(\omega)\right] \end{aligned} \tag{91}$$

The two first order conditions can then be adjusted similar to section B.3.1 and be written

as

$$
\begin{aligned}
0 = \quad & (1-p_t)E_t^N \Lambda_{t,t+1} R_{t+1}^K [\theta\lambda_{t+1} + (1-\theta)](1-\overline{\omega}_{t+1}^j) + \\
& \lambda_t((1-p_t)E_t^N[\Lambda_{t,t+1}R_{t+1}^K \overline{\omega}_{t+1}] + p_t E_t^R[\Lambda_{t,t+1}R_{t+1}^K] - 1) \qquad (92) \\
0 = \quad & -\beta(1-p_t)E_t^N \Lambda_{t,t+1}[\theta\lambda_{t+1} + (1-\theta)] + \lambda_t \beta(1-p_t)E_t^N \Lambda_{t,t+1} \\
& -\kappa_t \beta \Big\{ (1-p_t)E_t^N \Lambda_{t,t+1} \left[(\theta\lambda_{t+1} + 1 - \theta)\, \tilde{F}_{t+1}(\overline{\omega}_{t+1}^j) \right] \\
& + p_t E_t^R \Lambda_{t,t+1} \left[(\theta\lambda_{t+1} + 1 - \theta) \left(1 - \tilde{F}_{t+1}(\overline{\omega}_{t+1}^j) \right) \right] \Big\} \qquad (93)
\end{aligned}
$$

Using the same strategy as in B.3.1, the guess about the equalized multipliers can be verified. Similarly, it can be shown that leverage is the same across intermediaries. This then verifies that the guess of the run probability $p_t^j = p_t$ is verified as the cutoff value is the same across intermediaries as shown in equation (85). I additionally assume that in case of a run on the entire financial sector, a intermediary that survives shuts down and returns their net worth. This implies that $E_t^R \lambda_{t+1} = 1$. The participation constraint is given as:

$$
(1-p_t)E_t^N[\beta \Lambda_{t,t+1} \bar{R}_t D_t] + p_t E_t^R[\beta \Lambda_{t,t+1} R_{t+1}^K Q_t S_t^B] = D_t. \qquad (94)
$$

The incentive constraint is given as:

$$
\begin{aligned}
(1-p_t)E_t^N[\Lambda_{t,t+1}R_{t+1}^K(\theta\lambda_{t+1} + (1-\theta))[1 - e^{\frac{-\psi}{2}} - \tilde{\pi}_{t+1}]] = \qquad (95) \\
p_t E_t^R[\Lambda_{t,t+1}R_{t+1}^K(e^{-\frac{\psi}{2}} - \overline{\omega}_{t+1} + \tilde{\pi}_{t+1})],
\end{aligned}
$$

λ_t and κ_t are derived from the first order conditions in equations (92) and (93) are given as:

$$
\lambda_t = \frac{(1-p_t)E_t^N \Lambda_{t,t+1} R_{t+1}^K [\theta\lambda_{t+1} + (1-\theta)](1-\overline{\omega}_{t+1})}{1-(1-p_t)E_t^N[\Lambda_{t,t+1}R_{t+1}^K \overline{\omega}_{t+1}] - p_t E_t^R[\Lambda_{t,t+1}R_{t+1}^K]} \qquad (96)
$$

$$
\kappa_t = \frac{\beta(1-p_t)E_t^N \Lambda_{t,t+1}[\lambda_t - (\theta\lambda_{t+1} + 1 - \theta)]}{(1-p_t)E_t^N \Lambda_{t,t+1}\left[(\theta\lambda_{t+1} + 1 - \theta)\tilde{F}_{t+1}(\overline{\omega}_{t+1})\right] + p_t E_t^R \Lambda_{t,t+1}\left[(\theta\lambda_{t+1} + 1 - \theta)\left(1 - \tilde{F}_{t+1}(\overline{\omega}_{t+1})\right)\right]} \qquad (97)
$$

If $\lambda_t > 1$ and $\kappa_t > 0$, the participation and incentive constraint are binding.[27]

B.3.3 Binding of the Participation and Incentive Constraint: Numerical Check

When deriving the intermediaries problem and solving the model with the global solution method, I assume that the incentive constraint and participation constraint are always binding. This implies $\kappa_t > 0$ and $\lambda_t > 1$ in all periods. I verify these assumptions afterwards numerically using a simulation of 500000 periods and show that these assumptions hold in almost all periods (more than 99.5% of periods). As an example of the dynamics, Figure 11 shows the path of κ and λ based on the simulation of the boom-bust dynamics with the volatility shock in Section 3.2 (Figure 2), which is as follows: The economy is initially at its stochastic steady state (SS). From period 1 until period 8, the economy is hit by a one-standard-deviation negative volatility shock in every period. In period 9, a two-standard-deviation positive volatility shock materializes. Afterwards, no more shocks occur. No sunspot shock occurs in period 9,

[27] $\lambda_t > 1$ ensures that the intermediaries do not want to return their net worth to the households.

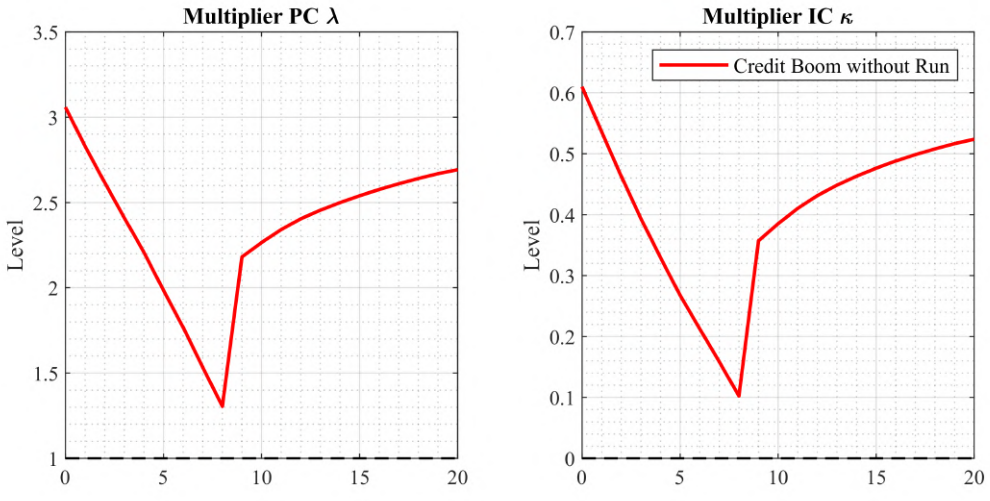

Figure 11: The dynamics of the participation constraint (λ_t) and incentive constraint (κ_t) multiplier during a credit boom. The simulation shows the impulse responses for a sequence of volatility shocks. The sequence is the same as in Figure 1. The economy is initially at its stochastic steady state (SS). From period 1 until period 8, the economy is hit by a one-standard-deviation negative volatility shock in every period. In period 9, a two-standard-deviation positive volatility shock materializes. Afterwards, no more shocks occur. No sunspot shock occurs in period 9, which implies no run.

which implies no run. The figure shows that the conditions are satisfied in this experiment. The constraints also hold in the other main experiments (the typical financial crisis (Figure 3) and the median path in the estimation (Section 4)).

The reason for these rare violations is that the intermediaries accumulate too much net worth. This could be addressed, for instance, by allowing for state-dependent dividend payments from the intermediaries to the households. The payments could be modeled as an occasionally binding constraint similar to the idea of equity injections as in Gertler et al. (2020a).

B.4 Endogenous Runs and Multiple Equilibria: Graphical Characterization

The importance of leverage can be shown by rewriting the recovery ratio $x_t^\star$:

$$x_t^\star = \frac{\phi_{t-1}}{\phi_{t-1}-1}\frac{[(1-\delta)Q_t^\star + Z_t^\star]}{Q_{t-1}\bar{R}_{t-1}}. \tag{98}$$

Elevated leverage levels make it more likely that the run equilibrium will occur. Furthermore, a contractionary shock, such as an increase in volatility or a negative TFP shock, reduces the return and can thus enable a run if the leverage of the financial sector is elevated.

Figure 12 illustrates how the combination of the volatility shock and leverage determine which region an economy falls into. The $x_t^\star = 1$ line is downward sloping and divides the two regions. First, it can be seen that a high level of previous period leverage and an increase in volatility push the economy into the fragile region, as discussed above. Second, low leverage is associated with the safe region. This highlights that the pre-crisis period is critical for the build-up of financial fragility. A period of low volatility reduces the risk-shifting incentives. The financial intermediaries increase their leverage and extend their credit supply. This credit boom brings with it financial fragility due to low loss absorbing capacities. In such a scenario with high leverage, a contraction shock can then cause a roll-over crisis. To put it another way, tranquil periods sow the seed of a crisis.

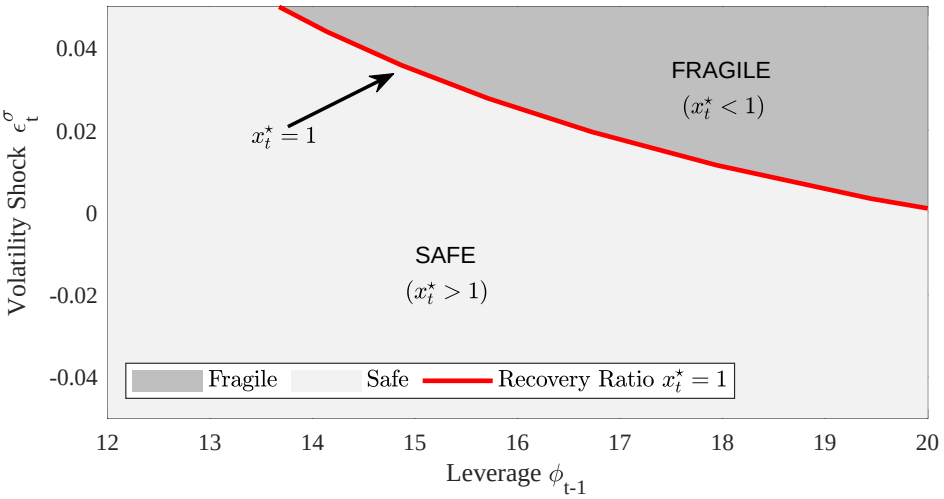

Figure 12: Illustration showing how the safe and fragile regions are dependent on leverage ϕ_{t-1} and the volatility shock ϵ_t^σ.

C Global Solution Method

The model is solved with global methods that can account for the multiplicity of equilibria and occasionally binding constraints. The state variables are $X_t = \{S_{t-1}, N_t, \sigma_t, A_t, \iota_t\}$, where I used N_t as state variable instead of $\overline{D}_{t-1}$ for computational reasons. The parameters of the model are summarized as Θ^P. I solve for the following policy functions $Q(X_t;\Theta^P), C(X_t;\Theta^P), \overline{b}(X), \Pi(X_t;\Theta^P), \lambda(X_t;\Theta^P)$, the law of motion of net worth $N'(X_t, \varepsilon_{t+1};\Theta^P)$ and the probability of a run next period $P(X_t;\Theta^P)$. These objects can be used to solve all remaining variables.

The algorithm to find the described policy functions uses time iteration with linear interpolation based on Richter et al. (2014). In other words, the functional space for the policy function approximation is piecewise linear.[28] The expectations are evaluated using Gauss-Hermite quadrature, where the matrix of nodes is denoted as ε.

In addition to this, the solution method features a non-standard aspect. To account for the multiplicity of equilibria due to possibility of a run, I use an additional piecewise approximation of the policy functions similar to Aruoba et al. (2018) and Aruoba et al. (2021).[29] In particular, I derive separate policy functions to approximate the run and normal equilibrium. Thus, the piecewise approximation of the policy functions $Q_t(X;\Theta)$ is postulated as

$$Q(X_t;\Theta) = \begin{cases} f_Q^1(X_t;\Theta^P) & \text{if no run takes place in period } t \\ f_Q^2(\tilde{X}_t;\Theta^P) & \text{if a run takes place in period } t \end{cases} \tag{99}$$

and similar for the remaining policy functions $(C(X_t;\Theta^P), \overline{b}(X), \Pi(X_t;\Theta^P), \lambda(X_t;\Theta^P), P(X_t;\Theta^P), N'(X_t, \varepsilon_{t+1};\Theta^P))$. The distinct functional space for the functions $f_Q^1(X_t;\Theta)$ and $f_Q^2(X_t;\Theta)$ is piecewise linear. The state variables for the run equilibrium are $\tilde{X}_t = \{S_{t-1}, \sigma_t, A_t\}$.

Even though the used solution method can account for the nonlinear dynamics, using such an "additional" piecewise element to distinct the equilibria related to the run can improve the accuracy. The reason is that the net worth value during a run is given from the other state variables so that I can reduce the state space from to three variables. Figure 13 shows the policy function for the asset price $Q(X_t;\Theta^P)$. The blue line describes $f_Q^1(\cdot)$ - the piece related to the no-run equilibrium, while the red line displays $f_Q^2(\cdot)$ - the piece related to the run equilibrium. Net worth N_t is varied on the left plot and volatility on the right plot, while the other state variables are fixed. The grid points of the discretized state space are marked as crosses and the policy functions are approximated using linear interpolation between the grid points. The function $f_Q^2(\cdot)$ is described only with one point on the left plot. The reason is that the net worth value during a run is given from the other state variables so that I

[28] An alternative to the piecewise linear functions could have been e.g. Chebyshev polynomials.

[29] The ZLB introduces additional multiple equilibria (see e.g. Benhabib et al. 2001 and Aruoba et al. 2018). I focus only on one specific equilibrium, namely the targeted-inflation equilibrium, by choosing starting values for the policy function iteration that are taken from the targeted-inflation equilibrium. Therefore, I abstract from the multiplicity arising from the zero lower bound.

can reduce the state space from four to three variables. Therefore, the policy function is only solved at this point for the specific values of the remaining state variables. This is also the reason why using such a piecewise linear approximation can improve the accuracy. The reason is that the net worth value during a run is given from the other state variables so that I can reduce the state space from four to three variables.

The gain in accuracy can be evaluated when inspecting the difference to the function $f_Q^1(\cdot)$. This is the case because the function $f_Q^1(\cdot)$ can also cover the run equilibrium, namely the level of net worth corresponds to the value during a run. This is possible because the value of net worth depends only on the level of previous period securities. This shows that the gains are rather small. The same finding is also for the right plot, where net worth is fixed to the level that occurs during a run and the volatility shock takes place. Thus, a method without piecewise approach could account very well for the nonlinear dynamics related to the run. However, the piecewise approach increases the accuracy and provides security that the run equilibrium is sufficiently accurate solved. Another advantage is that it can also capture if the run and no run economy has a different structure. For instance, if the central bank has a specific policy that it only implements after a run, it is strictly necessary to have the piecewise approach.

While $f_Q^1(X_t;\Theta^P)$ can represent the policy function over the entire considered level of net worth, it would be less precise to describe a run. The reason is that during the run period, I have pinned down the exact level of net worth, which is slightly positive as new banks enter in this period. Thus, there would be a larger approximation error if I would not define a second function for this run equilibrium.

The algorithm to find the policy functions is summarized below:

1. Define a state grid $\boldsymbol{X} \in [\underline{S}_{t-1}, \overline{S}_{t-1}] \times [\underline{N}_t, \overline{N}_t] \times [\underline{\sigma}_t, \overline{\sigma}_t] \times [\underline{A}_t, \overline{A}_t]$ and integration nodes $\boldsymbol{\epsilon} \in [\underline{\epsilon^{\sigma}}_{t+1}, \overline{\epsilon^{\sigma}}_{t+1}] \times [\underline{\epsilon^{A}}_{t+1}, \overline{\epsilon^{A}}_{t+1}]$ to evaluate expectations based on Gauss-Hermite quadrature

2. Guess the piecewise linear policy functions to initialize the algorithm, which includes a separate guess for each of the pieces that are related to the equilibriau (e.g. $f_Q^1(\tilde{X}_t;\Theta^P)$ and $f_Q^2(\tilde{X}_t;\Theta^P)$).)[30]

   (a) the "classical" policy functions $Q(X_t;\Theta^P), C(X_t;\Theta^P), \bar{b}(X), \Pi(X_t;\Theta^P), \lambda(X_t;\Theta^P)$,

   (b) a function $N'(X_t, \varepsilon_{t+1};\Theta^P)$ at each point from the nodes of next period shocks based on Gauss-Hermite quadrature

   (c) the probability $P(X_t;\Theta^P)$ that a run occurs next period

3. Solve for all time t variables for a given state vector assuming that no run occur to first solve for the functions related to no-run equilibrium (e.g. $f_Q^1(X_t;\Theta^P)$). Take from the previous iteration j the law of motion $N'(X_t, \varepsilon_{t+1};\Theta^P)$ and the probability of

[30] In practice, it can be helpful to solve first for the economy with only one shock, for instance the volatility shock, and solve this model in isolation. The resulting policy functions can then be used as starting point for the full model with two shocks.

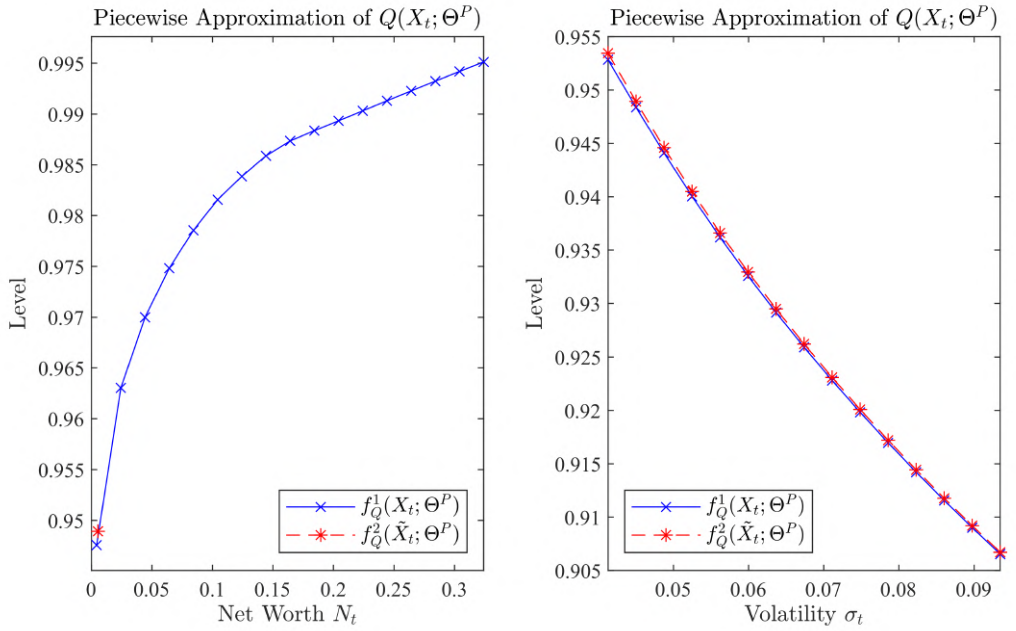

Figure 13: The figure shows the piecewise approximation of the policy function for the asset price $Q(X_t;\Theta^P)$. The function $f_Q^1(X_t;\Theta)$ describes the approximation of the policy function if no run occurs. The crosses are the grid points and the lines show the linear interpolation between these points. The function $f_Q^2(\tilde{X}_t;\Theta)$ describes the policy function of a run takes place in this period. In the left graph, the state variable net worth N_t is varied, while the remaining state variables are fixed. The function $f_Q^2(\tilde{X}_t;\Theta)$ displays only a single dot in the left graph because the level of net worth is predefined during a run (conditional on fixing the other state variables). In the right graph, the level of volatility is varied, while the remaining state variables are fixed. Net worth in the no run case is fixed to the level implied in the run case.

a run $P(X_t;\Theta^P)$ as given and calculate time $t+1$ variables using the guess j policy functions with X_{t+1} as state variables. The expectations are calculated using numerical integration based on Gauss-Hermite quadrature. A numerical root finder with the time t policy functions as input minimizes the error in the following five equations:

$$\text{err}_1 = (\tfrac{\Pi_t}{\Pi_{SS}} - 1)\tfrac{\Pi_t}{\Pi_{SS}} - \left(\tfrac{\epsilon}{\rho^r}\left(\varphi_t^{mc} - \tfrac{\epsilon-1}{\epsilon}\right) + \Lambda_{t,t+1}(\tfrac{\Pi_{t+1}}{\Pi_{SS}} - 1)\tfrac{\Pi_{t+1}}{\Pi_{SS}}\tfrac{Y_{t+1}}{Y_t}\right), \tag{100}$$

$$\text{err}_2 = 1 - \beta\Lambda_{t,t+1}\tfrac{i_t}{\Pi_{t+1}}1, \tag{101}$$

$$\text{err}_3 = (1-p_t)E_t^N\left[\beta\Lambda_{t,t+1}\bar{R}_t D_t\right] + p_t E_t^R\left[\beta\Lambda_{t,t+1}R_{t+1}^K Q_t S_t^B\right] - D_t, \tag{102}$$

$$\text{err}_4 = (1-p_t)E_t^N\left[\Lambda_{t,t+1}R_{t+1}^K(\theta\lambda_{t+1} + (1-\theta))(1 - e^{\frac{-\psi}{2}}\tilde{\pi}_{t+1})\right] - p_t E_t^R\left[\Lambda_{t,t+1}R_{t+1}^K(e^{-\frac{\psi}{2}} - \overline{\omega}_{t+1} + \tilde{\pi}_{t+1})\right], \tag{103}$$

$$\text{err}_5 = \lambda_t - \tfrac{(1-p_t)E_t^N\Lambda_{t,t+1}R_{t+1}^K[\theta\lambda_{t+1}+(1-\theta)](1-\overline{\omega}_{t+1})}{1-(1-p_t)E_t^N[\Lambda_{t,t+1}R_{t+1}^K\overline{\omega}_{t+1}]-p_t E_t^R[\Lambda_{t,t+1}R_{t+1}^K]}. \tag{104}$$

4. Take the iteration j policy functions , $N'(X_t,\varepsilon_{t+1};\Theta^P)$ and $P(X_t;\Theta^P)$ as given and solve the whole system of time t and $(t+1)$ variables. Calculate then N_{t+1} using the

"law of motion" for net worth

$$N_{t+1} = \max\left[R^K_{t+1} Q_t S^B_t - \overline{R}_t D_t, 0\right] + (1-\theta)\zeta S_t. \tag{105}$$

A run occurs at a specific point if

$$R^K_{t+1} Q_t S^B_t - \overline{R}_t D_t \leq 0. \tag{106}$$

In such a future state, the weight of a run is 1. In the other state, the weight of a run 0.[31] This can be now used to evaluate the probability of a run next period based on Gauss-Hermite quadrature so that I know p_t.

5. Repeat steps 3 and 4 for the run equilibrium so that the piece of the policy functions related to the run equilibrium is solved for (e.g. $f^2_Q(X_t;\Theta^P)$)

6. Update the policy policy functions $Q(X_t;\Theta^P), C(X_t;\Theta^P), \bar{b}(X), \Pi(X_t;\Theta^P), \lambda(X_t;\Theta^P)$ slowly. For instance for consumption policy function, this could be written as:

$$C_{j+1}(X_t;\Theta^P) = \alpha^{U1} C_j(X_t;\Theta^P) + (1-\alpha^{U1}) C_{sol}(X_t;\Theta^P), \tag{107}$$

where the subscript *sol* denotes the solution for this iteration and α^{U1} determines the weight of the previous iteration. Furthermore, $N'(X_t, \varepsilon_{t+1};\Theta^P)$ and $P(X_t;\Theta^P)$ are updated using the results from step 4:

$$N'_{j+1}(X_t, \varepsilon_{t+1};\Theta^P) = \alpha^{U2} N'_j(X_t, \varepsilon_{t+1};\Theta^P) + (1-\alpha^{U2}) N'_{sol}(X_t, \varepsilon_{t+1};\Theta^P), \tag{108}$$

$$P_{j+1}(X_t;\Theta^P) = \alpha^{U3} P_j(X_t;\Theta^P) + (1-\alpha^{U3}) P_{sol}(X_t;\Theta^P). \tag{109}$$

7. Repeat steps 3 - 6 until the errors of all functions, which are the classical policy functions $Q(X_t;\Theta^P), C(X_t;\Theta^P), \bar{b}(X), \Pi(X_t;\Theta^P), \lambda(X_t;\Theta^P)$ together with the law of motion of net worth $N'(X_t, \varepsilon_{t+1};\Theta^P)$ and the probability of a run $P(X_t;\Theta^P)$, at each point of the discretized state are sufficiently small.

[31] This procedure would imply a zero and one indicator, which is very unsmooth. For this reason, I use the following functional forms based on exponential function: $\frac{\exp(\zeta_1(1-D_{t+1}))}{1+\exp(\zeta_1*(1-D_{t+1}))}$ where $D_{t+1} = \frac{R^k_{t+1}}{R^D_t}\frac{\phi}{\phi-1}$ at each calculated N_{t+1}. ζ_1 is set to 2500. This large value of ζ ensures sufficient steepness so that the approximation is close to an indicator function of 0 and 1.

D Relationship between Leverage and Run Probability

The dynamics of leverage are very important and influence the run probability strongly. In general, extensive leverage makes the shadow banking system runnable, thereby raising the vulnerability of the economy to future financial crises. However, as it turns out, the relationship is complex and highly nonlinear.

The relationship between leverage and the run probability is complex and highly nonlinear. To show this result, the upper plot of Figure 14 shows a mapping between leverage and the run probability. The mapping results from increasing the level of the state variable S_{t-1} (securities) and calculating its impact on leverage and the run probability.[32] For instance, if previous period securities S_{t-1} are at 8.1, then leverage is around 20.2 and the run probability p is 0. Increasing S_{t-1} to 9.0 (while keeping constant all other state variables), leverage increases to around 20.9 and the run probability goes up to almost 5%. The graph confirms the general dynamics: higher leverage is associated with a higher run probability. At the same, the relationship is highly nonlinear. If leverage is below some varying threshold value, e.g. 20.4 for the displayed scenario, the probability of a run stays is zero. Once leverage increases above the threshold, then the probability of a run starts to increase. Importantly, the increase in the run probability accelerates, as the curve becomes steeper. This shows that the dynamics are nonlinear.

However, the mapping from leverage to the probability of a run is even more complicated in some states of the world. For instance, if the financial sector is relatively small, that is the share of its securities relative to total securities is low, then a high level of leverage is associated with rather low systemic risk for the financial sector. In contrast to this, if leverage is high and the share of intermediaries' securities is large, then there is substantial financial vulnerability. The lower plot of Figure 14 shows that such a relationship, in which the same leverage level is associated with altering run probabilities, can occur. The figure shows the same mapping between ϕ and p as the upper plot. However, the mapping is analyzed for different levels of net worth. Each level of net worth is shown as a distinct line. For orientation, the blue line corresponds to the scenario shown in the upper plot. Once net worth increases further and thus the share of securities held by the financial intermediaries, the relationship between leverage and the run probability can become backward bending. These backward bending curves show that a higher level of securities initially increases leverage and the run probability simultaneously. But the dynamics can change at one point. If the level of total securities increases further, the probability of a run continues to increase. However, leverage then starts to reverse and fall. The reason is that the run risk becomes too large, which forces intermediaries to reduce their leverage.[33] An important implication is that the same level of leverage can have many outputs. To express this in more mathematical terms, the model

[32]The mapping between leverage ϕ_t and the run probability p_t is shown for varying previous period total securities S_{t-1}. Total securities S_{t-1} are increased from 8.1 to 9.0, which then gives the changes in ϕ_t and p_t. To calculate the mapping, all other state variables (net worth, volatility and TFP) are fixed.

[33]The implication of this property is that the run probability is a tail risk in the model. Once it would become too large, intermediaries are forced to reduce their leverage, which limits financial fragility. This also implies that run probability also increases at a slower pace.

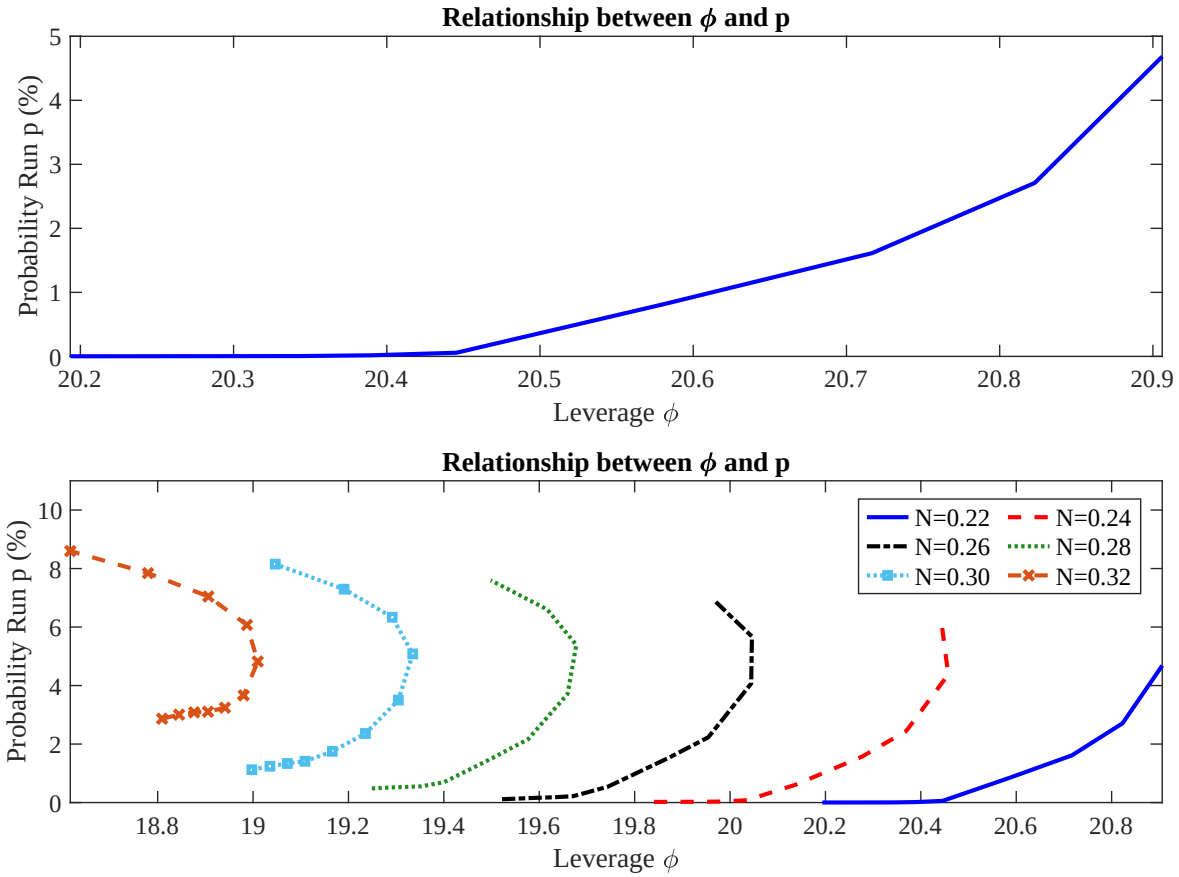

Figure 14: Relationship between leverage ϕ and the probability of a run for the period ahead p. The upper plot of Figure shows the mapping between leverage and the run probability if the level of previous period total securities S_{t-1} is varied. Total securities S_{t-1} are increased from 8.1 to 9.0. For instance, if previous period securities S_{t-1} are at 8.1, then leverage is around 20.2 and the run probability p is 0. Increasing securities to 9.0 (while keeping constant all other state variables), leverage increases to around 20.9 and the run probability goes up to almost 5%. To calculate the mapping, all other state variables (net worth, volatility and TFP) are fixed. The lower plot shows the same mapping for varying levels of net worth.

does not have a function that assigns to each level of leverage a unique run probability.[34]

Another way of showing that same level of leverage can result in different run probabilities depending on the economic circumstances is to use a scatter plot of leverage and run probability, as shown in Figure 15. The plot is based on based on a simulation over 500,000 periods. The figure highlights that the same level of leverage can result in different run probabilities in line with the statement. Nevertheless, a very important result is that higher leverage in general is associated with an elevated run probability, which is also indicated by the figure. Furthermore, the scatter plot also shows that there are some scenarios with very high leverage and a run probability of basically zero. The reason behind these observation

[34]The different lines are also overlapping horizontally. This also permits to have a function that gives a direct mapping from leverage to the run probability.

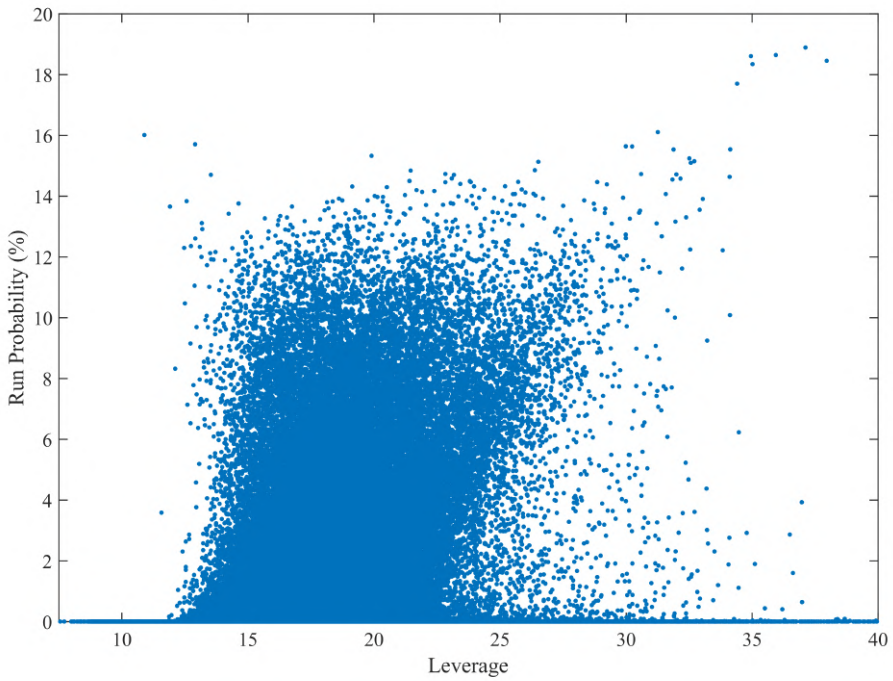

Figure 15: The figure shows a scatter plot of leverage and the run probability based on a simulation over 500,000 periods.

is that these data points are associated with periods, in which the financial sector had just started to rebuild after a run. While leverage is very high in this period, the run probability is basically zero as almost all securities are already hold by the households.

Thus, the relationship is not mechanic, and leverage alone is not a sufficient statistic to get the mapping to the probability of a run. This underlines why it is important to use the particle filter (instead of assuming a mechanic relationship) to extract the probability of a run over time.

E Particle Filter

I use a particle filter with sequential importance resampling based on Atkinson et al. (2020) and Herbst and Schorfheide (2015). The algorithm is adapted to incorporate sunspot shocks and endogenous equilibria similar to Aruoba et al. (2018), who have a model with sunspot shocks that directly determine the equilibria. I extend this approach to include the circumstance that the probability of equilibria is endogenously time-varying. The total number of particles M is set to 10000 as in Aruoba et al. (2018).

1. **Initialization** Use the risky steady state of the model as a starting point and draw $\{v_{t,m}\}_{t=-24}^{0}$ for all particles $m \in \{0, ..., M\}$. I set $\{\iota_{t,m} = 0\}_{t=-24}^{0}$, which excludes a run in the initialization. The simulation of these shocks provides the start values for the state variables $\mathbb{X}_{0,m}$.

2. **Recursion** Filter the nonlinear model for periods $t = 1, ..., T$

   (a) Draw the sunspot shock $\iota_{t,m}$ and the structural shocks $v_{t,m}$ for each particle $m = \{1, ..., M\}$. The sunspot shock is drawn from a binomial distribution with realizations $0, 1$:

   $$\iota_{t,m} \sim \mathcal{B}(1, \Upsilon), \tag{110}$$

   where 1 indicates the number of trails and Υ is the probability of $\iota = 1$.[35] The structural shocks are drawn from a proposal distribution that distinguishes between the realizations of the sunspot shock :

   $$v_{t,m} \sim N(\overline{v_t}^{\iota=0}, I) \quad \text{if} \quad \iota_{t,m} = 0, \tag{111}$$
   $$v_{t,m} \sim N(\overline{v_t}^{\iota=1}, I) \quad \text{if} \quad \iota_{t,m} = 1. \tag{112}$$

   As the regime selection is endogenous in the model, the proposal distribution can be the same for the two realizations of the sunspot shock. This is the case if the model does not suggest the realization of a run. The difference in using the proposal distribution is that instead of drawing directly from a distribution, I draw from an adapted distribution. I derive the proposal distribution by maximizing the fit of the shock for the average state vector $\overline{\mathbb{X}}_{t-1} = \frac{1}{M}\sum_{m=1}^{M} \mathbb{X}_{t-1,m}$

   i. Calculate a state vector $\overline{\mathbb{X}}_t$ from $\overline{\mathbb{X}}_{t-1}$ and a guess of $\overline{v}_t$ for the possible realizations of the sunspot shock:

   $$\mathbb{X}_t^{\iota=0} = f(\overline{\mathbb{X}}_{t-1}, \overline{v}_t^{\iota=0}, \iota_t = 0) \tag{113}$$
   $$\mathbb{X}_t^{\iota=1} = f(\overline{\mathbb{X}}_{t-1}, \overline{v}_t^{\iota=1}, \iota_t = 1) \tag{114}$$

   ii. Calculate the measurement error from the observation equation for the two

[35] In practice, I draw from a uniform distribution bounded between 0 and 1 and categorize the sunspot accordingly.

cases

$$u_t^{\iota=0} = \mathbb{Y}_t - g(\mathbb{X}_t^{\iota=0}), \tag{115}$$
$$u_t^{\iota=0} = \mathbb{Y}_t - g(\mathbb{X}_t^{\iota=1}). \tag{116}$$

The measurement error follows a multivariate normal distribution, so that the probabilities of observing the measurement error for the different sunspot shocks are given by

$$p(u_t^{\iota=0}|\mathbb{X}_t^{\iota=0}) = (2\pi)^{-n/2}|\Sigma_u|^{-0.5}\exp\left(-0.5(u_t^{\iota=0})'\Sigma_u^{-1}(u_t^{\iota=0})\right), \tag{117}$$
$$p(u_t^{\iota=1}|\mathbb{X}_t^{\iota=1}) = (2\pi)^{-n/2}|\Sigma_u|^{-0.5}\exp\left(-0.5(u_t^{\iota=1})'\Sigma_u^{-1}(u_t^{\iota=1})\right), \tag{118}$$

where Σ_u is the variance of the measurement error and n is the number of observables, which is 2 in this setup.

iii. Calculate the probability of observing $\mathbb{X}_t^{\iota=0}$ respectively $\mathbb{X}_t^{\iota=1}$ conditional on the average state vector from the previous period

$$p(\mathbb{X}_t^{\iota=0}|\overline{\mathbb{X}}_{t-1}) = (2\pi)^{-n/2}\exp\left(-0.5(\overline{v_t}^{\iota=0})'(\overline{v_t}^{\iota=0})\right), \tag{119}$$
$$p(\mathbb{X}_t^{\iota=1}|\overline{\mathbb{X}}_{t-1}) = (2\pi)^{-n/2}\exp\left(-0.5(\overline{v_t}^{\iota=1})'(\overline{v_t}^{\iota=1})\right). \tag{120}$$

iv. To find the proposal distribution, maximize the following objects with respect $\overline{v_t}^{\iota=0}$ respectively $\overline{v_t}^{\iota=1}$:

$$p(\mathbb{X}_t^{\iota=0}|\overline{\mathbb{X}}_{t-1})p(u_t^{\iota=0}|\mathbb{X}_t^{\iota=0}), \tag{121}$$
$$p(\mathbb{X}_t^{\iota=1}|\overline{\mathbb{X}}_{t-1})p(u_t^{\iota=1}|\mathbb{X}_t^{\iota=1}). \tag{122}$$

This provides the proposal distributions $N(\overline{v_t}^{\iota=0}, I)$ and $N(\overline{v_t}^{\iota=1}, I)$.

(b) Propagate the state variables $\mathbb{X}_{t,m}$ by iterating the state-transition equation forward given $\mathbb{X}_{t-1,m}$, $v_{t,m}$ and $\iota_{t,m}$:

$$\mathbb{X}_{t,m} = f(\mathbb{X}_{t-1,m}, v_{t,m}, \iota_t). \tag{123}$$

(c) Calculate the measurement error

$$u_{tm} = \mathbb{Y}_t - g(\mathbb{X}_{t,m}). \tag{124}$$

The incremental weights of the particle m can be written as

$$w_{t,m} = \frac{p(u_{t,m}|\mathbb{X}_{t,m})p(\mathbb{X}_{t,m}|\mathbb{X}_{t-1,m})}{f(\mathbb{X}_{t,m}|\mathbb{X}_{t-1,m},\mathbb{Y}_t,\iota_{t,m})} \tag{125}$$

$$= \begin{cases} \frac{(2\pi)^{-n/2}|\Sigma_u|^{-0.5}\exp\left(-0.5u_{t,m}'\Sigma_u^{-1}u_{t,m}\right)\exp\left(-0.5v_{t,m}'v_{t,m}\right)}{\exp\left(-0.5(v_{t,m}-\overline{v}_t^{\iota=0})'(v_{t,m}-\overline{v}_t^{\iota=0})\right)} & \text{if } \iota_{t,m}=0 \\ \frac{(2\pi)^{-n/2}|\Sigma_u|^{-0.5}\exp\left(-0.5u_{t,m}'\Sigma_u^{-1}u_{t,m}\right)\exp\left(-0.5v_{t,m}'v_{t,m}\right)}{\exp\left(-0.5(v_{t,m}-\overline{v}_t^{\iota=1})'(v_{t,m}-\overline{v}_t^{\iota=1})\right)} & \text{if } \iota_{t,m}=1 \end{cases} \tag{126}$$

where the density $f(\cdot)$ depends on the realization of the sunspot shock. The

incremental weights determine the log-likelihood contribution in period t:

$$\ln(l_t) = \ln\left(\frac{1}{M}\sum_{m=1}^{M} w_{t,m}\right). \tag{127}$$

(d) Resample the particles based on the weights of the particles. First, the normalized weights $W_{t,m}$ are given by:

$$W_{t,m} = \frac{w_{t,m}}{\sum_{m=1}^{M} w_{t,m}}. \tag{128}$$

Second, the deterministic algorithm of Kitagawa (1996) resamples the particles by drawing from the current set of particles adjusted for their relative weights. This gives a resampled distribution of state variables $\mathbb{X}_{t,m}$.

3. **Likelihood Approximation** Determine the approximated log-likelihood function of the model as

$$\ln(\mathcal{L}_t) = \sum_{t=1}^{T} \ln(l_t). \tag{129}$$

F Estimation of Financial Fragility: Additional Results

This section contains additional results for the estimation of financial fragility with the particle filter in Section 4. Three robustness checks (additional observable, measurement error, shocks post 2009) are conducted. Furthermore, the role of multimodality and tail risk is evaluated.

F.1 Robustness Checks

The three robustness checks are now described in detail.

F.1.1 Additional Observable: Credit Spread

One advantage of the particle filter is that it can handle more observables than shocks. To provide an example of flexibility of the approach, I include credit spreads as an additional observable in the observation equation as a robustness check. The spread is calculated as the difference between the BAA bond yield and a 10 year Treasury bond. The adapted observation equation is:

$$\begin{bmatrix} \text{Output Growth}_t \\ \text{Leverage}_t \\ \text{Credit Spread}_t \end{bmatrix} = \begin{bmatrix} 100 \ln\left(\frac{Y_t}{Y_{t-1}}\right) \\ \phi_t \\ 400 E_t(R^K_{t+1} - R^f_{t+1}) \end{bmatrix} + u_t, \tag{130}$$

where the risk free rate is defined as $R^f_{t+1} = i_t/\Pi_{t+1}$.

Figure 16 compares the baseline observation equation to a scenario with credit spreads as additional observable. Even though there are some changes for the filtered series relative to the baseline scenario with two series, the estimated probability of a run still predicts a strong build-up before 2008 and that the run itself occurred in 2008:Q4. However, it should be noted that the filter gives now a much higher run probability. The underlying reason is that the dynamics of the TFP shock are different when spreads are included. The level of TFP is elevated to the baseline scenario, which increases the security holdings of financial intermediaries as well as the overall level. This elevated level of TFP contributes to a boom and increases the run probability.

17 compares the dynamics of the credit spread with three observables to the baseline. While it highlights that the data is now (unsurprisingly) much better captured, the prediction of the baseline model for the credit spread is also mostly in line with the data. This provides another external validation of the estimation as credit spreads are a key variable.

F.1.2 Alternative Measurement Error

I choose a rather higher measurement error with 25% of the sample variance for two reasons. First, the leverage series is potentially very noisy because variables related to the shadow banking sector are hard to measure exactly. Second, the computational requirements to run the global solution method requires to exclude some important model elements that help to

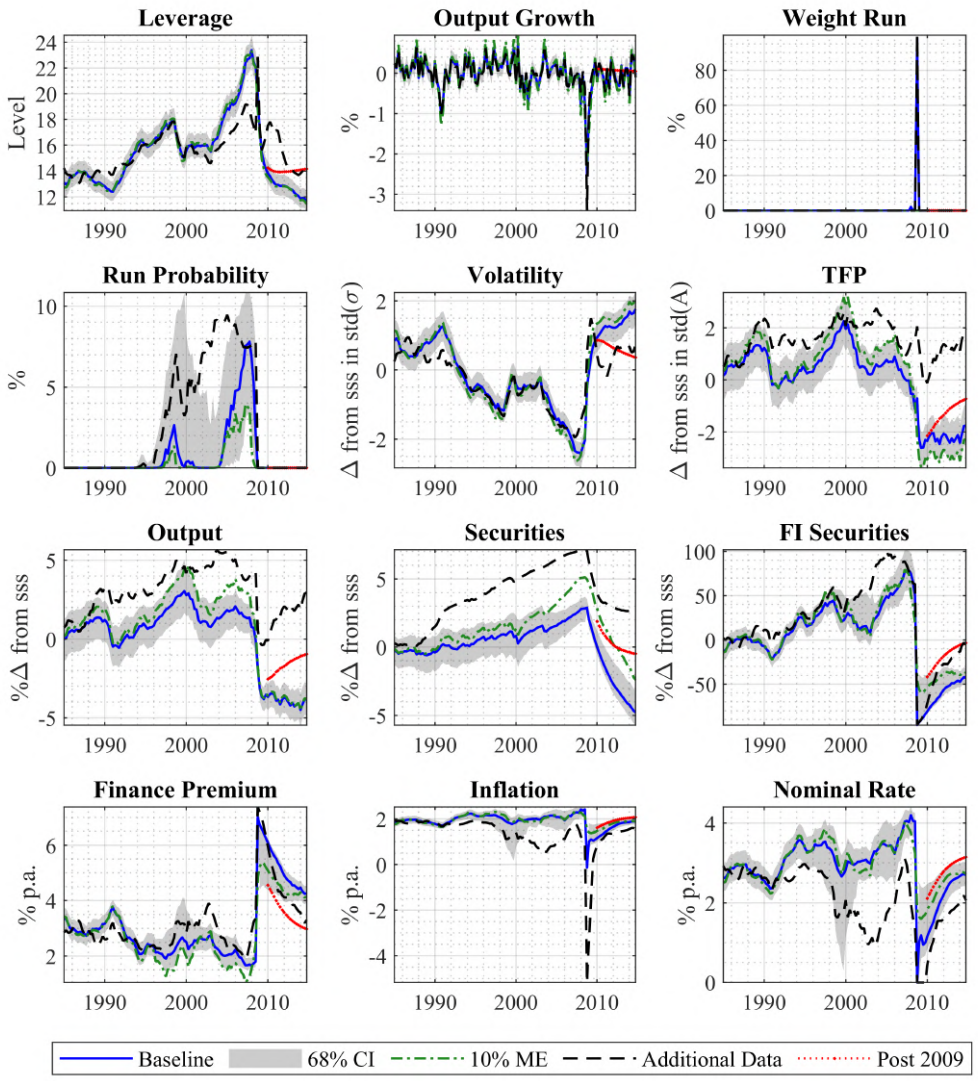

Figure 16: Comparison of the baseline estimation to alternative specifications, in which the measurement error is lowered to 10%, the credit spread is included as additional variable and no shocks hit the economy post 2009. The solid blue line shows the filtered median with its 68% confidence interval (grey shaded) for the baseline. The dash-dotted green line shows the filtered median for a lower measurement error of 10%. The dashed black line shows the filtered median if the credit spread is included as additional observable. The dotted red line shows the path from 2010, in which no shock post 2009 materializes. Note that for the third plot the weight of the run regime is shown. The scales are either percentage deviations from the stochastic SS (%Δ), deviations from the stochastic SS measured in the unconditional variance of the variables, annualized percent, percent, or the level.

match the data (e.g. habit or persistence for investment). As a robustness check, I include now a scenario with a measurement of 10% to check how robust the results are, as shown in Figure 16. The dynamics are quite similar to the baseline. There is a strong increase in run

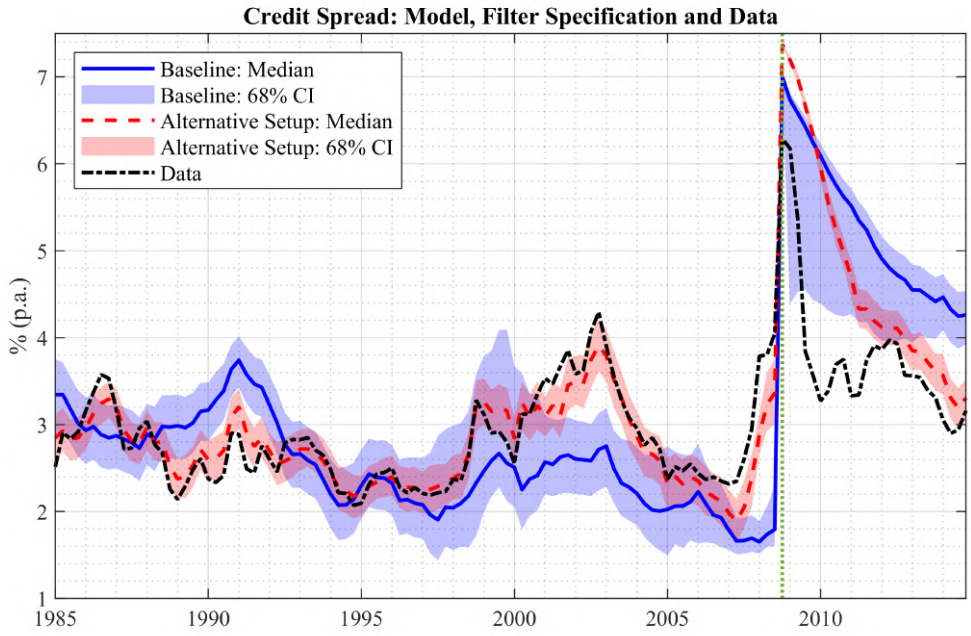

Figure 17: External validation of the credit spread and alternative model specification. The blue solid line and shaded area shows the filtered credit spread series for the baseline specification with output growth and leverage as observables. The red dashed line and shaded area shows the same series for a scenario with credit spread as additional observable. The black dash-dotted line shows the data, which is the spread between the BAA yield and the 10 year government bond. The data proxy, which is a measure of cross-sectional variance of industry level TFP, is the black dashed line. The level of the data is shifted by 0.7 percentage points to account for the difference between the simulated mean of the model and the data.

risk prior to 2008 and the filter locates a run to 2008:Q4. One difference is that there is a larger increase in the run risk around 2000.

F.1.3 Economic Activity Post 2009

Figure 16 compares the behavior of key time series if no shocks hit the economy beyond 2009. The average GDP growth rate between 2010 and 2014 has been smaller due to the shocks. Therefore, the additional shocks help to generate a slower recovery than the model alone would suggest. Output would be -1% below its steady state value in this counterfactual scenario without shocks compared to -4% in the actual estimation. This points out that the model does not have enough persistence in isolation. The shocks also help to keep leverage levels down. Leverage would be around 14 instead of 12 as in the actual data. This disparity could potentially be attributed to the changes in the regulatory environment, which is not accounted for in the model.

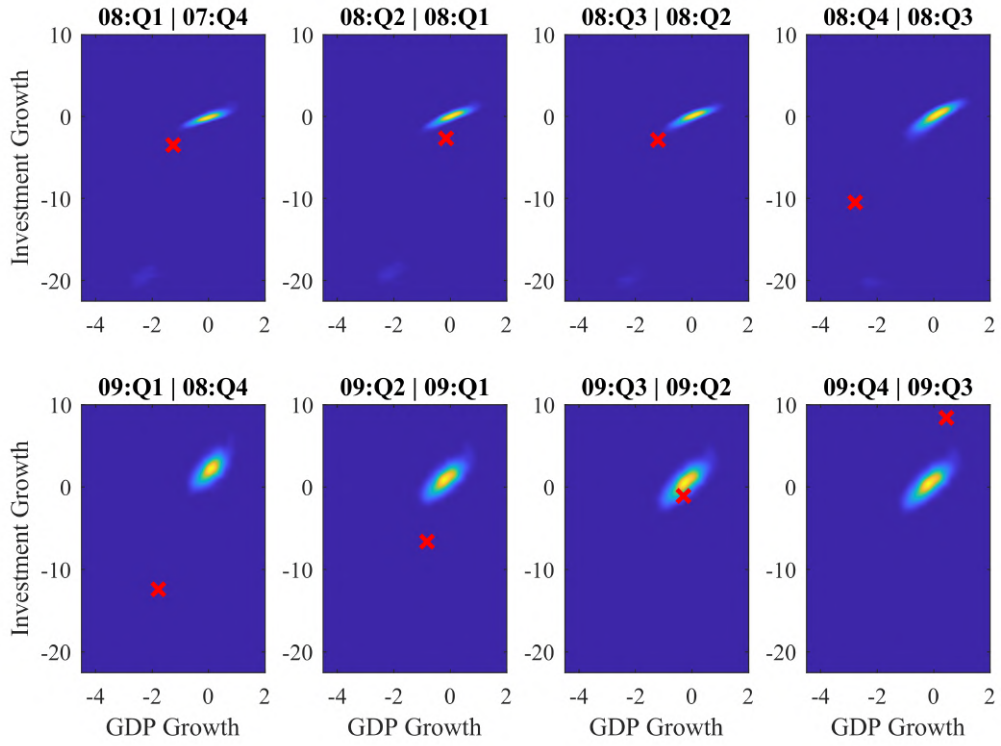

Figure 18: The contour plots displays the one-quarter-ahead joint distribution of GDP growth and investment growth over time. It shows that the multimodality arises due to the run equilibrium. GDP growth is on the horizontal axis, while investment growth is on the vertical axis. Yellow indicates a high density, while dark blue indicates a low density The red square shows the actual data realization in the forecasted period. The forecasts are conditioned on the median realization.

F.2 Macroeconomic Tail Risk and Multimodality

The increase in the run probability induces substantial macroeconomic downside risk. To better understand the downside risk, I evaluate the joint one-quarter-ahead distribution of output growth and investment growth. Figure 18 shows a contour plot of the one-quarter-ahead joint distribution of the variables from 2008:Q1 until 2009:Q4. It shows that the multimodality arises due to the run equilibrium. While most mass is on the no run equilibrium with GDP growth centered around 0, there is significant tail risk of a large fall in output due to a run. This is the slighlty blue area around -2.5% GDP growth and investment growth in the charts for the quarters in 2008. After the run, the distribution is overwhelmingly unimodal as there is no financial fragility. The model can explain the fall in GDP 2008:Q4 with a run because its 2008:Q4 forecast conditional on 2008:Q3 allows for a large fall in output. However, the run lacks some persistence to explain the two data realizations in 2009:Q1 and 2009:Q2.

The analysis is the structural equivalent to the large body of literature on growth-at-risk starting with Adrian et al. (2019), where the downside risk over time is evaluated. Recent reduced-form empirical approaches also suggest that the downside risk comes from a bimodal

distribution, in line with my findings (see e.g Adrian et al., 2021, Caldara et al., 2021 and Mitchell et al., 2021). The work most closely related is that of Adrian et al. (2021), who estimate the conditional joint distributions of economic fundamentals and financial conditions. Similarly to the predictions in the model, they find the occurrence of a second equilibrium for 2008:Q4 conditional on 2008:Q3. They also find that the probability of the normal equilibrium is higher in line with these results.

G Monetary and Macroprudential Strategies: Additional Results

G.1 Montary Policy with Financial Considerations: Ex-ante and Ex-Post Components

While the rule that responds to financial conditions succeeds in increasing financial stability and welfare, the source is not yet explored. Does the financial gain stem mostly from leaning-against-the-wind or a credible commitment ex-post? To shed light on this, I analyze the ex-ante and ex-post interventions separately. I model leaning-against-the-wind in advance as:

$$R_t^I = \max\left\{R^I\left(\frac{\Pi_t}{\Pi}\right)^{\kappa_\Pi}\left(\frac{\varphi_t^{mc}}{\varphi^{mc}}\right)^{\kappa_y}\left[\mathbf{1}_{S_t^B>S^B}\left(\frac{S_t^B}{S^B}\right)^{\kappa_s}+\left(1-\mathbf{1}_{S_t^B>S^B}\right)\right],1\right\}, \tag{131}$$

where $\mathbf{1}_{S_t^B>S^B}$ is an indicator function that is equal to one when intermediaries' security holdings are above target ($St^B > S^B$). In this specification, the monetary authority only raises rates in response to financial stability consideration.

One challenge with analyzing leaning-against-the-wind is the stability since the solution procedure explodes once the level of κ_s is sufficiently large. To overcome this problem, I impose the leaning-against-the-wind component only at the relevant parts of the state space. In other words, I exclude the rule from areas of the state space, which are never or only very rarely visited. In particular, I restrict that net worth needs to be sufficiently large, securities need to be below some upper bound, leverage needs to be inside a range associated with financial stability, the volatility shock is sufficiently small and the TFP shock is sufficiently large: $N_t > 0.124$, $S_t < 8.8739$, $9 < \phi < 40$, $\xi < 0.0561$, $A_t > 0.4872$. This step allows to solve the model with an interestingly strong leaning-against-the-wind as the code otherwise does not converge.

The commitment to a loose policy ex-post is modeled analogously as:

$$R_t^I = \max\left\{R^I\left(\frac{\Pi_t}{\Pi}\right)^{\kappa_\Pi}\left(\frac{\varphi_t^{mc}}{\varphi^{mc}}\right)^{\kappa_y}\left[\mathbf{1}_{S_t^B<S^B}\left(\frac{S_t^B}{S^B}\right)^{\kappa_s}+\left(1-\mathbf{1}_{S_t^B<S^B}\right)\right],1\right\}, \tag{132}$$

where the indicator functions captures now that intermediaries' security holdings are below target ($St^B > S^B$). In this specification, the central bank only lowers the interest rate in response to financial conditions.

To analyse the impact of the different components (ex-ante leaning as well as the ex-post commitment to loosening), Table 2 compares the welfare, financial stability and economic outcomes for various rules. The baseline MP rule (column 1) represents the scenario, in which the monetary authority only responds to inflation and output deviations. The modified monetary policy thatthat responds to financial conditions is shown in column 2. The parameter κ_s is set to its welfare maximizing value. I then dissect the rule in its ex-ante and ex-post interventions using the same value for κ_s. While the impact of leaning-against-the-wind in isolation is shown in column 3, the credible ex-post commitment to loose monetary

Table 2: Welfare, financial stability and economic outcomes of various policies

	Baseline MP rule	Modified MP rule (κ_s^{opt})	Leaning ex-ante	Loosening ex-post	Leverage tax (τ_s^{opt})
Selected key moments					
Welfare W (CE)[a]	–	0.56	0.05	0.52	0.64
Run Probability[b]	1.91	0.02	1.80	0.05	0
Mean of selected variables[c]					
Consumption C	0.58	0.40%	0.04%	0.37%	0.39%
Labor L	1.01	0.08%	0.02%	0.07%	0.07%
Leverage ϕ	15.5	−0.82%	0.09%	−0.99%	−3.99%
Assets S	8.48	1.63%	0.20%	1.48%	1.51%
Share Financial S^B/S	0.35	4.57%	0.37%	4.28%	4.37%
Standard deviation of selected variables[d]					
Consumption C	0.01	0.22%	−1.36%	1.58%	−3.19%
Labor L	0.006	−46.4%	−5.05%	−33.0%	−48.3%
Leverage ϕ	2.92	−9.86%	0.04%	−11.3%	−48.6%
Assets S	0.14	32.9%	−0.11%	35.3%	8.70%
Share Financial S^B/S	0.10	−24.8%	−1.67%	−22.4%	−53.6%

[a] Welfare gain/loss expressed as consumption equivalent relative to baseline rule in %.
[b] Annual run probability in %.
[c] The level is shown for the baseline economy. The other scenarios display the mean as percentage deviations relative to the baseline economy.
[d] The level is shown for the baseline economy. The other scenarios display the standard deviation as percentage deviations relative to the baseline economy.

policy is displayed in column 4. The outcomes are also compared to the leverage tax, where the parameter τ_s is the lowest value that reduces the run frequency to zero.

There are three key results from our analysis. First, leaning-against-the-wind has a positive, albeit small, impact on financial stability and welfare. When the central bank only leans against the wind by raising rates, the run probability is slightly reduced to 1.80% (from 1.91%) and welfare increases by 0.05% in terms of consumption equivalents. It also has a rather small effect on the mean and standard deviation of most variables. The model implications are different than the findings of Schularick et al. (2021), who argue that leaning-against-the-wind is more likely to increase crisis risk using historical data. My model suggests that the benefits of leaning-against-the-wind are slightly outweighing its costs. Thus, the policies has the potential to improve welfare and financial stability. However, the gains are likely to be rather small. But, it should ne noted that unanticipated monetary policy hikes can also trigger short-term financial instability before resulting in medium-term gains as I show by embedding a monetary policy shock in the model.

In contrast to leaning-against-the-wind, a credible commitment to loose policy ex-post provides a very large substantial and basically explain almost all of the welfare gains, as

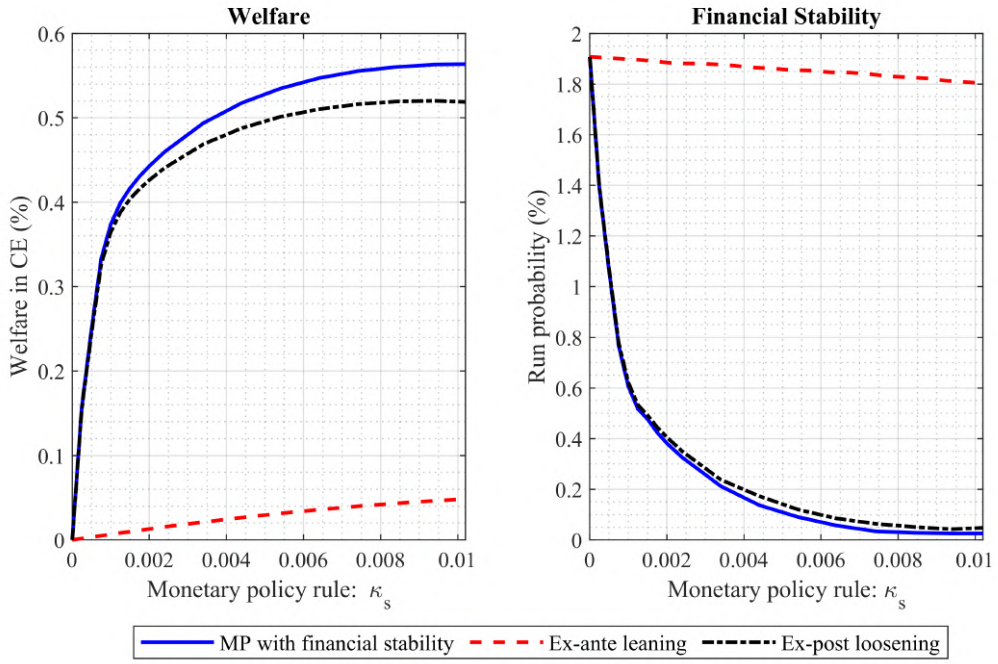

Figure 19: The figure shows the welfare and annual run probability under various policies. The monetary policy rule (blue solid) is compared to versions that only use its components. Only leaning-against-the-wind ex-ante is shown as dashed red line, while the commitment to a loose ex-post policy is shown as black dash-dotted line. The parameter of the financial stability element κ_s is varied between $[0, \kappa_s^{opt}]$

can be seen when comparing column 2 and column 4. However, this requires a credible commitment from the central bank. The result is in line with Devereux et al. (2019), who show in the context of sudden stops that the possibility to credibly commit to such ex-post policies is very effective in the avoidance of crises.

To further outlay the connection between these policies, Figure 19 compares the impact of the different components of the modified policy rule on welfare and financial stability. The response to the securities κ_s is varied between 0 and the optimal value κ_s^{opt}. This figure extends the subplot of Figure 9, as it now highlights the contribution of ex-ante leaning and ex-post commitment to loosening. The figure underlines that most gains come from a credible commitment to loose policy after a crisis. Leaning-against-the-wind in isolation can reduce the run probability only slightly and has therefore only a small positive on welfare.

Note that this result is robust to other specifications for the leaning-against-the-wind part such as changing the target value of securities S^B and or limiting the maximum contribution from leaning-against-the-wind in the policy rule. These experiments confirm the finding that leaning-against-the-wind has a positive, albeit small, effect.

G.2 Transmission of a Monetary Policy Shock

This section discusses the transmission of an unanticipated monetary policy shock during a boom. For this analysis, I assume that agents did not expect such a shock and do not expect

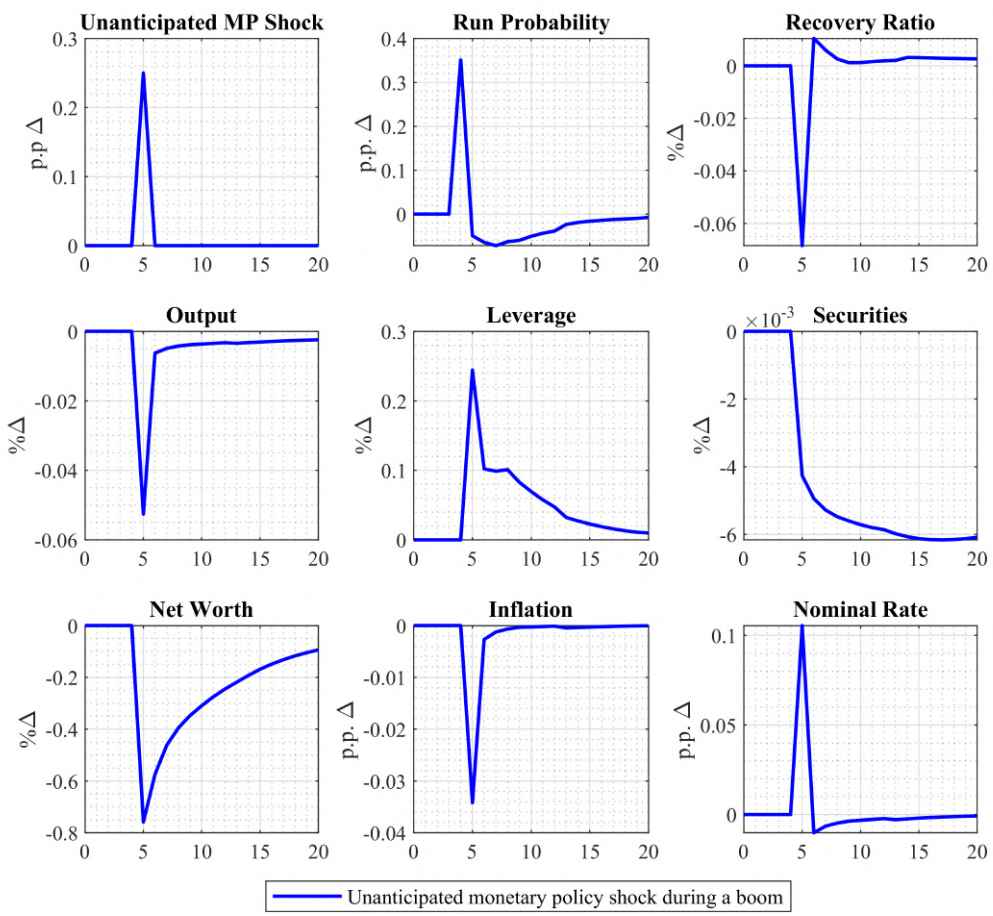

Figure 20: The figure shows the impact of an unanticipated monetary policy shock (25 bps) on the economy and financial stability during a boom scenario. The difference is either expressed in percentage points difference or percent relative to a scenario without a monetary policy shock is displayed. To generate the boom scenario, a sequence one-standard-deviation negative volatility shocks hits the economy in period 1 until period 8. Afterwards, no shock materializes.

a monetary policy shock in the future. The shock enters the Taylor rule (without a response to financial conditions) as follows:

$$R_t = \max\left\{R^I\left(\frac{\Pi_t}{\Pi}\right)^{\kappa_\Pi}\left(\frac{\varphi_t^{mc}}{\varphi^{mc}}\right)^{\kappa_y}, 1\right\}\exp\left(mp_t\right), \tag{133}$$

where mp_t is the monetary policy shock.

The following simulation assesses the transmission of an unanticipated interest rate hike during a boom. To create the boom, I assume that a sequence of one-standard-deviation negative volatility shocks hits the economy in period 1 until period 8 (starting from the stochastic steady state). The monetary policy shock, which is normalized to an annualized 25 basis points, occurs in period 5 (in the midst of the boom). Figure 20 shows the difference in the path between a scenario with and without a monetary policy shock. The contractionary

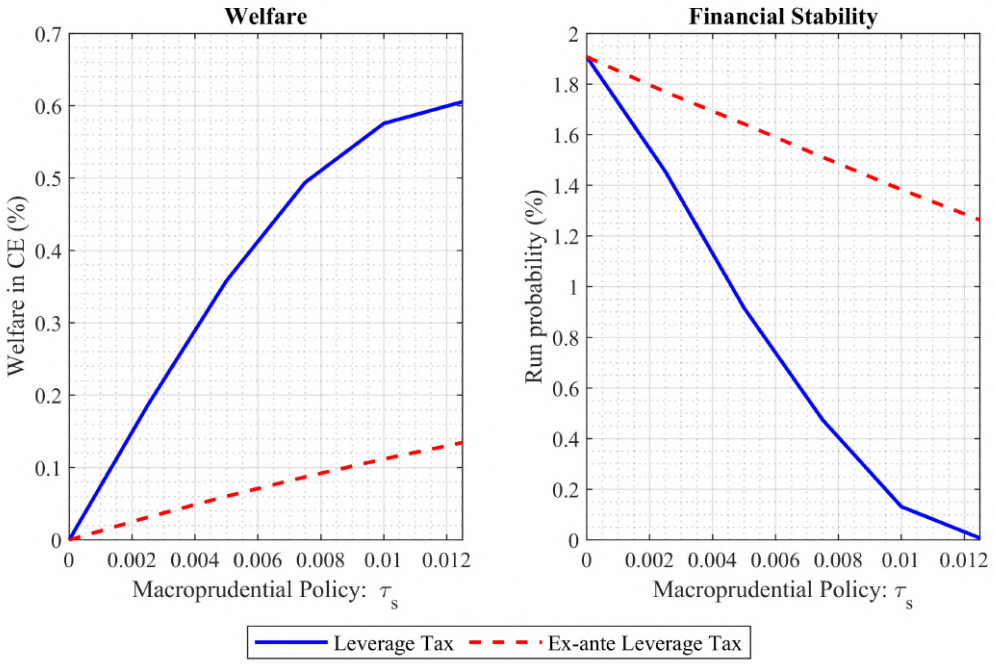

Figure 21: The figure shows the welfare and annual run probability for the leverage tax (blue solid) and a version with only an ex-ante component (dashed red line). The monetary policy rule is compared to versions that only use its components. The parameter of the response τ_s is varied between $[0, \tau_s^{opt}]$

monetary policy shock reduces output and inflation, while the interest rate increases, as expected. Initially, the monetary policy shock increases financial fragility, as the difference in the run probability goes up. The true run probability, that is if the unanticipated shock would have be known, increases by an additional 0.4% percentage points in period 4. This effect then reverses and financial stability improves as a result of the monetary policy hike. Furthermore, it also lowers total securities as well as net worth of the agents.

G.3 Macroprudential Policy: Ex-ante Component

I now also analyze separately the effects of ex-ante and ex-post macroprudential policy. The macroprudential authority responds to the security holdings of intermediaries similar to leaning-against-the-wind. If the security holdings are above the same target value, the central bank raises the tax. Otherwise, the tax is zero. The rule τ_t^{ϕ} is given as:

$$\tau_t^{\phi} = \mathbf{1}_{St^B > S^B} \left[\left(\frac{S_t^B}{S^B} \right)^{\tau_s} - 1 \right], \tag{134}$$

where τ_s is the response to deviations from the target value S^B set by the macroprudential authority. The target value S^B is calibrated to the same value as the other rules.

Figure 21 compares the leverage tax to its version with only the ex-ante component. The response to the securities τ_s is varied between 0 and the lowest value that reduces the run frequency to zero. This figure complements Figure 9, as it now highlights the contribution

of ex-ante and ex-post effects for the leverage tax. An important takeaway is that ex-ante macroprudential policy in isolation is rather effective in increasing financial stability, which is also in line with GKPb. This results contrasts the findings for monetary policy with a financial stability response, where the ex-ante effects were considerably smaller. In fact, the leverage tax can considerably further diminish the run probability if I would set $\tau_s > \tau_s^{opt}$. This also has important implications for the findings of the paper. While the results suggest that monetary policy can be a good substitute for macroprudential policy, this only holds if the authorities can credibly commit to ex-post policies.